THE RADIO BURSTS FROM THE OUTER CORONA

A Thesis
Submitted For the Degree of
Doctor of Philosophy in The Faculty of Science
BANGALORE UNIVERSITY

By

G. Thejappa

DECLARATION

I hereby declare that the matter embodied in this thesis is the result of the investigations carried out by me in the Indian Institute of Astrophysics, Bangalore and the Department of Physics, Central College, Bangalore, under the supervision of Prof.Ch.V.Sastry and Dr.M.N.Anandaram and has not been submitted for the award of any degree, diploma, associateship, fellowship, etc of any University or Institute.

(G.Thejappa)
Candidate

Ch.V.Sastry

M.N.Anandaram

Supervisors

Bangalore

Date   6|5|88

Dedicated to my beloved friend RAYA.

ACKNOWLEDGEMENTS

CONTENTS

ABSTRACT

Over the whole electromagnetic spectrum of the Sun the metre wavelength band (1 to 10m) is unique. Shorter wavelengths, from γ-rays to microwaves, come mostly from regions containing dense matter associated with the Visible Sun as we know it - the Photosphere and Chromosphere - and longer wavelengths come mainly from interplanetary space. Metre waves alone are generated in the tenuous Plasma known as the solar corona (ordinarily visible only at the time of a total eclipse), and they reveal a spectacular range of phenomena undreamt of before their discovery. It is here many types of Solar radio bursts are generated. Generally these radio bursts are excited by two types of disturbances : (1) Electron beams and (2) Collisionless shock waves. The Physics of the beam - plasma system is more or less understood both theoretically as well as experimentally, whereas the detailed study of the collisionless shock waves has been started recently by insitu experiments and subsequent theoretical advances. We study theoretically the acceleration of electrons, excitation of low as well as high frequency turbulence in the shock fronts and the subsequent radio emission processes. We apply this analysis to various burst phenomena such as Type I, Type II, absorption bursts, etc.

In the first chapter, we have broadly indicated the difference between inner and outer corona and classified the types of disturbances that perturb the corona into two classes: (1) electron

beams and (2) collisionless shock waves. The interrelation between these two types of disturbances is also discussed. We then give a preview of the results presented in the thesis.

In the second chapter, we study the type I burst phenomena. Assuming that weak shocks driven by newly emerging magnetic flux are responsible for type I radio bursts, we derive the dispersion relation for ion sound waves generated in a collisionless shock propagating perpendicular to the magnetic field. Using quasilinear analysis the energy density of the ion-sound turbulence is estimated and compared with the lower hybrid turbulence generated under similar conditions. We finally show that ion-sound turbulence is a better candidate for the generation of type I radio bursts in the solar corona. Since type I chains are the most direct evidence for the weak shocks responsible for their generation, measurements of the frequency drift rate and the bandwidth of these chains, can be used to estimate the upstream velocity and the density jump across the shock. The Alfven velocity and hence the coronal magnetic field can be calculated by substituting the above values in the modified Rankine - Hugoniot relation. Therefore we devise a method to estimate the radial dependence of the coronal magnetic field above mild active regions using the Type I chain data. These results are compared with the existing estimates and found to be in good agreement.

In chapter III, we describe the Radio telescope which was used to study the fine structure of the solar radio emission

at decameter wavelengths. The main fine structures observed using the above telescope are : (1) the peculiar time profiles of type III storm bursts and (2) absorption bursts. It has been shown that the peculiar time structures in type III profiles are not due to random superposition of bursts with varying amplitudes. It has also been shown that they are not manifestations of funda- mental - harmonic pairs. Some of these profiles can be due to superposition of bursts caused by ordered electron beams ejected with a constant time delay at the base of the corona. Regarding the absorption bursts, it has been shown that the ion- sound turbulence, generated by a laterally moving shock wave can act as an absorber of the decametric continuum radiation travelling radially outward, converting it into longitudinal Langmuir turbulence by three wave interactions. The duration of the absorp- tion, the depth and the bandwidth are explained selfconsistently in this model.

The most enigmatic type of decametric radio bursts are the drift pair bursts. The data on drift pair bursts obtained using the swept frequency spectrograph at Nancay, France, have been analysed in chapter IV. We have detected for the first time features like drfit pair chains and vertical drift pair bursts. The drift pairs and their associated phenomena like chains and vertical bursts can be interpreted if one assumes that the double plasma resonance layer, where the radiation is proposed to be generated is different at different instants of time so that one gets a slope in the frequency - time plane. If one

assumes considerable fluctuations in some microscopic parameters such as density and magnetic field, it is possible to have drift of all types. A steep variation in the magnetic field is derived assuming that the density is not affected by DP activity, in the case of vertical DPs.

In chapter V, it is proposed that the majority of shock waves responsible for the generation of type II radio bursts are supercritical. It is also proposed that the reflected ions behave like a beam in the foot and the ramp and like a ring in the downstream, i.e., just behind the overshoot. These are described by drifted Maxwellian and Dory-Guest-Harris distributions respectively. The ion beams are unstable and can drive the low frequency waves, whose frequency lies between the electron and ion cyclotron frequencies. These waves are absorbed by the ambient electrons, leading to the formation of electron "tails", in upstream as well as in downstream. On entering the cold background these hot electrons, in turn, drive the high frequency Langmuir oscillations to high level energy densities $\frac{W_L}{n_o T_e} \approx 10^{-5} - 10^{-4}$ in the upstream as well as in the downstream. The conversion of plasma waves into electromagnetic waves is caused by the induced scattering of plasma waves off ions or by merging of two Langmuir waves. The brightness temperatures in the lower and upper bands depend on the number densities in the accelerated beams. Since the number density of the electron beams in the downstream is less than that of upstream, the U band is fainter than L band as experimentally observed;

thus explaining naturally the band splitting in Type II bursts and the difference in brightness of the two bands. The role of nonlinear processes is also studied.

In chapter VI we briefly summarize the main conclusions of the thesis. We also briefly mention the importance of our results. The future observations and theoretical work to be done in these lines are also suggested.

CHAPTER I

INTRODUCTION

The study of the sun is of great importance not only because it provides us with an excellent testing ground for many physical laws that cannot be tested in the laboratory but also because it is the only star near enough for detailed scrutiny of its surface, atmosphere and activity. In the past, studies of the sun have always led to the development and understanding of many physical concepts. These include atomic spectra, the interaction of plasmas with matter and magnetic fields, and nuclear reactions.

Radioastronomy is the only means by which one can study cosmic plasmas, although the data obtained gives only partial information about the physical conditions. One of the serious limitations of Radio Astronomical studies is the poor resolving power that can be obtained. As the radio emissions are very closely connected with the physical processes going on in the comic objects, it is very essential to obtain as many observational details as possible. Since sun is sufficiently close to us and provides very rich information in the radio domain also, a study of these radio emissions provide important clues to the understanding of many complicated plasma processes taking place in the solar environment, which may be impossible to simulate on earth.

Some of these processes are collisionless shock waves, particle acceleration, wave particle interactions and wave-wave interactions. The solar corona is the very hot, tenuous, inhomogeneous and time varying atmosphere, which, with its extension

as the solar wind, continues from the transition region to the planets and beyond. Magnetic fields undoubtedly play an important role in its structure and motions, and probably also in its heating. This hot, inhomogeneous magnetoplasma can support a variety of plasma modes. In addition to this, the solar activity produces transients and disturbances of varied nature like shock waves and particle beams in the corona thereby pumping energy into the normal modes of the plasma. These growing modes can radiate directly if they are transverse electromagnetic modes; if they are electrostatic, they can interact among themselves to generate electromagnetic radiation. The physical conditions and the parameters such as plasma frequency, cyclotron frequency etc will decide the predominance of the particular type of modes that grow faster than others. The generated radiation can have specific polarization which again carry information about the physical environment from which the radiation emerges; The emerging radiation propagates through the outer coronal medium which impresses its own changes on the original radiation. The detection and analysis of such radiation, therefore, provides not only information about the coronal medium, but also about the various energy sources that pass through the corona.

The radio phenomena occur over a wide range of the electromagnetic spectrum starting from a few Kilo Hertz to thousands of Mega Hertz. The radio window provided by the earth's atmosphere can be used for ground based observations of the radio emission. The satellite data provide information at those wavelengths

which cannot pass through the earths atmosphere. Some types of radio phenomena occur over a wide range of frequencies suggesting that they extend from the inner corona to the outer corona and interplanetary space. Certain other radio phenomena occur only over a limited frequency range indicating their localized nature.

The inner corona is dense and permeated by high magnetic fields of varied structures. The outer corona has relatively weak magnetic fields and therefore the basic plasma processes going on in these regions may be quite different. While the inner corona contains closed as well as open magnetic fields of varied structures, the outer corona contains predominantly open magnetic fields. The study of radio emission from outer corona provides an excellent opportunity of understanding the solar activity which influences it.

Over the whole electromagnetic spectrum of the Sun the metre wavelength band (1 to 10 m) is unique. Shorter wavelengths, from γ-rays to microwaves, come mostly from regions containing dense matter associated with the visible Sun as we know it – the photosphere and chromosphere – and longer wavelengths come mainly from interplanetary space. Metre waves alone are generated in the tenuous coronal plasma (ordinarily visible only at the time of a total eclipse), and they reveal a spectacular range of phenomena undreamt of before their discovery.

In general, one can classify the types of disturbances in the solar corona that give rise to radio signatures into two catagories : charged particle beams (predominantly electron beams) and shock waves. But these two are not really independent since one requires low frequency turbulence to accelerate particles and the energy of the low frequency turbulence has to be transferred through some resonant wave particle interaction to the electrons. As the generated radio waves have to propagate through the corona before reaching us they should have sufficiently high frequency so that the plasma on their path will be transparent. Therefore the shock should produce sufficiently high frequency plasma waves. Otherwise the shock generated low frequency turbulence has to accelerate particles which in turn can release their energy to high frequency waves from which one expects radio wave generation.

As the density, temperature, magnetic field etc change continuously outward, these changes are also reflected in the radio emission. Identification of the signature of such changes helps us to determine the inhomogeneity characteristics of the corona. For example the slope of the dynamic spectrum of the radio waves gives information about the speed of the disturbance responsible for the emission and the density variation of the corona. In some case it can be related to the magnetic field variations, and this depends upon the actual emission mechanism.

Of the various types of radio emission the type I noise

storm is very special in the sense that it is seldom associated with flares. The active regions in which noise storm sources are located, are not conducive to flares. The mild shocks which develop out of magnetic pulses generated by newly emerging magnetic flux are recently proposed to be responsible for the Type-I emission (Spicer et al 1981) and this theory is under current development (Wentzel 1981, 1982, Gopalswamy and Thejappa, 1985). This theory needs low frequency turbulence to accelerate electrons and to interact with high frequency turbulence generated by these accelerated electrons in order that radio emission occurs. In the literature lower hybrid turbulence is proposed as the low frequency turbulence. We have investigated this problem and found that the ion-sound turbulence could be a better alternative to the lower hybrid turbulence. We support this claim by bringing in a suitable acceleration mechanism and the effectiveness of the resonant three wave interaction. Coronal magnetic fields can be estimated if a realistic model is used to interpret the radio data. On the basis of data from many sources including radio data, Tanstrom and Benz (1978) and Dulk and McLean (1978) derived an empirical formula for the radial dependence of coronal magnetic field. They had left out the type I radio data basically because, the theory of type I emission was not clear at that time. Since the type I theory is fairly clear now, we collected the data of type I chains from literature and used the emerging flux theory to estimate the coronal magnetic fields and derived an empirical relation. Our values are smaller than those of

Dulk and McLean (1978), which is quite natural because the type I emission originates from mild active regions where the magnetic field will be less compared to the active regions responsible for other radio bursts as they are flare associated. The modification of the emerging flux theory and the estimation of coronal magnetic field using this theory are dealt with in chapter II in detail.

The outer corona can be studied using radio telescopes, operating at low frequencies as the local plasma frequency in the outer corona lies in the low frequency range. The Gauribidanur radio telescope operates around 35 MHz and is being used to study many interesting features in decametric radio emission. In chapter III we consider two features that have been recorded by this telescope. First one discusses the fine structures in the observed type III bursts which provide valuable information regarding various damping processes for the excited Langmuir waves that get converted into radiation and the electron beam injection mechanism. The second one deals with absorption features produced in the decametric continuum. From the observational characteristics we have interpreted it as the effect of a "Screen" of ion-sound turbulence generated by a laterally moving shock which absorbs the continuum radiation as it propagates. The requirements to be fulfilled by the ion-sound turbulence in order to produce the observed emission are discussed.

The drift pair bursts are still enigmatic to the solar radio

astronomers. Although they have been observed quite some time ago (Roberts, 1958), they are still not fully understood. We collected data using the Gauribidanur radio telescope as well as the swept frequency spectrograph at Nancay (Boischot et al 1980). Analysis of this data has brought out many new features such as DPs with very large drift rate and the chains of drift pairs, which may provide important clues to the understanding of these DPs. From the frequency drift characteristics we are led to the conclusion that the movement of a physical agency cannot cause the observed drift rates. We propose that the drift has to be determined by the characteristics of the medium. We derive the functional behaviour of the magnetic field and the density in the DP active regions. We critically review the existing theories of DPs and provide a basis for further development of the theory of DP bursts in Chapter IV.

In chapter II, we dealt with weak shocks causing type I emission. The type II emission is also attributed to the shocks but they are relatively strong. We propose in chapter V that the majority of the shocks responsible for type II bursts are supercritical. In such shocks, the ion reflection becomes an important dissipation mechanism.

The reflected ions which act like a beam in the foot and ramp of the shock front and like a ring just behind the overshoot excite low frequency turbulence with an anisotropy

in the phase velocities i.e., the phase velocity of the waves parallel to magnetic field is much greater than perpendicular to the magnetic field. Therefore the magnetized ambient electrons quickly absorb these waves which leads to the formation of non-Maxwellian electron tails both in the upstream as well as in the downstream. We derive the distribution functions for these accelerated electron beams. These hot electrons in turn, drive high frequency Langmuir oscillations with $\omega \approx \omega_{pe}$ upto very high level $W_L/_{n_o T_e} \approx 10^{-5}$ - 10^{-4} in the ambient cold plasma both in the upstream and downstream. The conversion of plasma waves into electromagnetic waves is caused by the induced scattering of plasma waves off ions ($\omega \approx \omega_{pe}$) or by Coalescence of two Langmuir waves ($\omega \approx 2\omega_{pe}$). The role of nonlinear processes is also studied. The brightness temperature calculated from the theory, $T_b \approx 10^{11}$ K appears to be in very good agreement with observations. The observed frequency splitting will be determined by the jump in plasma frequency (due to density Jump) across the shock. The difference in the brightness temperatures in the upper and lower frequency bands also is explained by this model. Therefore we present a self consistent theory of the Type II radio bursts which includes the acceleration process, radio emission, the frequency splitting, and the unequal brightness in the upper and lower bands.

In the concluding chapter VI, we summarise our results and highlight the main conclusions. We also critically evaluate our work and suggest necessary work to be carried out both in theory and observations.

CHAPTER II

EXCITATION OF THE ION-SOUND TURBULENCE IN THE COLLI-

SIONLESS SHOCK WAVES AND TYPE I RADIO BURSTS.

ESTIMATION OF CORONAL MAGNETIC FIELDS USING TYPE I

- CHAIN DATA

2.1 Introduction

Historically, Hey (1942) was first to recognize the sun spot association noise storms from the Sun. On the radio spectrograph the type I storm consists of many shortlived, narrow-band bursts scattered at random across the frequency-time plane. Occasionally the bursts appear in chains which drift slowly to higher or lower frequencies. The bursts are sometimes superimposed on a background continuum of emission. The low-frequency edge of such storms may be anywhere from about 150 MHz down to about 50 MHz. A typical example of the type I storm is given in the fig.2.1. Except near the limb the radiation is generally strongly circularly polarized in the sense of the ordinary mode (Le Squeren 1963). The observed polarization and heights are generally taken as evidence that the emission process is a plasma process at or near the local plasma frequency. The low frequency type III component of noise storms indicates the escape of electrons from the source region, and it is often assumed that before the electrons escape they play a role in the type I emission process also (Aubier et al 1978). The evidence presented by Duncan (1981) lends support to this idea.
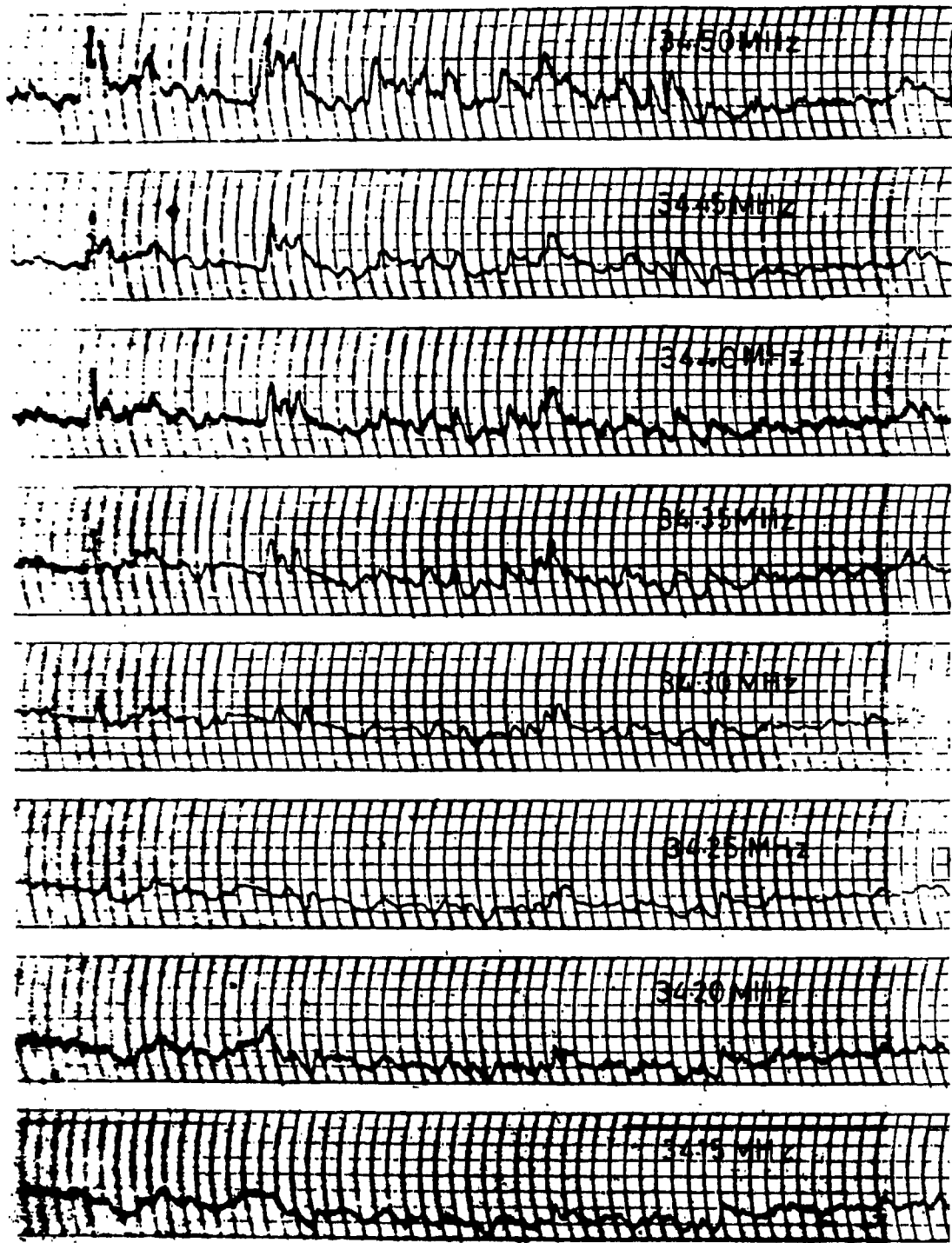
Fig. 2.1. An example of type I noise storms recorded using
Gauribidanur Radio Telescope.

Observations of noise storm characteristics have been extensively reviewed by Kundu (1965) and Elgaroy (1977). Although the type I storms are historically the first class of radio bursts that was identified, they are today among the least known manifestations of solar radio emission. Despite their connection with large sunspots on the solar disk, they seem to be entirely coronal phenomenon.

The frequency drifts associated with groups of type I bursts (chains) are attributable to weak shocks. The absence of second harmonic radiation and the narrow bandedness of the type I bursts show that the shocks responsible for type I storms are slightly super Alfvenic. Zaitsev and Fomichev (1973) were first to suggest that type I bursts are due to the currents driven perpendicular to an ambient magnetic field by a shock without identifying the free energy that drives the shock. They have also assumed that $\frac{\omega_{pe}}{\Omega_e} \ll 1$ where ω_{p_e} and Ω_e are the plasma and cyclotron frequencies respectively and Alfven Mach number $M_A \simeq 1.5$, which are as strong as flare assocaited shocks. The shocks causing type I emission therefore correspond to evolving active regions in a quasi-stationary corona where the magnetic field and density are not conducive for flares. The inequality $\omega_{p_e}^2 \ll \Omega_e^2$ can satisfy only at frequencies much higher than 300 MHz, which is in the cut off range for type I bursts (Melrose, 1982). The transition between type I sotrms to type III storms Indicates that the trapped particles in the closed magnetic field are responsible for type I storms (Aubier et al 1978). Wentzel

(1981) proposed that the interaction of upper hybrid (UH) waves generated by the loss cone distribution of electrons trapped in the closed magnetic fields with the lower hybrid (LH) waves generated by a shock wave gives rise to type I emission. Spicer et al (1981) identified the newly emerging magnetic flux as the agency which drives the shocks perpendicular to the magnetic field. They also estimate the LH turbulence level in the perpendicular shocks, which stochastically accelerates the electrons, which in turn generate UH waves, once they develop a loss cone. The interaction between UH and LH waves gives rise to the radiation. The chain is produced when the shock moves out in the corona producing bursts at various places where the resonance conditions are satisfied. The bursts could be generated intermittently due to the random weakening or strengthening of the shock (Spicer et al 1981) because of fluctuations in the corona (Yakobalev, 1980) or due to the fact that emissions occur at those places in the corona where the plasma frequency matches with integral multiples of the UH frequency during the lifetime of the shock (Wentzel, 1981).

Ion-Acoustic turbulence as another alternative low frequency turbulence to interact with higher frequency electrostatic waves was proposed by many authors (Melrose, 1977 Benz and Wentzel, 1981, Malara et al, 1985). According to Benz and Wentzel (1981), ion-sound turbulence is generated by parallel currents due to coronal evolution. Then the slope of the chains in the dynamic spectrum cannot be explained by such a model. In the emerging

flux theory of Spicer et al (1981) the perpendicular currents due to shock gradients feed the LH waves. We propose here that ion-sound waves can be generated by the perpendicular currents and these IS waves can interact with the UH waves to generate the Type I radiation.

2. Ion-sound turbulence due to shock gradients in collisionless plasma

The generation of ion-sound turbulence is an interesting problem both in laboratory and in the astrophysical contexts (Kaplan and Tsytovich, 1973). The ion-sound instability is generated when the relative velocity between the ions and electrons in a plasma exceeds the ion-sound velocity. The growth of ion-sound waves, therefore, depends upon the drift current present in the plasma. When shock waves propagate through a magnetized plasma the shock gradients generate currents perpendicular to the magnetic field. These currents generate ion-sound waves propagating perpendicular to the magnetic field. In non-isothermal plasmas, the generation is very efficient. Even in isothermal plasmas, ion-sound waves can be generated with a high energy density, provided the Buneman instability generated in the front of the shock heats the electrons differentially so that non-isothermality is generated (Galeev, 1976; Kaplan and Tsytovich, 1973).

In this section we derive the expression for the growth rate of the ion sound waves generated by shock gradients and the energy density of the ion sound (IS) turbulence saturated

by quasilinear effect. We compare the energy density of the lower hybrid (LH) turbulence with that of IS turbulence generated under similar conditions and show that the IS turbulence grow to higher levels. We also show that IS turbulence could be a better candidate for the low frequency turbulence needed to generate type I solar radio bursts.

2.2 Dispersion relation for ion-sound waves generated by
shock waves

We consider a collisionless shock wave propagating perpendicular (in the x-direction) to the magnetic field in the z direction. Since the ion Larmor radius exceeds the shock thickness, ions are treated as unmagnetised. The electrons gyrate many times in the magnetic field in the shock transit time and hence they are magnetised. In the shock frame, the density and magnetic field gradients are in the x-direction. As the electrons are decelerated in the x-direction due to induction and the ions are unaffected, there is a net charge separation in the shock-front so that an electric field E_x arises.

By assuming $\vec{B} = \hat{e}_z B_0 (1 - \epsilon_B x)$ represents the magnetic field in the neighbourhood of a point of inflection in the wave (where $B = B_0$, $V_x = U_0$ etc), we get:

$$\frac{\partial B}{\partial x} = - B_0 \epsilon_B = - \frac{4\pi n e V_{ye}}{c} \tag{2.1}$$

But in the above field configuration, $\dot{E}_x$ in the magnetosonic wave is given by

$$E_x = -\frac{B_o}{c} v_{ye} \qquad (2.2)$$

Therefore we obtain:

$$E_x = -\frac{\varepsilon_B B_o^2}{4\pi n e} \qquad (2.3)$$

where

$$\varepsilon_B = \frac{d(\ln B_o)}{dx} \qquad (2.4)$$

is the magnetic field gradient, B_o is the ambinet magnetic field at x = 0, n and -e are the density and charge of the electrons. This electric field gives rise to a cross-field drift given by

$$V_E = -\frac{c E_x}{B_o} = \frac{c B_o}{4\pi n e} \varepsilon_B \qquad (2.5)$$

The gradients in density and magnetic field give rise to the drifts

$$V_n = \frac{\varepsilon_n v_e^2}{\Omega_e} \qquad (2.6)$$

and

$$V_B = \frac{\varepsilon_B v_\perp^2}{\Omega_e} \qquad (2.7)$$

where $\varepsilon_n = \frac{d(\ln n)}{dx}$ is the gradient in density, $\Omega_e = \frac{e B_o}{m_e c}$

is the electron cyclotron frequency, V_e is the electron thermal velocity, m_e is the electron mass and c is the velocity of light in free space.

We are interested in solving the Valsov-Poisson equations to obtain the linear dispersion relation. The equilibrium distribution function can be obtained in terms of the following integrals of motion:

$$W_T = \frac{1}{2} m v^2 - F x \quad \text{(total energy)} \tag{2.8}$$

$$P_y = m v_y - \frac{e}{c} \int B_o(x)\, dx, \text{(y-momentum)} \tag{2.9}$$

$$P_z = m V_z \quad \text{(z-momentum)} \tag{2.10}$$

Here F is the force due to the charge separation electric field:

$$F = -e\, E_x \tag{2.11}$$

The simplest equilibrium which reduces to a Maxwellian in the absence of inhomogeneities may be given as,

$$f_{oe}(x,\vec{v}) = \left(\frac{m_e}{2\pi T_e}\right)^{3/2} \left[1 + \alpha\left(x - \frac{v_y}{\Omega_e}\right)\right] \exp\left[-\frac{m_e v^2}{2 T_e} - F x\right] \tag{2.12}$$

where T_e is the electron temperature and α is the parameter characterizing the spatial variation. It is related to the density gradient by the relation,

$$\varepsilon_n = \alpha + \frac{F}{T_e} \tag{2.13}$$

The perturbation of such an equilibrium can be described by the linearized Vlasov equation:

$$\frac{\partial f_1}{\partial t} + \vec{v} \cdot \frac{\partial f_1}{\partial \vec{x}} - \frac{e}{m} \left[\frac{\vec{v} \times \vec{B_0}(\vec{x})}{c} - \frac{F}{e}\vec{e_x} \right] \cdot \frac{\partial f_1}{\partial \vec{v}} = \qquad (2.14)$$
$$= -\frac{e}{m} \vec{\nabla}\varphi(\vec{x},t) \cdot \frac{\partial f_{oe}}{\partial \vec{v}}$$

where

$$f_1 \left(\vec{x}, \vec{v}, t \right) = f_e \left(\vec{x}, \vec{v}, t \right) - f_{oe} \left(x, \vec{v} \right) \qquad (2.15)$$

is the perturbed distribution function and $\varphi(\vec{x}, t)$ is the perturbed potential. Equation (2.14) can be solved using the method of characteristics (see e.g. Krall and Trivelpiece 1973). The characteristics are

$$\frac{d\vec{x}}{dt} = \vec{v}$$
$$\frac{d\vec{v}}{dt} = -\Omega_e \left(1 - \varepsilon_B x \right) \vec{v} \times \hat{e_z} + \frac{F}{m_e}\hat{e_z} \qquad (2.16)$$

where we have assumed the magnetic field variation in the form,

$$B_o (x) = B_o \left(1 - \varepsilon_B x \right) \qquad (2.17)$$

The particle trajectories $\vec{x}'$, $\vec{v}'$ which arrive at $\vec{x}$, $\vec{v}$ when $t' \to t$ can be obtained from (2.16) as,

$$v_x' = v_\perp \cos\left[\theta + \Omega_e (t'-t)\right] + v_E \sin \Omega_e (t'-t)$$

$$v_y' = v_\perp \sin\left[\theta + \Omega_e (t'-t)\right] - v_E \left[\cos \Omega_e(t'-t) - 1\right] - v_B$$

$$v_z' = v_z$$

$$(2.18)$$

and

$$x' = x + \frac{V_\perp}{\Omega_e}\left\{\sin\left[\Theta + \Omega_e(t'-t)\right] - \sin\Theta\right\}$$
$$+ \frac{V_E}{c}\left\{1 - \cos\Omega_e(t'-t)\right\}$$

$$y' = y - \frac{V_\perp}{\Omega_e}\left\{\cos\left[\Theta + \Omega_e(t'-t)\right] - \cos\Theta\right\}$$
$$- \frac{V_E}{\Omega_e}\sin\Omega_e(t'-t) + V_E(t'-t) - V_B(t'-t)$$

$$z' = z + V_z(t'-t)$$

$$(2.19)$$

Here, $V_x = V_\perp \cos\Theta$, $V_y = V_\perp \sin\Theta$. We have neglected terms of order ϵ_B^2, under the assumption of weak spatial gradient. Equation (2.14) can be formally integrated as

$$f_1(\vec{x}, \vec{v}, t) = -\frac{e}{m}\int_{-\infty}^{t} dt' \, \nabla\varphi(\vec{x}', t') \cdot \frac{\partial f_{oe}(x', \vec{v}')}{\partial \vec{v}'}$$

$$(2.20)$$

Taking

$$\varphi(\vec{x}, t) = \varphi(x) \, e^{i k_y y + i k_z z - i\omega t}$$

$$(2.21)$$

and assuming that the local approximation (Krall, 1968) is valid (i.e., $\varphi(x) = \varphi(o)$) one can perform the integration in (2.20) with the aid of (2.18) and (2.19). The result is

$$f_1^{(e)} = \varphi(o)\frac{e}{T_e} f_{oe}(x, \vec{v}) \cdot$$
$$\cdot \left[1 - (\omega - \omega^*)\sum_{P,\ell} \frac{J_P\left(\frac{k_y V_\perp}{\Omega_e}\right) J_\ell\left(\frac{k_y V_\perp}{\Omega_e}\right)\exp(i(P-\ell)\Theta)}{(\omega - k_y V_E + k_y V_B - P\Omega_e)}\right] \quad (2.22)$$

where $\quad \omega^* = k_y V_E - k_y V_n$

Since the ions are unmagnetised, their distribution is simple:

$$f_1^{(i)} = -\frac{e}{m_i} \varphi(o) \frac{\vec{k} \cdot \frac{\partial f_{oi}}{\partial \vec{v}}}{(\omega - \vec{k} \cdot \vec{v})} \tag{2.23}$$

where

$$f_{oi} = n_o \left(\frac{m_i}{2\pi T_i}\right)^{3/2} \exp\left[-\frac{m_i v^2}{2 T_i}\right] \quad , \tag{2.24}$$

T_i, m_i being ion temperature and ion mass respectively. Substituting (2.22) and (2.23) in the Poisson's equation,

$$-\nabla^2 \varphi = 4\pi e \int d^3\vec{v} \left[f_1^{(i)} - f_1^{(e)}\right] \quad , \tag{2.25}$$

one can eliminate $\varphi(o)$ to get the dispersion relation,

$$D(x=o, k, \omega) = 1 + \chi_i + \chi_e = 0 \quad , \tag{2.26}$$

where

$$\chi_i = \frac{k_i^2}{k^2} W\left(\frac{\omega}{k v_i}\right) \tag{2.27}$$

and

$$\mathcal{X}_e = \frac{k_e^2}{k^2} \left\{ 1 + \frac{m_e}{T_e} \left(\frac{m_e}{2\pi T_e} \right)^{1/2} \int_0^\infty V_\perp dV_\perp \int_{-\infty}^\infty dV_z \cdot \right.$$

$$\left. \cdot \sum_P \frac{(\omega - \omega^*) J_P^2 \left(\frac{k_y V_\perp}{\Omega_e} \right)}{(\omega - k_y V_E + k_y V_B - k_z V_z + P\Omega_e)} \exp\left(-\frac{V_\perp^2 + V_z^2}{2 V_e^2} \right) \right\}$$

(2.28)

where k_α and V_α are the Debye wave number and thermal velocity of species α ($= e, i$). The W-function is defined as

$$W(z) = \frac{1}{\sqrt{2\pi}} \int_{-\infty}^\infty \frac{x\, e^{-x^2/2}\, dx}{x - z}$$

(2.29)

We consider the range of frequencies $k_y V_i < \omega < \Omega_e$. In this range, one can neglect terms of order $\omega / P\Omega_e$, $P = \pm 1, \pm 2,$ and expand $W\left(\omega / k_y V_i \right)$ asymptotically. From the Rankine-Hugoniot relations, we note that the jump in magnetic field and density across a laminar shock are of the same order. Defining an average gradient-B drift, $\overline{V}_B = \frac{\mathcal{E}_B V_\perp^2}{\Omega_e} \approx \frac{\mathcal{E}_n V_e^2}{\Omega_e}$, We find that $\overline{V}_B \sim V_n$. Hence we get

$$\frac{\omega - k_y V_E + k_y V_n}{\omega - k_y V_E + k_y \overline{V}_B} \simeq 1$$

(2.30)

With further assumption that $k_y V_e > \Omega_e$ and $\frac{k_z}{k_y} > V_E/V_e$ we can solve the dispersion relation (2.26) to get the frequency ω_γ and growth rate $\gamma \left(\omega = \omega_\gamma + i \gamma ; \; \left| \frac{\gamma}{\omega_\gamma} \right| \ll 1 \right)$ as,

$$\omega_\gamma = \pm \frac{\omega_{p_i} \left(1 + 3 \, T_i/T_e \right)}{\cdot \left[1 + \frac{k_e^2}{k^2} \left(1 + \Lambda_0 \right) \right]^{1/2}} \qquad (2.31)$$

and

$$\frac{\gamma}{\omega_\gamma} = - \left(\frac{\pi}{8} \right)^{1/2} \frac{k_i^2}{k^2} \left(\frac{\omega_\gamma}{k_y V_i} \right) e^{- \omega_\gamma^2 / 2 k^2 V_i^2}$$

$$- \left(\frac{\pi}{2} \right) \frac{k_e^2}{k^2} \left(\frac{V_E}{\bar{V}_B} - \frac{\omega_\gamma}{k_y \bar{V}_B} - 1 \right) J_0^2 \left[\frac{k_y V_e}{\Omega_e} \left(2 \left(\frac{V_E}{\bar{V}_B} - \frac{\omega_\gamma}{k_y \bar{V}_B} \right) \right)^{1/2} \right] \cdot$$

$$\cdot \left(1 + \frac{k_z^2 V_e^2}{k_y^2 V_E^2} \right) \exp \left[- \frac{V_E}{\bar{V}_B} - \frac{\omega_\gamma}{k_y \bar{V}_B} + \frac{k_z^2 V_e^2}{k_y^2 V_E^2} \right]$$

$$(2.32)$$

where

$$k^2 = k_y^2 + k_z^2$$

Here

$$(2.33)$$

$$\Lambda_0 = I_0 \left(\frac{k_y^2 V_e^2}{\Omega_e^2} \right) \exp \left(- \frac{k_y^2 V_e^2}{\Omega_e^2} \right) \simeq \frac{1}{\sqrt{2\pi}} \frac{\Omega_e}{k_y V_e} \ll 1 \cdot \qquad (2.34)$$

The frequency of the waves given by (2.31) is nothing but the ion-sound frequency because $\Lambda_e < 1$ and $T_e \gg T_i$. The frequency can be written as

$$\omega_\gamma = \pm \frac{k c_s \left(1 + 3 T_i/T_e\right)}{\left[1 + \frac{k^2}{k_e^2}\left(1 - \Lambda_e\right)\right]^{1/2}}$$

(2.35)

where $c_s = \sqrt{T_e/m_i}$ is the ion sound velocity.

The first term in (2.32) is the ion-Landau damping. The second term is due to electron Landau damping and drifts. The mode with lower sign in (2.32) grows when

$$\frac{V_E}{V_B} + \frac{|\omega_\gamma|}{k_y V_B} > 1$$

(2.36)

Now, $\frac{V_E}{V_B} = \frac{2}{\beta} > 1$, and hence the instability criterion is easily satisfied provided the ion Landau damping is negligible. This is in fact so because of the condition $T_e \gg T_i$. Differentiating (2.32) with respect to k, we find that γ reaches a maximum value of $\sqrt{\frac{m_e}{m_i}} \Omega_e$ when $k \sim k_e$. When the wavenumber decreases, γ also decreases and $\gamma = \frac{1}{2} \sqrt{\frac{m_e}{m_i}} \Omega_e$ when $k \sim k_e \frac{\Omega_e}{\omega_{p_e}}$. Hence one can conclude that the maximum growing modes lie in the range, $\left[k_e \frac{\Omega_e}{\omega_{p_e}}, \; k_e \right]$

2.3 Quasilinear saturation of ion-sound instability

Once the ion-sound waves start growing, the electrons

in the resonance region start diffusing in velocity space due to quasilinear interaction. Therefore, the equilibrium distribution function of electrons changes slowly with time. Because of this, the energy density of the ion-sound waves saturates. The change in equilibrium distribution function can be found as

$$\frac{\partial f_o}{\partial t} = \left< \frac{c}{B_o^2} \left[\vec{\nabla}\varphi \times \vec{B_o} \right] \cdot \vec{\nabla} f_1 + \frac{e}{m_e} \frac{\partial \varphi}{\partial z} \frac{\partial f_1}{\partial v_z} \right>$$

(2.37)

where $\left< \cdots \right>$ denotes average over fast time scale. f_1 is the rapidly fluctuating part of the distribution and $f_o \gg |f_1|$. Calculating as in the linear case, we get

$$\frac{\partial f_o}{\partial t} = \frac{e^2}{m^2} \sum_k \left[k_z \frac{\partial}{\partial v_z} + 2\omega \frac{\partial}{\partial v_\perp^2} - k_y \frac{\partial}{\partial (v_y - \Omega_e x)} \right] J_o^2 \left(\frac{k_y v_\perp}{\Omega_e} \right) \cdot$$

$$\cdot \left[k_z \frac{\partial}{\partial v_z} + 2\omega \frac{\partial}{\partial v_\perp^2} - k_y \frac{\partial}{\partial (v_y - \Omega_e x)} \right] f_o \cdot$$

$$|\varphi|^2 \delta (\omega - k_y v_E + k_y v_B - k_z v_z)$$

(2.38)

The calculation is similar to that of Krall and Book (1969). But in our case the resonance region is determined by V_E rather than V_B. Since most of the waves propagate in a narrow cone around the direction of drift, we assume $k_z = 0$ and we get the effective collision frequency due to ion-sound turbulence as

$$\nu_{eff} = \frac{\int v_y \left(\frac{\partial f_o}{\partial t} \right) d^3\vec{v}}{\int v_y f_o \, d^3\vec{v}}$$

(2.39)

The change in the equilibrium function due to quasilinear effect, viz, $\frac{\partial f_o}{\partial t}$ is obtained from (2.38). This change is proportional to the energy density of IS waves which enters through the quasilinear diffusion coefficient. Evaluation of the integral (2.39) yields,

$$\gamma_{eff} = \left(\frac{m_e}{m_i}\right)^{1/2}\left(\frac{\beta}{2}\right)\left(\frac{\Omega_e \, \omega_{Pe}^2}{c^2 \, \epsilon_B^2}\right)\left(1+\ell n \frac{\omega_{Pe}^2}{\Omega_e^2}\right)\frac{W_s}{nT_e}$$

(2.40)

where $W_s = \sum_{k} k^2 |\varphi|^2$ the energy density of the ion-sound waves.

We can take the scale length of magnetic field variation in the shock as

$$\epsilon_B \simeq \frac{\Delta B}{B_o} L_s^{-1}$$

(2.41)

where $\Delta B = \left(B_2 - B_1\right)$ is the jump in magnetic field (see Fig.2) across the shock and L_s is the shock thickness. Putting this in the marginal stability case of (2.36) viz,

$$\frac{2}{\beta} - \frac{c_s}{V_e^2} \frac{\Omega_e}{\epsilon_B} = 1$$

(2.42)

we get an expression for the shock thickness L_s:

$$L_s = \left(\frac{\Delta B}{B_o}\right)\left(\frac{2}{\beta} - 1\right)\frac{V_e^2}{\Omega_e c_s}$$

(2.43)

The shock thickness is also related to the effective collision frequency due to the instability generated in the shock by (Spicer et. al., 1981)

$$ L_s = \frac{\vartheta_{eff}\, c^2}{\omega_{p_e}^2\, V_A} \quad \frac{M_A}{M_A^2 - 1} $$

$$(2.44)$$

where $M_A = V_1 / V_A$ is the Alfvenic Mach number,

$V_A = B_o / \sqrt{4\pi n m_i}$ is the downstream Alfven velocity and

V_1 is the velocity of the shock. Relations (2.43) and (2.44) can be used along with (2.40) to find

$$ \frac{W_s}{n T_e} = \frac{\left(\frac{m_i}{m_e}\right)^{1/2} \frac{\Delta B}{B_o}\, \frac{C_s V_A}{V_e^2} \left(\frac{M_A^2 - 1}{M_A}\right)\, \frac{2}{2-\beta}}{\left[\, 1 + \ln\, \frac{\omega_{p_e}^2}{\Omega_e^2}\, \right]} \cdot $$

$$(2.45)$$

The above expression indicates that the energy density of the ion-sound turbulence depends upon the jump in magnetic field ΔB, the electron temperature T_e, the Alfvenic Mach number M_A, the coronal plasma β and the ratio of the plasma frequency ω_{pe} to the electron cyclotron frequency Ω_e.

2.4 Comparison with lower hybrid turbulence

For weak shock waves, the energy density of the LH turbulence has been calculated by Spicer et. al. (1981) as

$$\frac{W_{LH}}{n T_e} = \sqrt{\frac{m_e}{m_i}} \quad \frac{\Omega_e^2}{\omega_{Pe}^2} \frac{V_A}{c_s} \frac{\Delta B}{B_0} \frac{M_A^2 - 1}{M_A}$$

(2.46)

comparing the expressions (2.46) and (2.45) one gets

$$\frac{W_{LH}}{W_S} = \frac{\Omega_e^2}{\omega_{Pe}^2} \left(1 - \frac{1}{2} \beta \right) \left(1 + \ell_n \frac{\omega_{Pe}^2}{\Omega_e^2} \right)$$

(2.47)

In most of the plasmas of interest, $\Omega_e^2/\omega_{Pe}^2 \ll 1$ and hence the LH turbulence saturates at a lower level compared to the IS turbulence. The other factors in equation (2.45) are not important. In the coronal region where type-I bursts occur, say 100 MHz level, the magnetic field is $\sim$ 1 G (Gopalswamy et. al. 1984), which corresponds to a cyclotron frequency of 2.8 MHz. Then the ratio $\Omega_e^2/\omega_{Pe}^2 \sim$ 2.8 x 10^{-2} and hence $\frac{W_{LH}}{W_S} \sim$ 4.5 x 10^{-3}. Under such circumstances, clearly, IS turbulence is important.

Though we have compared the LH and IS turbulences under identical conditions, one should note that we have assumed $T_e \gg T_i$. The solar corona is usually isothermal ($T_e \approx T_i$) under which case the Landau damping for the IS waves will be dominant. But it has been pointed out (Galeev, 1976; Tidman and Krall, 1971) that a variety of instabilities are excited at the shock

front and most of them essentially heat the electrons and quenched at the initial portion of the shock front itself. Deeper into the shock, the condition $T_e > T_i$ is established and IS waves grow and these waves determine the structure of the shock wave by limiting the perpendicular current, quasilinearly. The situation is explained in Fig.2.2. The Buneman instability is first to occur with $V_E \sim V_e$ near the front of the shock which heats the electrons and increases T_e/T_i . Deeper into the shock $V_E < V_e$, and the Buneman instability is quenched whereas IS instability is excited. In fact, the magnetic field gradient ε_B needed for generating the Buneman instability can be obtained as

$$ V_E \simeq \frac{c\, B_0}{4\pi n e} \qquad \varepsilon_B = V_e $$

$$ \varepsilon_B \simeq 7.8 \times 10^{-3}\ cm^{-1} $$

<div align="right">(2.48)</div>

For IS waves, $\varepsilon_B \simeq 1.8 \times 10^{-4}\ cm^{-1}$.

This means the density gradient at the initial portion should be 43 times more than that in the interior. This will be satisfied in the shock configuration assumed by Vlahos et. al. (1982). Moreover, Møller-Pederson et. al. (1977) have concluded that whatever be the initial value of T_e/T_i, ultimately IS turbulence will be generated.

Now, let us consider the generation of type-I radio bursts. Basically we need high frequency waves to coalesce with low frequency waves to produce electromagnetic radiation as type-I radio bursts. The generation of these waves must be due to
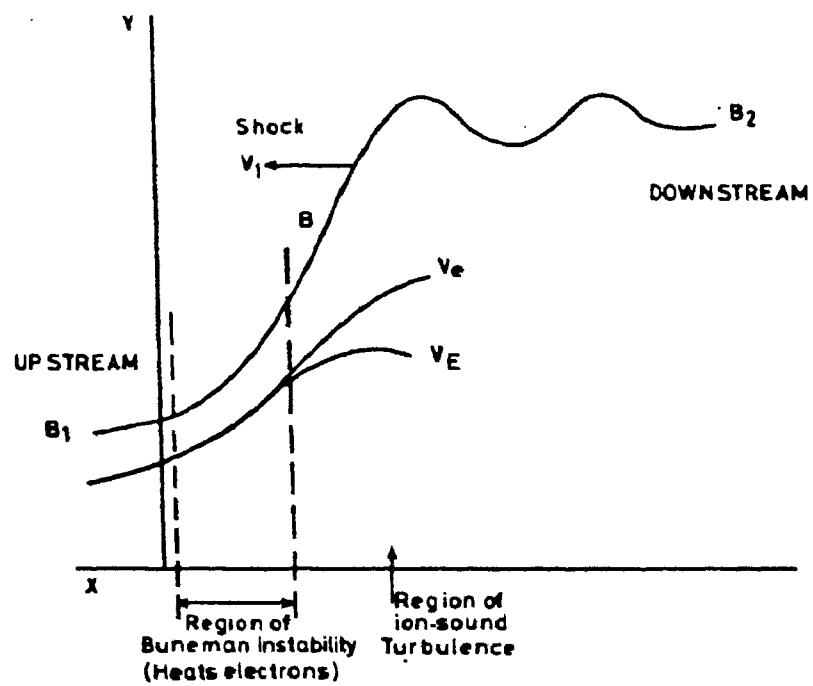
Fig. 2.2. The profiles of B, V_e and V_E at various portions of the shock; the regions of ion-sound and Buneman instabilities are also indicated.

some agency moving through the corona. The small drift rate of type-I chains indicates that the agency must be a weak shock. The weak shock, therefore, should generate both high and low frequency turbulence. In the emerging flux theory of Spicer et. al. (1981), the high frequency waves are UH waves generated by energetic electrons stochastically accelerated by LH waves. We argue that the IS turbulence is a plausible candidate for the low frequency waves because of their higher level of saturation energy and the larger width in wave number space so that the resonance conditions for the interaction with high frequency turbulence is easily satisfied. We consider these points in detail below.

2.5 Energy requirement of low frequency waves

For the UH waves to provide adequate brightness temperature, the low frequency waves should have an energy density,

$$\frac{W^{\sigma}}{nT_e} \gtrsim \frac{6\sqrt{3}}{\pi} \frac{V_e \, c}{\omega_{p_e} L_N \, V_{\varphi}^{\sigma}}$$

(2.49)

where σ represents any suitable low frequency waves that interact with the UH waves to produce the radiation; L_N is the scale height of coronal electron density variation and V_{φ}^{σ} is the phase velocity of the low frequency waves. For a coronal plasma frequency of 100 MHz, $L_N \approx 10^{10}$ cm. For typical phase velocities of the low frequency waves in the million degree

corona, one gets from (2.49)

$$\frac{W^{\sigma}}{n T_e} \gtrsim 1 \cdot 3 \times 10^{-6}$$

<div align="right">(2.50))</div>

This condition is satisfied only marginally by the LH waves whereas the energy density of IS waves is much larger than the limit (2.50) as is evident from the discussion in section (2.4).

2.6   Acceleration of electrons to generate high frequency waves

Now, the low frequency turbulence should generate energetic electrons. The energetic electrons should develop a loss cone distribution to generate the necessary high frequency waves. The LH waves can stochastically accelerate the electrons to high energies while the IS waves cannot (Lampe and Papadopoulos, 1977; Kaplan et. al., 1974). But there is another efficient process by which the IS waves can produce energetic particles with a loss cone distribution in order to generate UH waves. Whistler waves and IS waves have the same range of frequencies. Hence, the IS waves can get converted into whistler waves through non-linear scattering from the ions and electrons. The characteristic time of conversion is :

$$\tau_s = \frac{20}{\beta} \left(\frac{W_s}{n T_e} \right)^{-1} \Omega_e^{-1}$$

<div align="right">(2.51)</div>

where $\beta = \dfrac{8 \pi n T}{B_0^2}$ and Ω_e is the electron cyclotron frequency.

These whistlers have electric field normal to the magnetic field and hence increase the transverse energy of the electrons as they are absorbed by the electrons. Once the transverse velocity of the particle exceeds certain threshold value determined by the mirror ratio, the electrons are trapped. The characteristic time over which this trapping occurs is :

$$\tau_h = \frac{6}{\pi} \left(\frac{\omega_{pe}}{\Omega_e} \right) \left(\frac{V_h}{V_e} \right)^2 \left(\frac{W_w}{n T_e} \right)^{-1} \Omega_e^{-1}$$

(2.52)

where W_w is the energy density of whistler waves. For a V_h (velocity of the heated electron due to whistler absorption) of $\sim 7 \cdot V_e$ and $W_w \simeq 0.5\ W_s$ one gets $\tau_{scatter} \sim 0.01$ s and $\tau_{heat} \sim 0.5$ s. Both these time scales are well within the collisional damping time (Kaplan and Tsytovich 1973).

$$\tau_{coll} = \left(\frac{T_i}{T_e} \right)^{3/2} \frac{N_D}{\omega_{pi}}$$

(2.53)

where

T_i, ω_{pi} -ion temperature and ion plasma frequency, N_D-Debye number $= n\ \lambda_D^3$, λ_D being electron Debye radius. Hence the ion sound turbulence provides an alternative mechanism to produce loss cone distribution of energetic electrons.

2.7 Overlap in wavenumber space

For the efficient interaction of the high and low frequency

waves, the following resonance conditions should be satisfied:

$$\vec{k}_L + \vec{k}_\sigma = \vec{k}_t$$

(2.54)

$$\omega_L + \omega_\sigma = \omega_t$$

(2.55)

where (k , ω) are the wave number and frequency, and L, σ , t represent the UH, low frequency and transverse waves respectively. Since $k_t \ll k_L, k_\sigma$ one needs $k_L \sim k_\sigma$. For maximum growing modes (Wentzel 1981),

$$k_L \simeq 2 k_e \left(\frac{V_e}{V_h} \right) ,$$

(2.56)

$$k_{LH} \leq k_e \left(\frac{\Omega_e}{\omega_{P_e}} \right)$$

(2.57)

and for the ion sound waves,

$$k_s \in \left[k_e \frac{\Omega_e}{\omega_{P_e}} , k_e \right]$$

(2.58)

Since $\frac{\Omega_e}{\omega_{P_e}} \ll 1$ for the coronal plasma level at 100 MHz, we see that there is a better overlap in the k-space in the case of IS waves compared to the LH waves. The equation (2.57) demands that V_h must be atleast 20 V_e to satisfy the resonance condition while moderate electron heating is sufficient in the case of ion sound wave because of its wider range of maximum growth.

It is clear from the above discussions that the IS turbulence excited by the weak shocks is more likely candidate for the generation of type-I bursts in the solar corona.

2.8   Estimation of coronal magnetic field using type I emission

The coronal magnetic fields can be estimated only indirectly from the various types of radio emissions emanating from different heights in the solar atmosphere.   Because of solar activity it is difficult to define an average magnetic field in the solar corona.   Like density and temperature, magnetic field also is enhanced in the active regions.   These parameters, moreover, vary from one active region to another.   The magnetic field also depends on the evolution of the active region in time. The estimation of magnetic field using a particular radiation applies only to that situation which gives rise to the radiation in question.   For example, if one estimates magnetic field using noise storm measurements, then the field corresponds to a slowly varying active sun.   If the magnetic field is derived using other radio bursts, like Type-II etc, then it corresponds to a fast changing active sun because of their close association with flares.

Using the properties of various radio emissions, Newkirk (1967, 1971) estimated the magnetic field strength, Dulk and McLean (1978) re-evaluated the sources of data and improved the estimates by eliminating those data which involved an interpretaion in terms of out moded, incorrect or inapplicable plasma

concepts. The radio emission based estimates included in the analysis of Dulk and McLean (1978) and Tanstorm and Benz (1978) correspond only to fast changing active regions because all these radio bursts are flare associated. The type-I bursts, which correspond to a slowly changing active region, are not used for magnetic field estimates mainly because the theories of these bursts were uncertain at that time.

Apart from slowly varying component, (Kakinuma and Swarup, 1962) the type-I storms are probably the only phenomena that could be used to estimate the magnetic field in the active regions in the absence of flares. The understanding of the type-I phenomenon has improved very much after the emerging flux theory of Spicer et al., (1981). A working model based on this theory has been proposed by Wentzel (1982). It is therefore worthwhile attempting the magnetic field estimation using type-I storms. This provides an opportunity to compare the estimates with those of Dulk and McLean (1978) who excluded estimates from type-I phenomena. Wild and Tlamicha (1964) made use of the spectral characteristics of type-I chains to estimate the coronal magnetic field. This was included in the compilation of Newkirk (1967, 1971). It was mentioned by Wild and Tlamicha (1964) that shock waves could generate the type-I bursts. They assumed that the velocity of the exciting disturbance to be the same as Alfven velocity and estimated the radial field. Actually the shock wave has super-Alfvenic velocity and therefore their estimate may correspond to the upper limit of the magnetic

fields. Takakura (1966) attempted to use the polarization proper-
ties of the type-I bursts to calculate the radial field which sets
a lower limit. The result was nearly 10 Gauss at 50 MHz which
is a very high value. This is basically because the theory used
by him has severe draw backs (Melrose, 1980). In this chapter
we derive the coronal magnetic fields at various heights based
on type-I chain observations assuming that the emission is at
local plasma frequency. The velocity of the shock, calculated
from the drift rate of the chains, and the density jump across
the shock, obtained from the observed bandwidth, are used as
the imput in the Rankine-Hugoniot relations and the magnetic
field is calculated.

One of the interesting features of the type-I bursts is
their narrow bandwidth, which implies that the density jump
across the shock must be only of the order of a few percent
of the ambient density (Spicer et al., 1981). Since $\Omega_e \ll \omega_{pe}$ the
emission is assumed to be at the local plasma frequency, the
bandwidth and relative density jump could be related as follows:

$$\omega_{pe}^2 = \frac{4\pi n e^2}{m} \tag{2.59}$$

$$\left| \frac{\Delta \omega}{\omega} \right| = \frac{1}{2} \frac{\Delta n}{n} \tag{2.60}$$

where n, e and m are the ambient density, charge and mass
of electrons and Δn is the density jump. As the bandwidth
of the type-I chains is very small, the shock travels only a small
distance in the corona compared to the coronal scale height.

Suppose the emission starts at a frequency f_1 corresponding to a plasma layer of density n_1 and the emission stops at the frequency f_2 corresponding to a layer with density n_2. Because of the closeness of the layers, the difference ($n_1 - n_2$) will be very small compared to the average density. When the shock reaches the n_2 layer, the n_1 layer will be within the shock wake as the shocked region takes a long time to relax to the equilibrium situation (Lampe and Papadopoules, 1977; Lacombe and Møller-Pederson, 1971) compared to the time taken for the shock to travel from the n_1 layer to the n_2 layer. Hence one can assume that the density remains almost same from immediately behind the shock to the starting layer. Therefore one can equate the density jump Δn across the shock to the difference ($n_1 - n_2$) and hence relate it to the bandwidth $\Delta f = f_1 - f_2$. (wentzel, 1981; Spicer et al 1981; Wentzel, 1982).

The chains of type-I bursts (Wild and Tlamicha, 1964, Hanasz, 1966, De Groot et al. 1976) have very small drift rates. Assuming a particular density model above the active regions, the observed drift rate can be converted into radial velocity V_1 of the agency (the shock) causing the bursts as follows:

$$V_1 = - \frac{df}{dt} \; \frac{1}{|\vec{\nabla} f_{p_e}|}$$

$$(2.61)$$

where $f_{p_e} = {}^{\omega}p_e / 2\pi$, $\frac{df}{dt}$ is the frequency drift and $\vec{\nabla} f_{p_e}$ is the gradient of the plasma frequency of the corona. Since $f_{p_e}^2 = \frac{n(\lambda) e^2}{\pi m}$, the radial velocity depends upon the assumed

density model. If we assume strictly perpendicular shocks, then V_1 corresponds to the upstream velocity. The density jump and the upstream shock velocity are related to the Alfven velocity and ion-sound velocity through the Rankine – Hugoniot (RH) relation (Tidman and Krall, 1971) as follows:

$$\frac{\Delta n}{n} = 1 - \frac{1}{8}\left[\frac{5\,c_s^2}{V_1^2} + 1 + \frac{5}{2}\frac{V_A^2}{V_1^2} + \left\{\left(\frac{5\,c_s^2}{V_1^2} + 1 + \frac{5}{2}\frac{V_A^2}{V_1^2}\right)^2 + 8\frac{V_A^2}{V_1^2}\right\}^{1/2}\right]$$

(2.62)

where

$$V_A = \frac{B}{\sqrt{4\pi n m_i}}$$

is the Alfven velocity, m_i is the ion mass, c_s is the ion sound velocity and B is the ambient magnetic field. If the coronal temperature is assumed to be constant ($T_e \approx 10^6 k$) then c_s is a constant. Knowing $\Delta n/n$ and V_1 from observations, V_A and hence the magnetic field can be estimated.

We used type-I chain data, covering the range from 250 to 46 MHz (De Groot, 1966; Karlicky and Jiricka, 1982; Wild and Tlamicha, 1964; Elgaroy and Ugland, 1970; Tlamicha, 1982; Aurass et al., 1982; and Aubier et al., 1978) which approximately lies between one and two solar radii. This is the region in which the noise storm activity is maximum. The shock velocity and the density jump are used in the RH relation (2.62) to get,

$$\frac{V_A^2}{V_1^2} = \frac{8\left(1 - \frac{\Delta n}{n}\right)^2 - 2\left(1 - \frac{\Delta n}{n}\right)\left(1 + 5\frac{c_s^2}{V_1^2}\right)}{1 + 5\left(1 - \frac{\Delta n}{n}\right)}$$

(2.63)

Those data which give negative values for the right hand side of the relation (2.63) have been excluded. In other words C_s, V_1 and $\frac{\Delta n}{n}$ must satisfy the following inequality:

$$5 \frac{c_s^2}{V_1^2} < 3 - 4 \frac{\Delta n}{n} \qquad (2.64)$$

The type-I bursts occur at the top of the closed magnetic fields according to the emerging flux theory as well as other observations (Krüger, 1977). Therefore the plasma beta must be less than untiy or, in other words, the Alfven velocity has to exceed the ion-sound velocity. Therefore, (2.64) becomes,

$$\left[\frac{5}{\left(3 - 4 \frac{\Delta n}{n} \right)} \right] c_s^2 < V_A^2 < V_1^2 \qquad (2.65)$$

where we have also included the requirement that the shock velocity V_1 must exceed the Alfven velocity for the shock to exist (Tidman and Krall, 1971). We have used the density model,

$$n(\rho) = 4.2 \, x \times 10^{4 + 4.32/\rho} \qquad (2.66)$$

where $\rho = \frac{\Lambda}{\Lambda_\odot}$ is the radial distance in units of solar radius $\Lambda_\odot$, x = 2 for Newkirk streamer model and x = 4 for 2 times Newkirk's streamer model. The quantities ρ and n are related by

$$\zeta = \frac{4 \cdot 975}{\ln \left(f_6 / 2 \cdot 583 \right)} \quad ; \quad x = 2$$

(2.67)

and

$$\zeta = \frac{4 \cdot 975}{\ln \left(f_6 / 3 \cdot 65 \right)} \quad ; \quad x = 4$$

(2.68)

where $f_6 = f_{pe}/10^6$ is the frequency in MHz. The corresponding shock velocities are,

$$V_1 = - \frac{3 \cdot 463 \times 10^6}{\left[\ln \left(f_6 / 2 \cdot 583 \right) \right]^2} \frac{1}{f_6} \frac{\partial f_6}{\partial t} \quad m \, s^{-1}$$

(2.69)

and

$$V_1 = - \frac{3 \cdot 463 \times 10^6}{\left[\ln \left(f_6 / 3 \cdot 65 \right) \right]^2} \frac{1}{f_6} \frac{\partial f_6}{\partial t} \quad m \, s^{-1}$$

(2.70)

Actually, the factor x can vary from 2 to 5 or even more for specific active regions. We have taken these two models to show that the magnetic field estimate is model dependent.

The derived values of coronal magnetic field strengths

are plotted in Figs. 2.3 and 2.4 for x = 2 and x = 4 respectively. Also plotted are the values obtained by assuming that the shock velocity is the same as the Alfven velocity. For the sake of comparison, we have shown the curve obtained by Dulk and McLean (1978), Viz

$$B = 0.5 \left(S - 1 \right)^{-1.5} \tag{2.71}$$

This curve is obtained using the results of many techniques for coronal field estimation. The magnetic field values obtained from the Type-I chain data are given in Table I. The values can be fitted by straight lines to get the following single parameter formulae:

$$\left. \begin{aligned} B &= 0.41 \left(S - 1 \right)^{-0.89} \qquad V_1 > V_A \\ B &= 0.57 \left(S - 1 \right)^{-0.94} \qquad V_1 = V_A \end{aligned} \right\} ; \quad x = 2 \tag{2.72}$$

and

$$\left. \begin{aligned} B &= 0.7 \left(S - 1 \right)^{-1.1} \qquad V_1 > V_A \\ B &= 0.89 \left(S - 1 \right)^{-0.92} \qquad V_1 = V_A \end{aligned} \right\} ; \quad x = 4$$

$$\tag{2.73}$$

The above curves are depicted in the figures (23), (24) and (25). It is clear from figs. (23) and (24) and also from Table I that the magnetic fields obtained by the method ($V_1 = V_A$) of Wild and Tlamicha (1964) are slightly more than the values
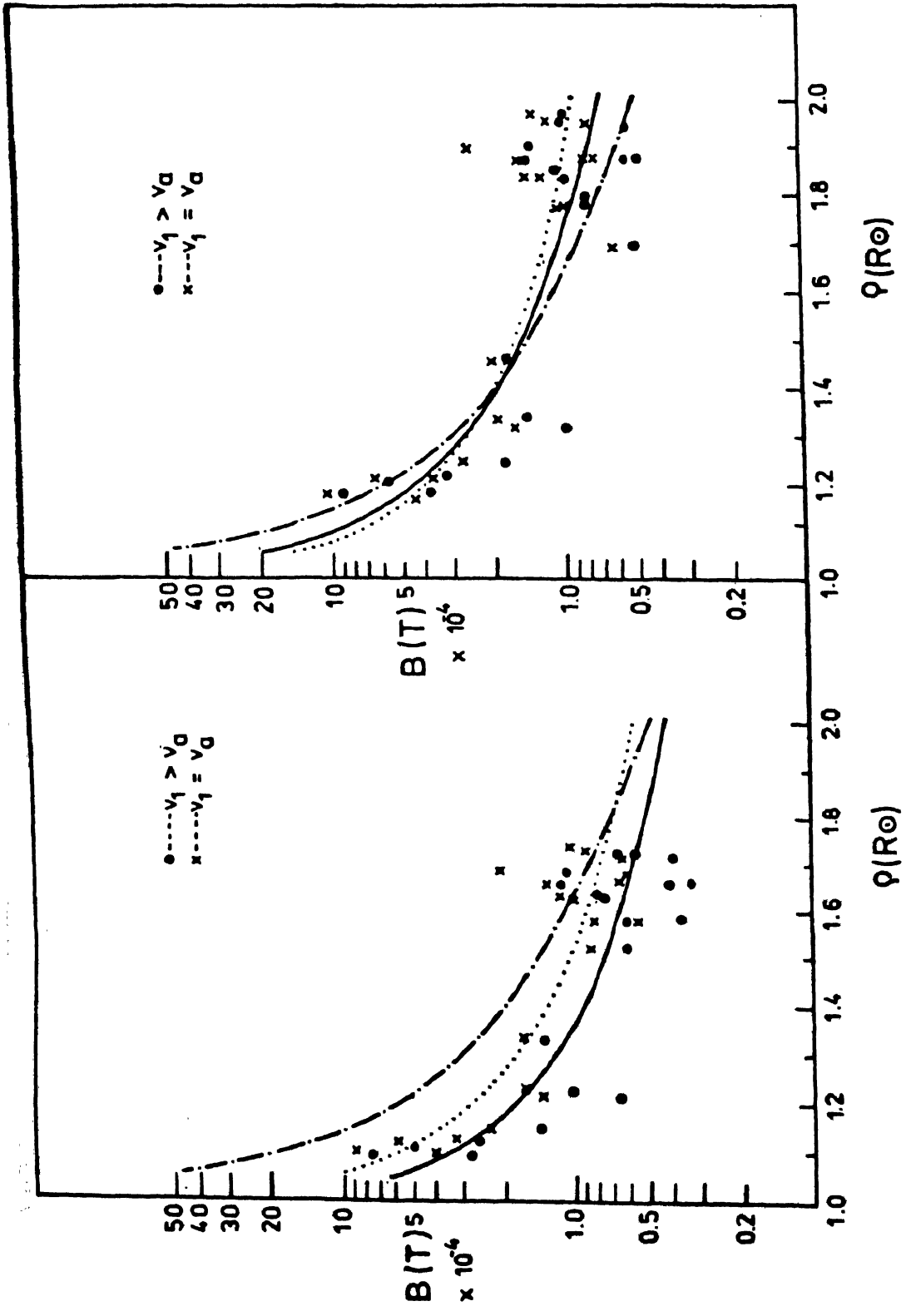
Fig.2.3. (for x = 2) : The magnetic field B, versus radial Fig. 2.4. (for x = 4): The magnetic field B. versus distance, (in units of solar radius $R_\odot$). The least radial distance, (in units of solar radius $R_\odot$). square fits for the $V_1 > V_A$ and $V_1 = V_A$ cases, The last square fits for the $V_1 > V_A$ and $V_1 = V_A$ are represented and..... respectively. The cases, are represented by ____ and ..... respectively. empirical fit of Dulk and McLean (1978) is respresen- The empirical fit of Dulk and McLean (1978) is ted by .--. represented by .--.

THE ESTIMATED MAGNETIC FIELDS FOR VARIOUS CASES

S.No.	Frequency (MHz)	x = 2 B (G) V V_A	x = 2 B (G) V = V_A	B (G) V = V_A	B (G) V = V_A	x = 4 B (G) V = V_A	B (G) V = V_A	References
1	250	1.09	7.510	8.444	1.177	8.960	10.02	De Groot (1966)
2	244.5	1.093	2.810	3.836	1.183	3.750	4.493	Karlicky and Jiricka
3	230	1.108	5.001	5.581	1.201	6.020	6.645	De Groot (1976)
4	219	1.121	2.630	3.157	1.215	3.250	3.766	"
5	197.5	1.147	1.410	2.298	1.247	1.820	2.710	Wild and Tlamicha (1964)
6	158.5	1.208	0.663	1.347	1.319	0.992	1.605	Karlicky and Jiricka (1982)
7	150	1.225	1.060	1.594	1.339	1.490	1.932	Elgaroy and Ugland (1970)
8	109	1.329	1.350	1.607	1.465	1.730	1.980	Tlamicha (1982)
9	68	1.520	0.613	0.843	1.700	0.525	0.620	Aurass et al., (1982)
10	60.5	1.578	0.618	0.820	1.772	0.830	1.036	Wild and Tlamicha (1964)
11	60	1.582	0.369	0.538	1.780	0.824	0.950	Aubier et al., (1978)
12	55	1.627	0.752	0.993	1.834	.990	1.263	Wild and Tlamicha (1964)

							Wild and Tlamicha (1964)
13	54.5	1.632	0.813	1.106	1.840	1.070	1.409	
14	52.25	1.654	1.125	1.222	1.869	1.460	1.558	"
15	52.0	1.657	0.403	0.621	1.873	0.570	0.793	"
16	51.75	1.660	0.340	0.602	1.876	0.497	0.763	"
17	50.0	1.679	1.090	2.090	1.901	1.402	2.577	"
18	47	1.715	0.402	0.616	1.947	0.564	0.793	"
19	46.5	1.721	0.575	0.880	1.955	1.020	1.134	"
20	46	1.728	0.750	1.013	1.963	0.990	1.308	"
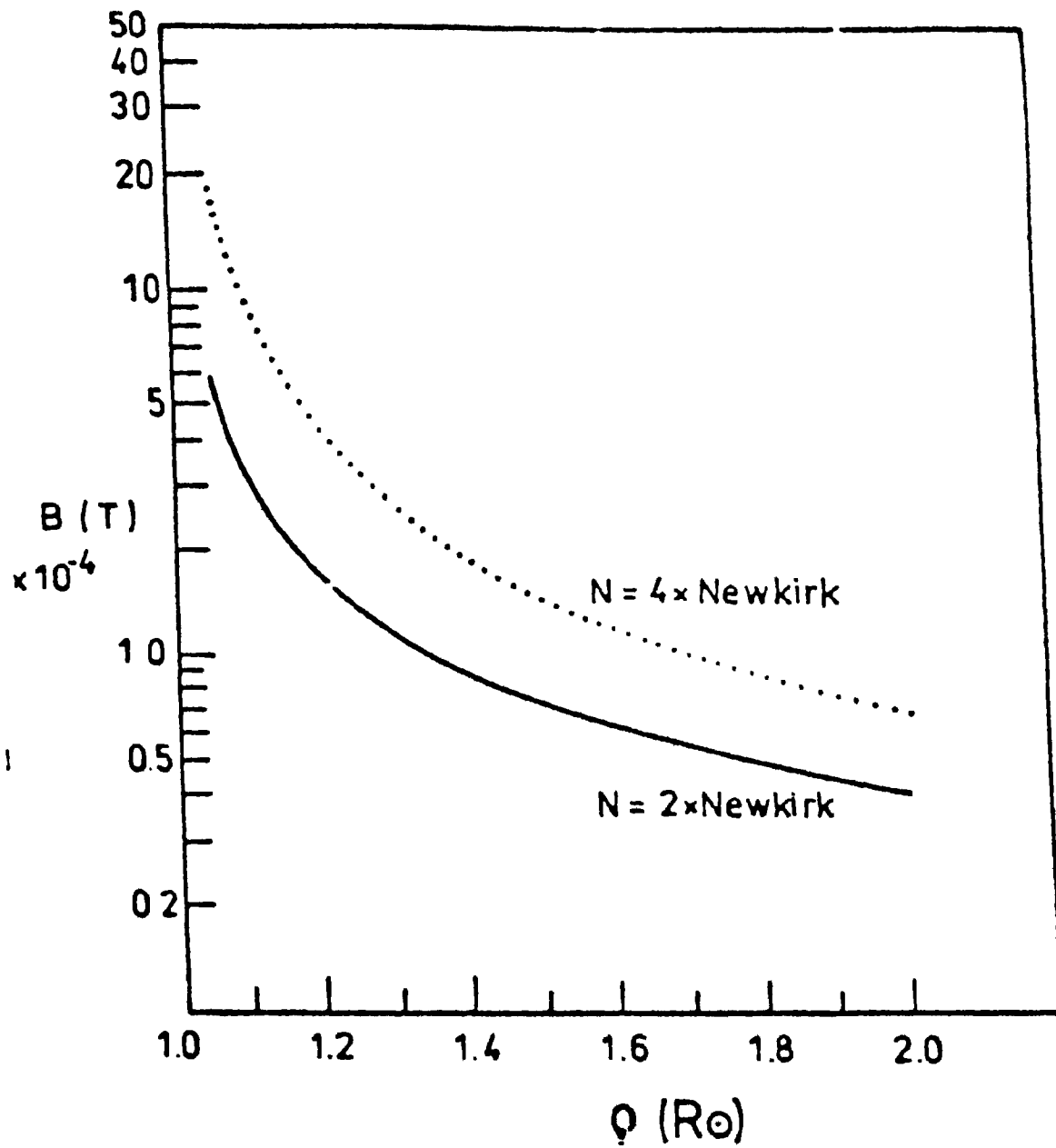
Fig. 2.5. The magnetic field versus radial distance, (in units of $R_\odot$) for the cases $V_1 > V_A$. (Newkirk $= 4.2 \times 10^{4 + \frac{4.32}{f}}$).

obtained by our method ($V_i > V_A$). The field strengths obtained by Dulk and McLean (1978) are larger compared to both $V_i = V_A$ and $V_i > V_A$ cases for the density model, x = 2 while all the values come closer for x = 4 model. The qualitative behaviour of the magnetic field as a function of the radial distance is almost same in all the cases. It is clear from fig.(25) that an enhancement in electron density leads to higher values of the magnetic field.

2.9 Conclusions

In this chapter we have discussed two aspects of type I solar radio emission. The first one deals with low frequency turbulence generated in the shock fronts responsible for type I radiation. Here we derived the dispersion relation for the ion sound waves excited by the perpendicular currents in the shock fronts and the growth rates are estimated. The saturation level of ion-sound turbulence is obtained from a quasilinear analysis and compared with that of lower hybrid waves generated under similar conditions. It is found that the ion-sound turbulence saturates at a higher level compared to the lower hybrid turbulence and therefore, the former is a better candidate compared to the latter because of the higher energy density and the fact that there is a better overlap in the wave number space also. The shock waves produced by the newly emerging flux give rise to the ion-sound turbulence which, according to our analysis

is the most favourable candidate to interact with the high frequency waves to generate type I emission.

The second one concerns with the estimation of macroscopic parameters of the corona by assuming that weak shocks generated by the emerging magnetic flux are responsible for the type I radiation. The most important macroscopic coronal parameter is the magnetic field. The coronal magnetic fields are deduced mainly from the data of various radio emissions from the sun during its flare. The type-I emission is of particular importance because it is the only nonthermal emission which is not flare associated. There were a couple of attempts to estimate the magnetic fields using type-I bursts (Wild and Tlamicha, 1964, Takakura, 1966). The fields obtained by Takakura (1966) are overestimates because of the inadequate theory, used. The approach of Wild and Tlamicha (1964) is correct in that they assumed the velocity of the agency causing type-I chains to be equal to the Alfven velocity. It is known at present that the type-I emission is caused by super-Alfvenic shocks and hence the magnetic fields deduced will be less than the above. Since the type-I bursts correspond to mild variations in the active regions, the shocks have to be weak. Therefore the shock velocity will be slightly more than the Alfven velocity. Comparison of our values with those of Wild and Tlamicha (1964) supports this fact because our values are only slightly less.

The field strengths obtained by Dulk and McLean (1978)

are larger than both our values and those of Wild and Tlamicha (1964) for x = 2 density model. This is because the values obtained by Dulk and McLean (1978) correspond to active regions conducive for flares where one expects enhanced density and magnetic fields. In the x = 4 density model, the curves due to our method and of Wild and Tlamicha (1964) come closer to that of Dulk and McLean (1978) because we assume a higher density in this model which may not be a realistic approximation. This therefore provides an indirect evidence for the fact that the flare associated bursts correspond to a corona with enhanced density and magnetic fields.

The collected data of the type-I chains correspond to various times and locations in the corona and from instruments of various characteristics. Therefore the calculated field may not correspond to a particular active region.

In conclusion, we point out that our estimates agree well with those of. Wild and Tlamicha (1964) based on shock waves. It is also evident that the density and magnetic fields in the active regions from where type-I emissions originate must be less than those in the active regions associated with flares. In summary, the formula $B = 0.41 \, (\mathcal{S} - 1)^{-0.89}$ gives the coronal magnetic field B above mild active regions as a function of the radial distance

CHAPTER III

FINE STRUCTURE OF SOLAR DECAMETRIC RADIATION
OBSERVED USING THE GAURIBIDANUR RADIO TELESCOPE

3.1. Introduction

Fast microstructure in solar radio emission is quite well known in the wavelength range from a few millimeters to decameters (Slottje, 1972, 1978, Sastry, 1973, etc.). The outer corona can be studied using telescope operating at low frequencies. The radio telescope used to study the fine structure of the radio emission operates around 35 MHz and is located at Gauribidanur. There are many interesting features in the decametric radio emission both in continuum and bursts. We mainly concentrate on two distinct features: 1. the peculiar time structure of solar decametric type III radio bursts and 2. decametric absorption bursts.

Usually, time profile of a type III burst is characterized by a sharp rise followed by an exponential decay. If the decay is due to collisional damping, one can easily calculate the kinetic temperature of the corona where the bursts originate using the standard formulas. During the course of our observations of storm type III bursts (Thejappa and Sastry, 1982, Thejappa et al 1984) we found that the time profiles of these bursts can take a variety of forms; three distinct profiles are presented here 1. the intensity rise to a small steady value before the onset of the main burst, 2. the intensity of the main burst

reduces to a finite level and remains steady before it decays to the base level, and 3. the steady state is present during the rise as well as the decay phase of the main burst.

We have also detected many interesting absorption features during our observations of the microstructure of the decametric continuum. The characteristics of these absorption features are found to be different from those at short wavelengths (Sastry et al, 1983, Gopalswamy et al 1983, 1984 Thejappa et al, 1984).

In what follows, a summary of these observations are presented. A description of the Gauribidanur Radio Telescope can be found in Section 3.2. The peculiar time profiles of type III bursts is described in section 3.3, whereas in section 3.4, the observations and theoretical interpretation of decameter absorption bursts are presented.

3.2. Equipment

Decametric Radio Telescope located at Gauribidanur (Latitude 13°36'12" N, longitude 77°26'07"E) is a T-shaped array of one thousand broadband dipoles 640 in the east-west arm and 360 in the south arm. All dipoles accept east-west polarization. A full reflecting screen (area 60,000 m^2) is mounted 1.5 m below the dipoles. The entire structure is supported on a grid of 3500 wooden poles of varying lengths of upto 35 feet to compensate for the terrain. The dimensions of the array are shown in fig. 3.1. A photograph of the east-west array taken from the eastern
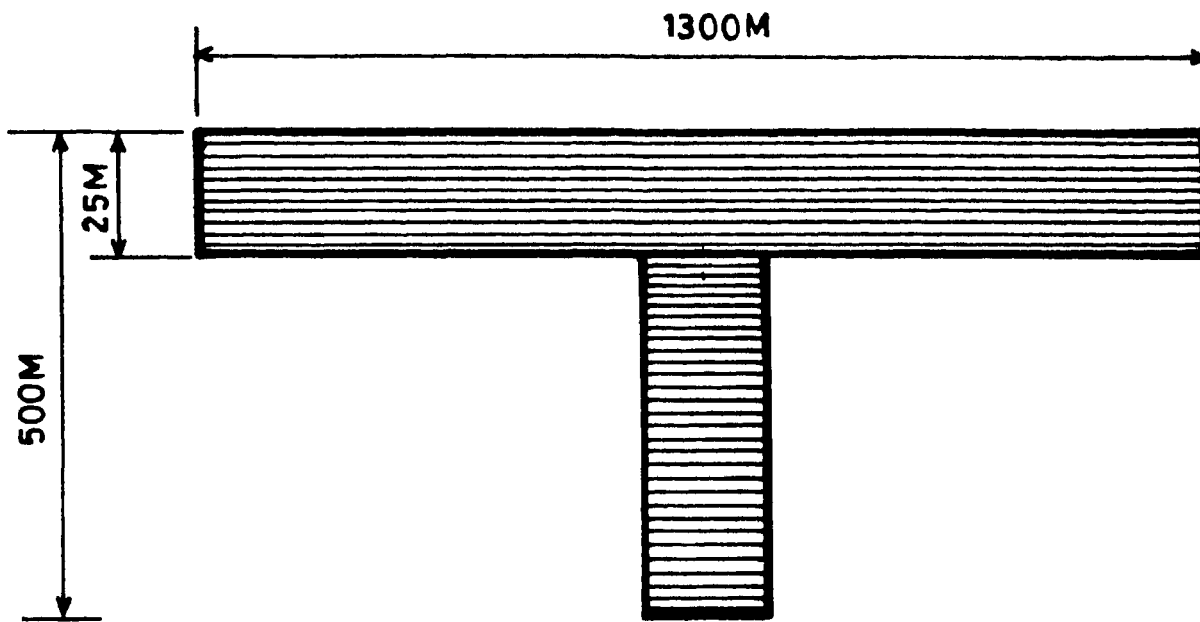
LOCATION:
　　Gauribidanur, Karnataka, INDIA
　　　　Longitude: 77°26'07"E
　　　　Latitude : 13°36'12"N
　　　　Frequency: 34 5 MHz
　　　　Beam width: 26'x38'
　　　　Effective area: 250 λ^2

Fig.3.1.　The Dimensions of the Array of the Gauribidanur
　　　　　Radio Telescope.

Fig. 3.2.   The east-west array of the Gauribidanur Radio Telescope.

Fig.3.3.　　The South arm as seen from its southern end.

end is shown in fig.3.2. and a photograph of the south array taken from the southern end is presented in fig.3.3. The outputs of the east, west and south arms are carried by coaxial cables to the centre of each arm and from there to the main observatory building. The signals are amplified and the sum of the east and west signals is correlated with that of the south arm. In this way a beam of about 26 x 38 arc minutes at the Zenith is produced at a frequency of 34.5 MHz.

The beam of the south arm can be pointed to anywhere within ± 60° of the zenith on the meridian. This is accomplished by adjusting the phase gradient across the aperture by using remotely controlled diode phase shifters. A special purpose digital control system sets the beam to the required position and also cycles it through several declinations sequentially. The time required to shift the beam from one position to another is of the order of a few milliseconds, and the number of declinations can be varied from one to sixteen. The beam of the E-W array can be tilted in hour angle to ±5° of the meridian by remotely operated diode phase shifters controlled by another special-purpose digital system. It is thus possible to track a source for about 45 minutes around the meridian transit.

In addition to the anolog system, a digital correlation system is also available. The hardware for this system consists of a 32-channel double sideband front end and a 128-channel one-bit digital correlator. The sampling rate is 2 MHz and the integration time can be varied from 2 to 256 ms. For this receiver

the N-S array is divided into 23 groups and each group is correlated with the E-W arm. At any instant the fourier transform of these correlations yields the brightness distribution of a strip of the sky of dimensions 26' (RA) X 15° (DEC). The 128-channel digital correlator can also be configured to measure the autocorrelation function of a signal.

The present observations were made with the NS array and a multichannel receiver. The NS array has a collecting area of approximately 9000 m^2 and beam widths of 15° and 0.5° in the EW and NS directions respectively. The center frequency of the receiver system is 3.45 MHz. The separation between the channels is 50 KHz and the bandwidth of each channel is 15 MHz. The time constant used is 10 ms. The minimum detectable flux density is about 1 SFU. The data were recorded both in analogue and digitial forms.

3.3 Time structure of solar decametre type III bursts

3.3a Observations

Our earlier observations on storm bursts are mainly of short duration ($\approx$ 1 s) and narrow band (Sastry 1969, 1971, 1972, 1973). In the present study we have considered time profiles of bursts whose total duration lies between 10-20 s. It is well known that the decametric noise storms consist of a succession of many Type III bursts. The duration of a Type III burst at frequencies around 30 MHz lies in the above range (e.g. Krishan, Subramanian and Sastry 1980; Subramanian, Krishan and Sastry

1981). The frequency drift of a Type III burst at these frequencies is of the order of 30 MHz s^{-1}. Since the duration is in the expected range and also there is no measurable frequency drift in our records we believe that the events we discuss here are Type III bursts. Also, all the other types of known solar bursts have completely different characteristics in this frequency range. Fig. 3.4 shows typical examples of bursts under study. In Fig. 3.4a one can see that the intensity rises to about 20 per cent of the level of the main peak and remains resonably steady for a period of about 4 s before the onset of the main burst, and we designate this as Type A profile. Another type of burst in which the intensity decays to about 30 per cent of the main peak level and remains steady for a period of 2 s before it decays to the base level is shown in Fig.3.4b, and is designated as Type B profile. In Fig. 3.4c, there is a small but steady rise in intensity for a period of 3 s before the onset of the main burst, and also the main burst decays to a constant level of about 20 per cent of the main peak and remains steady for a period of 3 s, which we call a Type C profile. Out of the total number of 165 bursts studied, 34 per cent belong to Type A, 45 per cent to Type B and 21 per cent to Type C profiles. We have measured the various characteristics of these bursts illustrated in Fig. 3.4, which are of interest to us in the following discussion.

Histograms depicting the variation of the number of bursts versus duration are given in Fig.3.5 for the three types of profiles
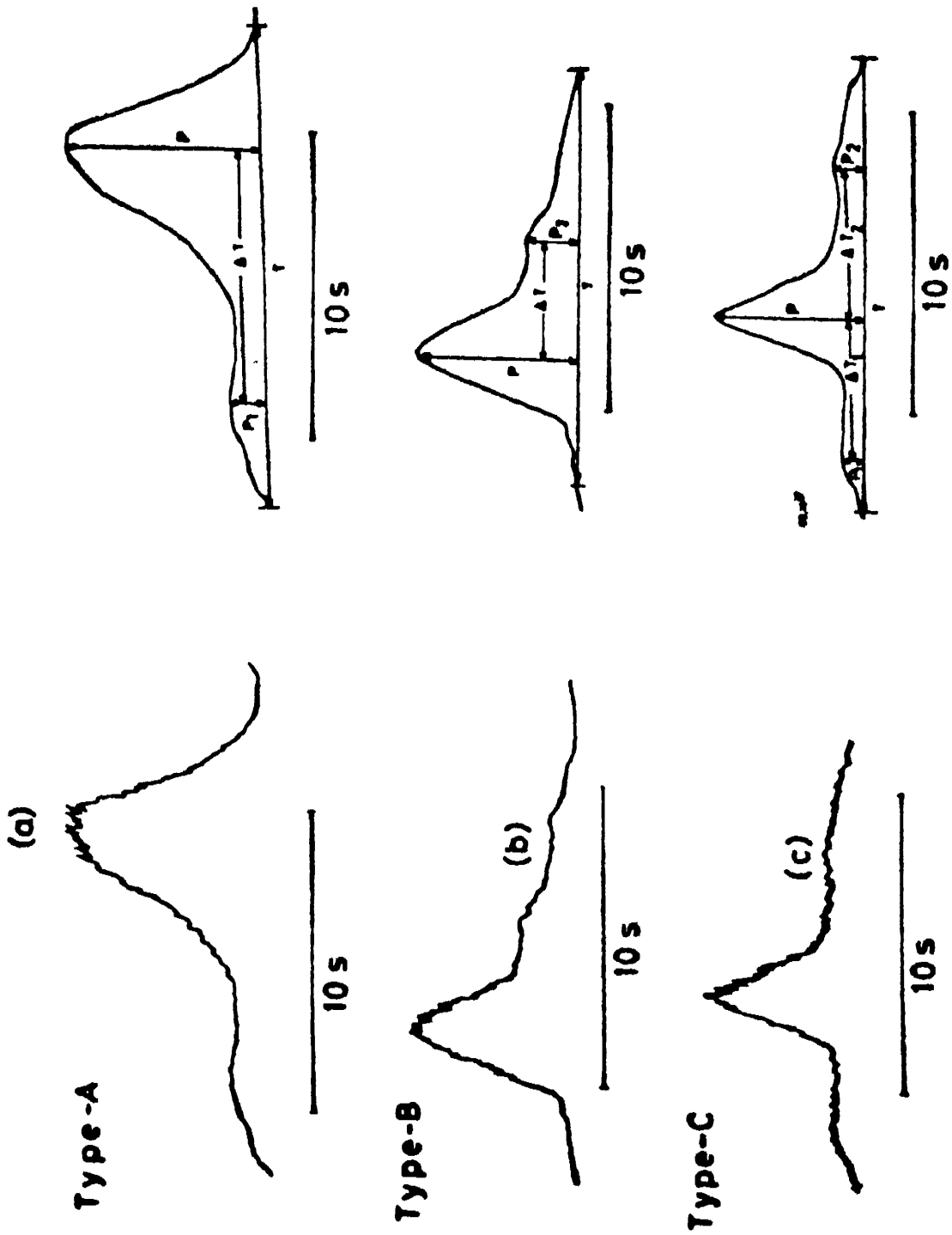
Fig. 3.4. Typical examples of Type III burst profiles and the definition of burst parameters.
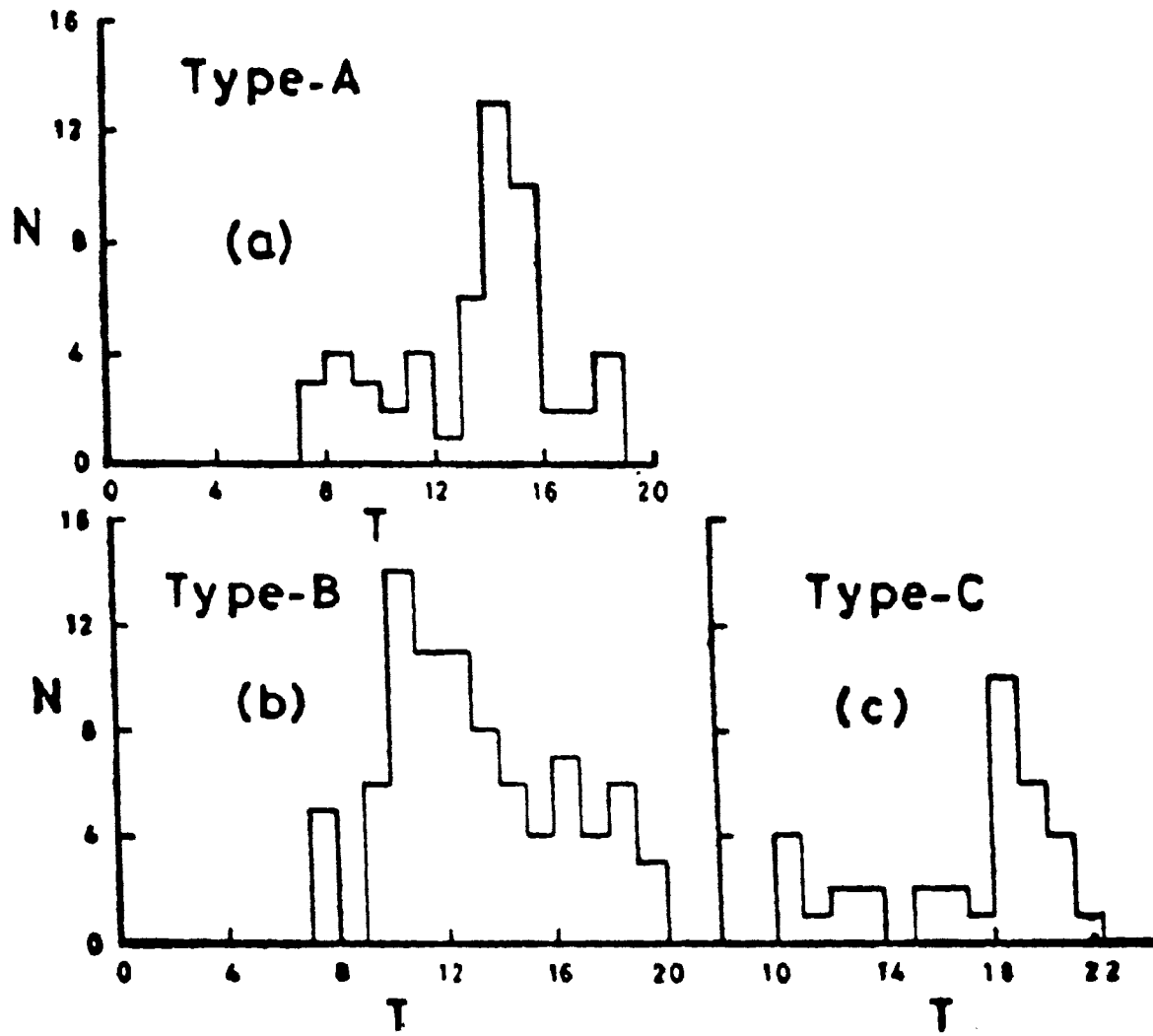
Fig. 3.5.   Histograms showing the number of bursts (N) versus
total duration (T).

It can be seen that in the case of Type A profiles the duration lies in the range 14-16 s and that for Type B lies in the range 10-15 s. The duration of Type C profiles is larger ($\gtrsim$ 18 s).

In Fig.3.6 the distribution of ΔT, the time interval between the peak of the main burst and the onset time of steady level in the case of Type A and the start of decay of the steady level in the case of Type B is shown. For Type A profiles, ΔT is about 5-6 s, whereas it lies between 3-6 s for Type B profiles. In the case of Type C profiles, ΔT_1 (interval between the main peak and the onset of steady level) ranges from 5-7 s and ΔT_2 (time interval between the main peak and the start of decay of the steady level) is ≤ 8 s.

The distribution of the following amplitude ratios are shown in Fig. 3.7: 1. the level of the pre-rise to that of the main peak P_1/P, 2. the level to which the main burst decays and remains steady to the level of the main peak P_2/P. It can be seen that the ratios P_1/P and P_2/P lie in the range 0.1 to 0.3 in all the profiles.

Following the procedure of Aubier and Boischot (1972) we have measured the decay constants of the main burst (τ_1) and also that of the final decay of the steady level (τ_2). Note that in the case of Type A profiles only τ_1 is present. From the histograms given in Fig. 3.8 it can be seen that the decay constants τ_1 and τ_2 lie in the range 1-4 s for all the three types of profiles. We did not find any strong correlation between
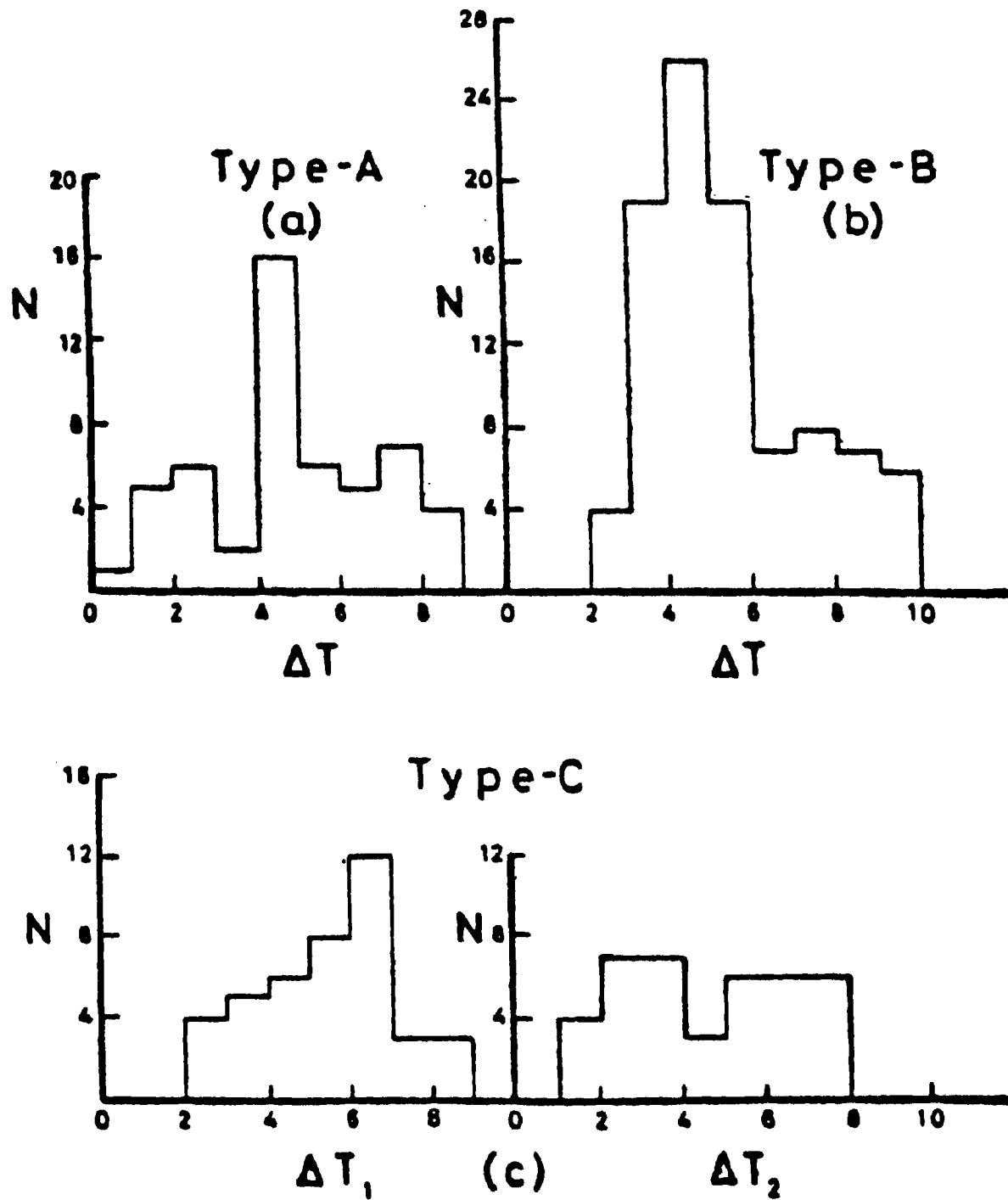
Fig. 3.6.   Histograms showing the distributions of time intervals
(ΔT).   See fig. 3.4 for the definition of ΔT_1 and
ΔT_2 in type c profiles.
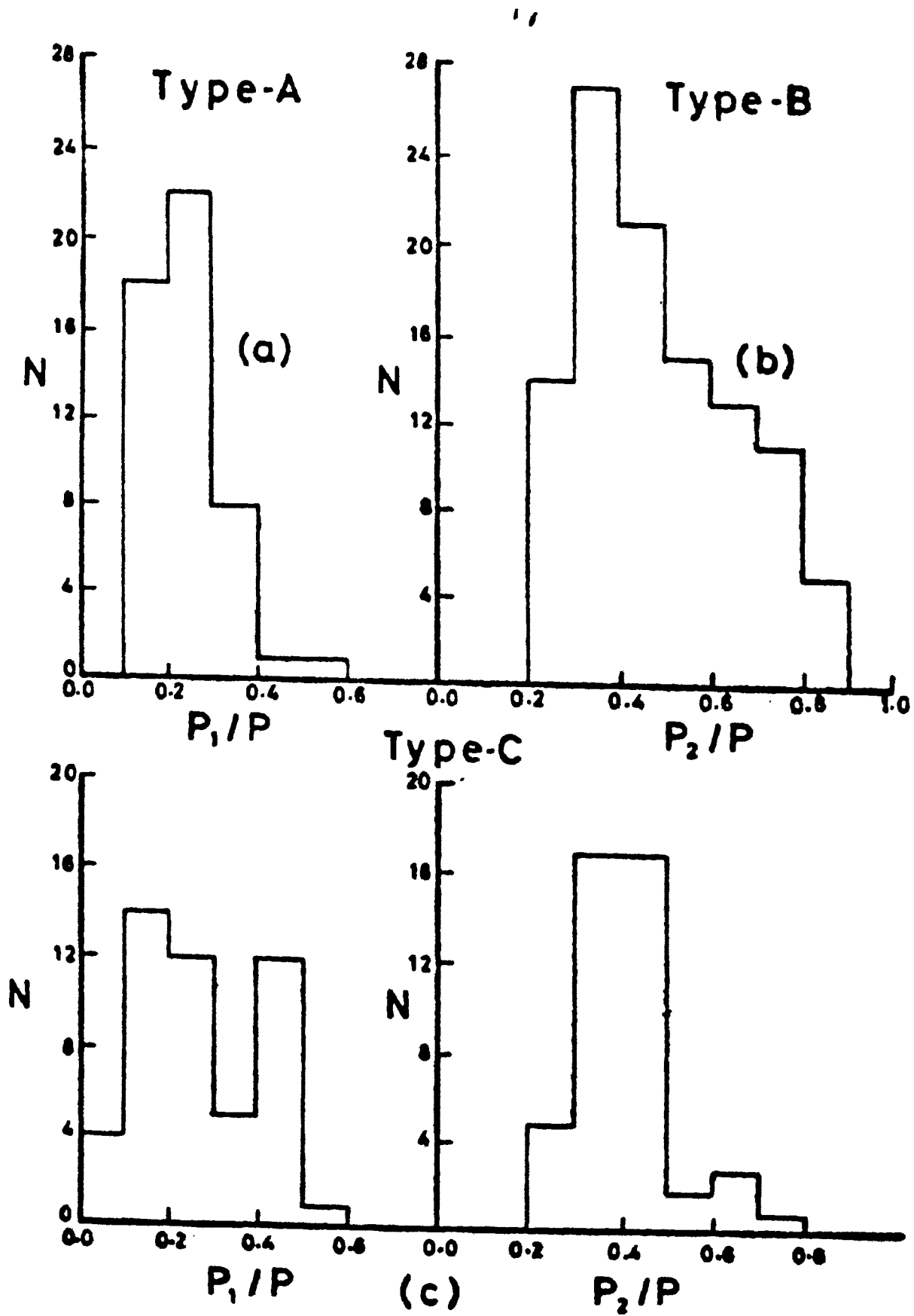
Fig. 3.7. Histograms depicting the distribution of amplitudes ratios P_1/P and P_2/P.
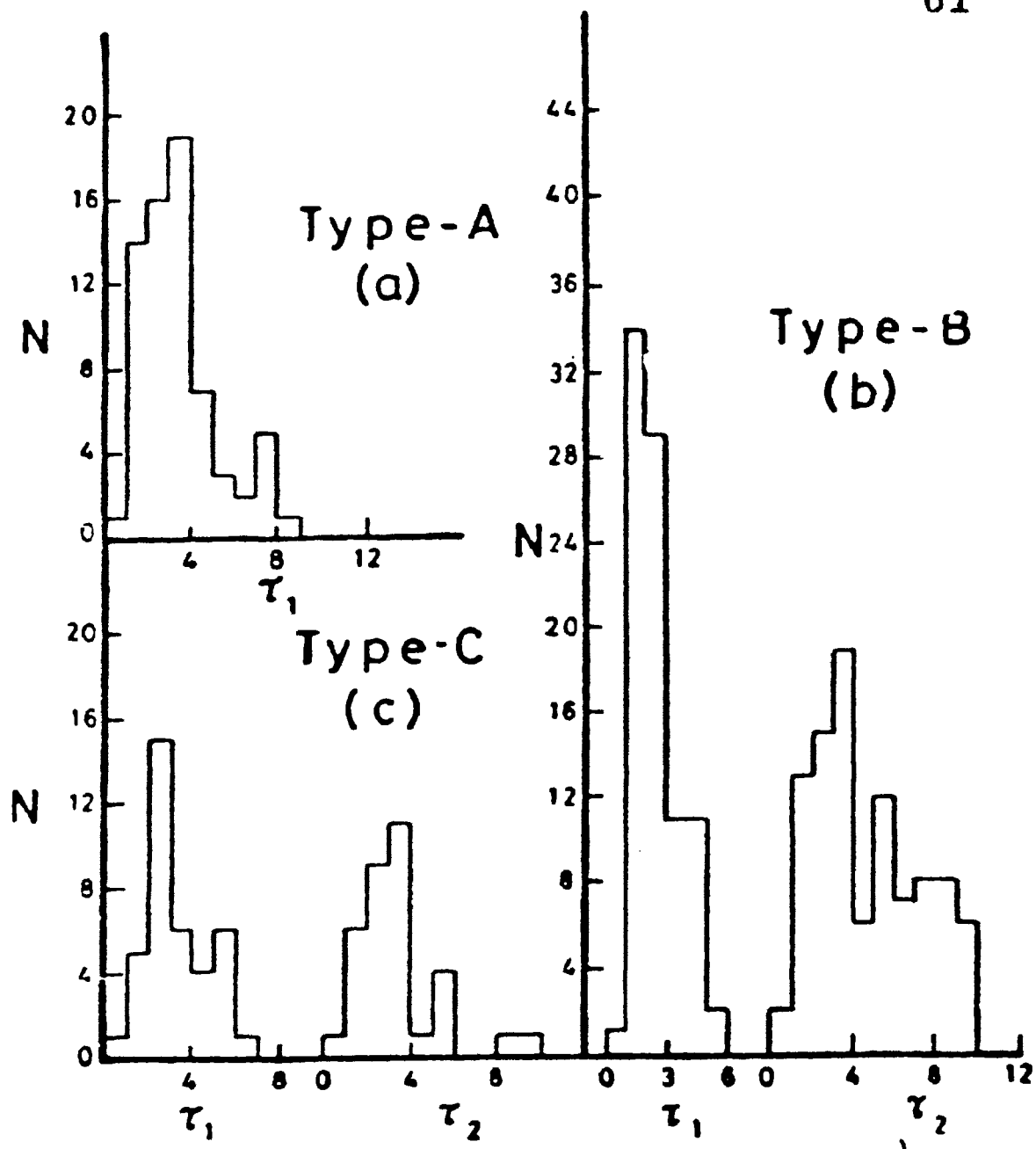
Fig. 3.8.   Histograms showing the distribution of decay constant τ_1 and τ_2.

the decay constant τ_1 and the duration of the exciter. Also τ_1 and the total duration T are uncorrelated.

3.3b. Discussion

During the periods of enhanced emission at decametre wavelengths we have observed that there can be single or groups of bursts occurring at random intervals. Therefore, the simplest possible explanation for the three types of profiles presented here can be that they are due to superposition of bursts occurring randomly in time. But it is found that the occurrence of the three types of profiles presented here is maximum only on particular days although the period of enhanced emission may last for a much longer time. The fact that the time interval, ΔT as defined above tends to lie in a rather narrow range irrespective of the total duration of the burst, indicates that the profiles are not produced by entirely random superposition of independent events. Also the measured ratio of amplitudes shows that the amplitudes of the initial and final phases are always a fraction of the main peak, and this ratio lies between 0.1-0.3. This need not be the case in case of bursts of various amplitudes occurring randomly in time.

The second possibility is that these profiles are the manifestations of fundamental harmonic (f-h) pairs. From the work of Daigne and Møller-Pedersen (1974) and Rosenberg (1975), it is clear that the time separation between the peaks of the fundamental and harmonic emission is, in general, constant

and is equal to about 4 s. It was also found that the amplitudes in f-h pairs are comparable (Rosenberg 1975). In the present case it is difficult to rule out the f-h pair hypothesis on the basis of the time intervals ΔT which are about the same as found by above authors. But the fact that the intensity ratios P_1/P and P_2/P observed by us are much less than unity does not lend suppost to this hypothesis. Also, according to Caroubalos, et al (1974) the ratio τ_F/τ_H of the decay constants of the fundamental and harmonic should be of the order of two if one assumes that the intensity of the fundamental $I_F \sim W$ (the energy density of plasma waves), the intensity of the harmonic $I_H \sim W^2$ and the temperatures in the regions of both fundamental and harmonic emissions are the same. Our observations show that τ_1 and τ_2 are in general same and in some case τ_2 can be greater than τ_1. Even if our Type A and Type B profiles are possible manifestations of f-h pairs, it is difficult to interpret type C profile on this basis. In the case of f-h pairs studied by Caroubalos, et al (1974) there are two clear-cut peaks in emission whereas in the profiles presented here no prominent subsidiary peak exists. Therefore, we believe that the profiles are probably not due to fundamental and harmonic emission. Zaitsev, et al (1972) have calculated the Type III burst profiles by solving the one-dimensional relativistic quasi-linear equations on a timescale $t \gg \tau$ where τ is the characteristic time for the development of two-stream instability (time taken for the plateau formation

$\tau = \omega_{pe}^{-1} \, n/n_s$ where ω_{pe} is the plasma frequency, n is the density of the background plasma and n_s is the density of electrons in the stream) and for the spatial scales $x \gg L$ where L is the intial thickness of the cloud under the initial conditions of a local explosion type. They have shown that at decametre and longer wavelengths—where the characteristic time of the absorption associated with collisions of electrons with ions in a 'cold' plasma, ν_{eff}^{-1} is much greater than the characteristic time of absorption due to Landau damping in the back of the stream $\Delta x/V_s$ (where Δx and V_s are the extent of the stream in the corona and its mean speed respectively) is satisfied-collisions can be neglected and only Landau damping in the tail of the stream. determines the dissipation of plasma wave energy. Their theoretical profiles agree well with the experimental data in the hectometre range under the assumption that electromagnetic wave generation takes place at the second harmonic of the plasma frequency. Zaitsev et al. (1974) extended the same in the case where the injection time of hot electrons from the region of the flare is considerably greater than the time of existence of the burst at a given fixed frequency. The dissipation mechanism is the same Landau damping on tail of the beam even at the decametre and metre wavelengths. The results of Zaitsev et al. (1974) have been confirmed by the extensive numerical work done by many authors (Takakura and Shibahashi 1976; Magelssen and Smith 1977; Grognard 1980)., The energy density of plasma waves is given by:

$$W_L(\xi) = \frac{n_s \, \epsilon_0}{3 \sqrt{2\pi}} \, \frac{(\epsilon_0/m)^{1/2}}{\eta_{eff} \, x} \left(\frac{2m\xi^2}{\epsilon_0}\right)^3 \exp\left(-\frac{2m\xi^2}{\epsilon_0}\right) \quad (3.1)$$

for the final momentum distribution of the stream:

$$f_0(P) = P \frac{n_s}{(2\pi m \epsilon_0)^{1/2}} \exp\left(-P^2/2m\epsilon_0\right) \quad (3.2)$$

The mean velocity of the beam

$$v_s = \left(\epsilon_0/m\right)^{1/2} \quad (3.3)$$

where n_s is the electron density in the beam, ϵ_0 is the intial energy of the beam, $\xi = x/t$, x is the distance between the photosphere and the respective plasma layer, m is the mass of an electron and η_{eff} is the effective number of collisions. The energy density reaches its maximum when

$$t = t_{max} = x \left(\frac{3}{2} \frac{\epsilon_0}{m}\right)^{-1/2} \quad (3.4)$$

It is possible that the profiles presented here are due to the superposition of two or three bursts caused by ordered electron beams ejected with a constant time difference. In the case of Type A profiles, the electron beam responsible for the main burst should reach the appropriate plasma level soon after the electron beam causing the pre-rise leaves the same level. Then the time interval ' ΔT' is equal to the time at which W_L (plasma wave energy density) causing the main burst reaches

its maximum. Since we know ΔT from observations, we can find the initial energy of the beam causing the main burst. From the observed ratio P_1/P, we can find the intial energy of the first beam. If we take $x = 1.1 \times 10^{11}$ cm and $\Delta T = 4$ s, the $V_2 = 1.856 \times 10^{10}$ cm s^{-1} and $V_1 = 0.37 \times 10^{10}$ cm s^{-1}, where V_1 and V_2 are the mean velocities of the first and second beams respectively. By computing the resultant time profile with the above initial energies of the beams, we are able to reproduce approximate profile of Type A and the rise part of Type C. It is not possible to reproduce the steady decay of Type B and Type C profiles in this manner. Note that the superposition of W_L is possible since we have used a combination of two beams which follow independent paths. It may be possible to construct all the time profiles by a combination of more than two beams. But it is not clear how the electron beams are accelerated to the above energies and ejected with constant time difference.

The other possible explanation for the observed profiles is that the conversion mechanism of plasma waves into electromagnetic waves and their decay show such a peculiar character.

3.3c. Conclusion

We have investigated three distinct time profiles of Type III bursts occurring during the periods of enhanced emission. These are: (1) profiles where the intensity rises to a small but

steady value before the onset of the main burst, (2) the intensity of the main burst reduces to a finite level and remains steady before it decays to the base level, and (3) the steady state is present during the rise as well as the decay phase of the main burst.

It was shown that these profiles are not due to random superposition of bursts with varying amplitudes. They are also probably not manifestations of f-h pairs. Some of the observed time profiles can be due to superposition of bursts caused by ordered electron beams ejected with a constant time delay at the base of the corona.

3.4 Decametric absorption bursts

The absorption or sudden reductions are common in decimeter and meter wavelengths (Young et al, 1961, de Groot 1970, 'Slottje' 1972, Benz and Kuijpers 1976). Among the observations of a variety of fine structures superimposed over decametric continuum (Gergely 1982, Melrose 1982, Sawant 1982) and of smooth continuum (Gergely and Kundu, 1975), interesting absorption features have been discovered (Sastry et al 1983, Gopalswamy et al 1983, Thejappa et al 1983). The absorption bursts were detected using the Gauribidanur Radio Telescope, described in section 3.2 of this chapter.

The interpretation of the absorption features depends

on the mechanism of radio emission and the propagation characteris-
tics of the radio waves. Since the generation of radiation itself
may be different at different frequency ranges, the absorption
mechanism also could differ. However, one can classify the
interpretations of the absorption bursts into two categories.
One is to attribute it to the temporary stoppage of the radiation
generation in the source itself and the other is to ascribe it
to the propagation effects. In the former case, if the radiation
generation is due to a plasma process then the reduction can
occur either due to the stoppage of the production of plasma
waves or due to the stoppage of the coversion of plasma waves
into radiation. For example, the reduction in microwave flux
observed by Kaufman et al (1968) could be interpreted as the
temperature dependence of optical depth. If an optically thin
flux tube from where the thermal radiation emanates is heated
by the passage of cyclotron waves or a shock wave then the
optical depth decreases, hence decreasing the observed brightness
temperature. In this paper we discuss the possibility of absorption
in the propagation stage and mention the possibility in the genera-
tion stage also.

3.4a Observations

In Fig.3.9a one can see a broad-band absorption feature
with a duration of 6 s at $06^h 52^m 09^s$. The absorption bursts
at $06^h 53^m 23^s$ UT is strong and has fine structure. The total
duration of the bursts is about 1.4 s. The fall time, i.e., the
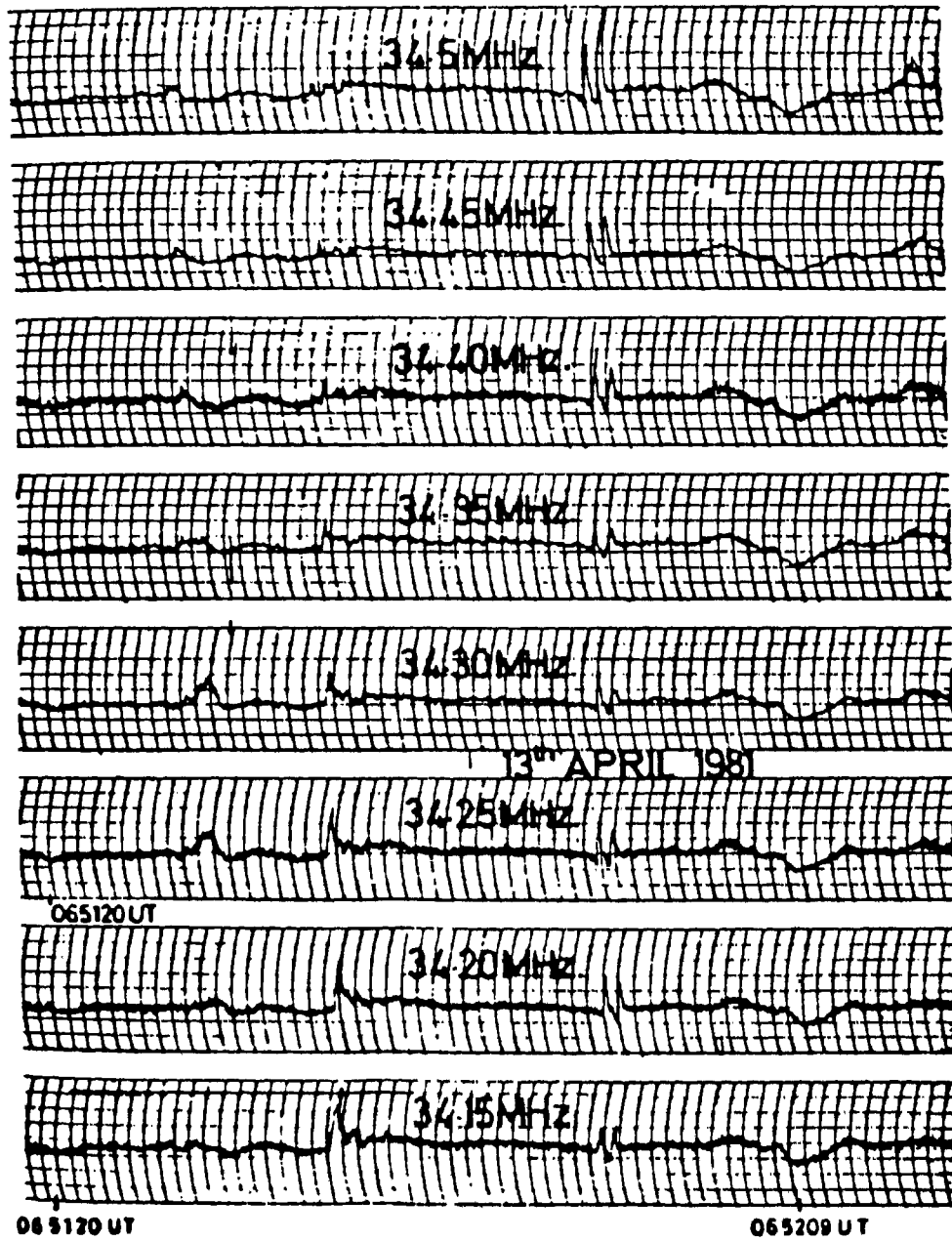
Fig. 3.9. 8-channel record obtained on 1981 April 13. The ordinate is the intensity of the radio emission.

Fig. 3.9 contd.,

25 JUNE 1981
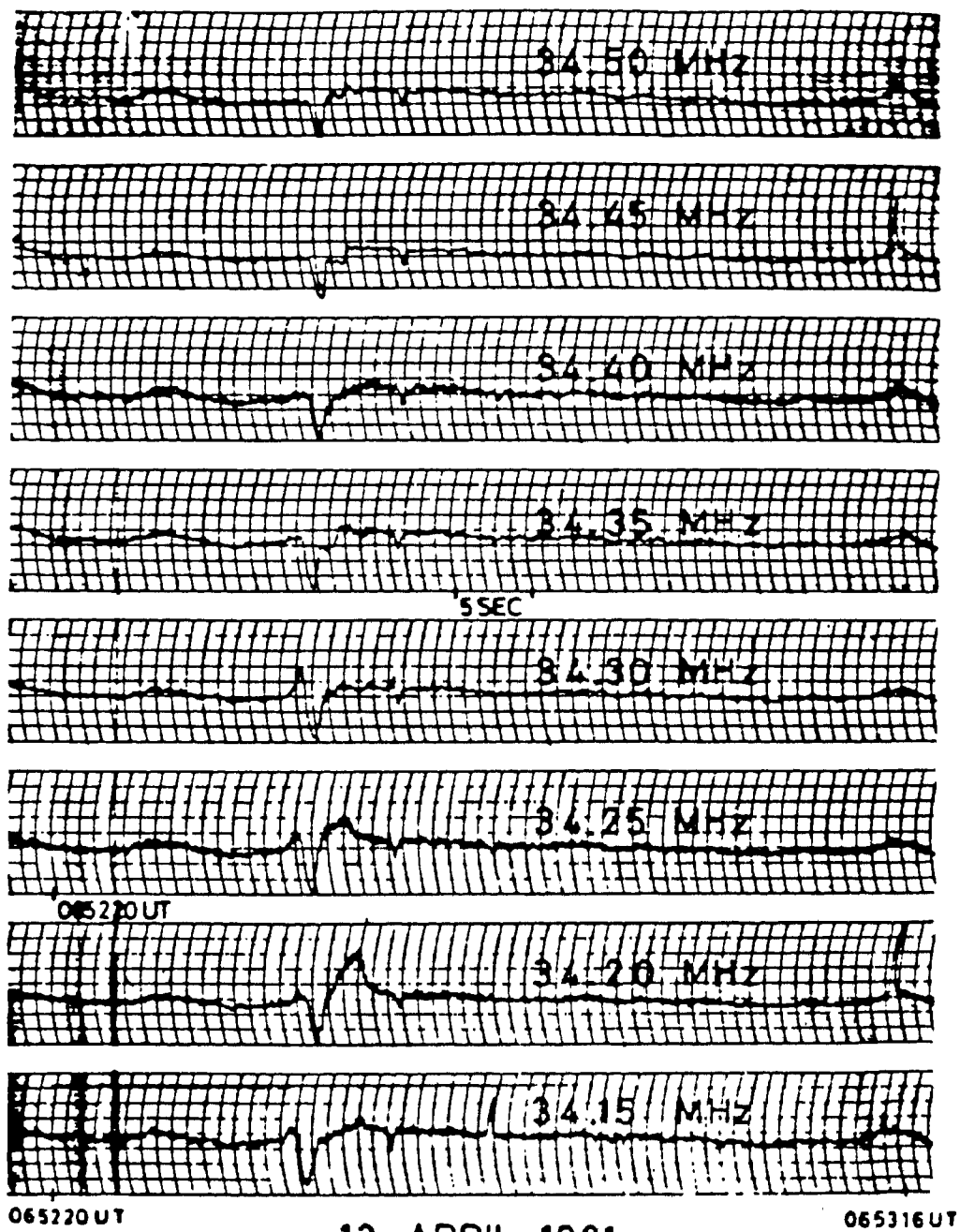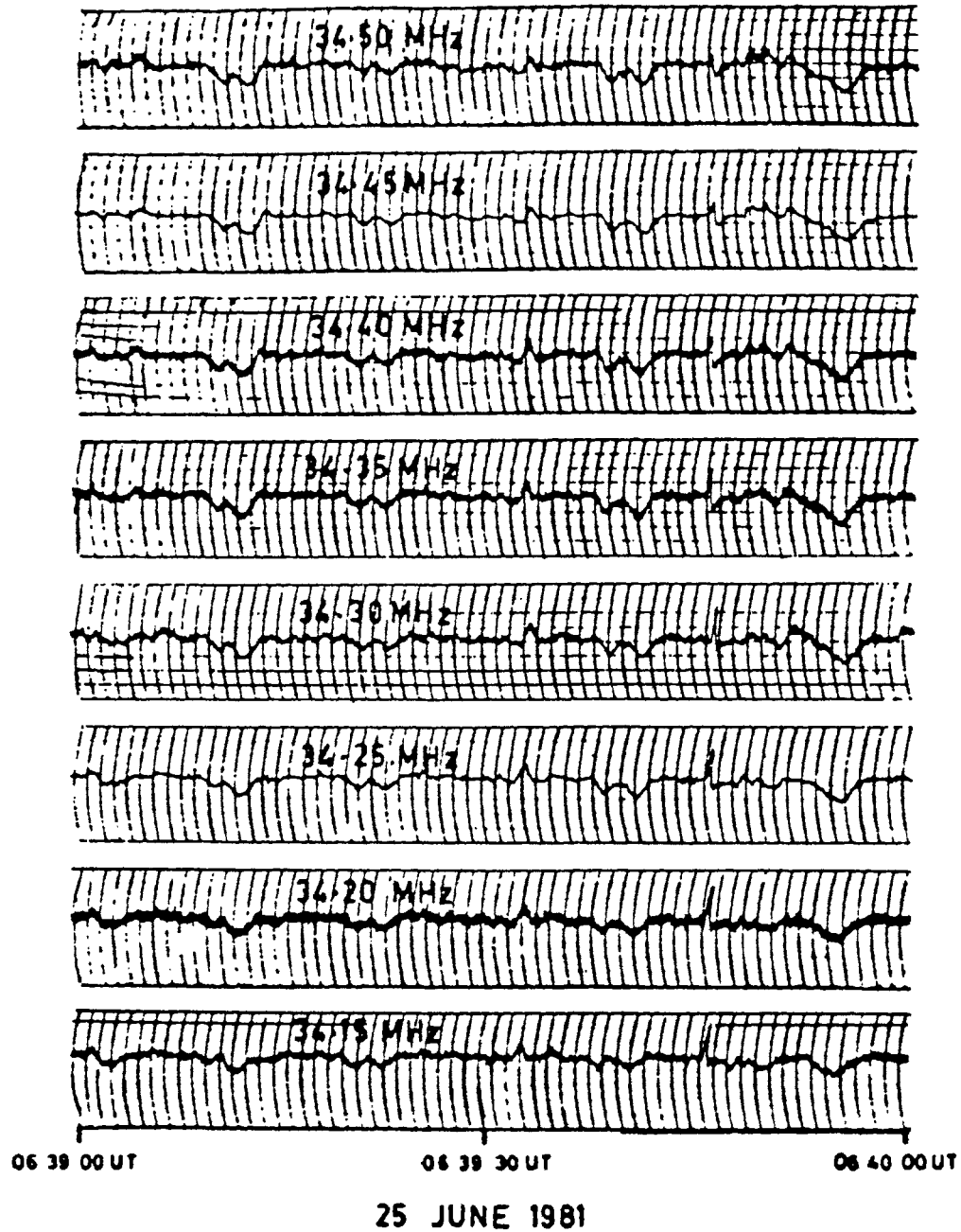
Fig. 3.10. Second example of the absorption bursts observed at Gauribidanur.

06 32 00 UT   06 32 30 UT
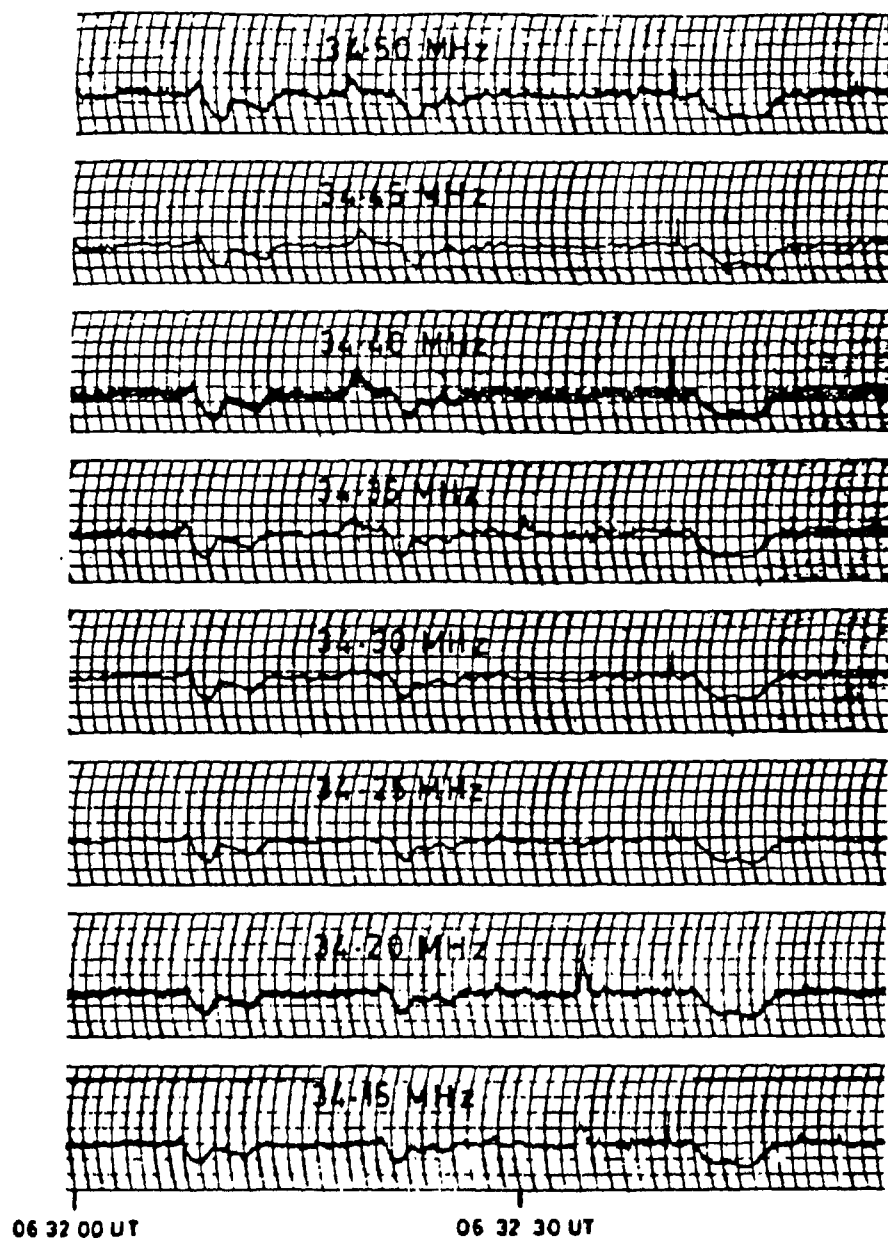
20 AUGUST 1981

Fig. 3.11. Another example of the absorption bursts observed at Gauribidanur.

time taken for the intensity to reach the minimum value is 400 ms and the rise time, i.e., the time taken for the intensity to reach the minimum value is 400 ms and the rise time, i.e., the time taken for the intensity to reach the preabsorption level is about 1 s. The bandwidth of the absorption burst is 500 KHz, whereas the associated emission burst is narrower. Another very-short duration (400 ms) broad-band absorption burst occurred at $06^h 53^m 28^s$ UT whose fall and rise times were very rapid (150 ms). Two more narrow-band absorption bursts with bandwidths of 200 KHz and 250 KHz respectively occurred at $06^h 52^m 32^s$ UT and $06^h 53^m 48^s$ UT. Note the double structure in the time profiles of absorption in some channels and that the emission bursts which occurred at the same time in some channels are very intense compared to the absorption bursts.

Part of another record obtained on 1981 June 25 is shown in Fig.3.10. One can see the reduction in intensity with both sudden and gradual onsets. Note the split time structure of some of the absorption bursts. Another record obtained on 1981 August 20 is shown in Fig. 3.11. Here we have shown examples of sudden decreases but with very slow recovery. A careful examination of the time profiles of the two bursts occurring at $06^h 32^m 08^s$ and $06^h 32^m 21^s$ UT shows that after the intial decrease the intensity recovers only to about half of the initial level and stays there for about two seconds before attaining the preabsorption level. It is interesting to note that

the time profiles of these two bursts occurring at different times are exactly similar to each other.

A statistical analysis of several hundred absorption bursts revealed the following characteristics.

1. The absorption bursts can occur isolated or can be followed or preceded by emission bursts. In come cases absorption and emission can occur simultaneously in different frequency channels.

2. The bandwidth of absorption bursts is always greater than about 500 KHz whereas those of emission bursts could be as narrow as 50 KHz.

3. The minimum duration of the absorption bursts is of the order of 1 s, whereas that of the emission bursts can be much smaller (100 ms).

4. The depth of the absorption is about 30-40 per cent of the continuum level. We also noticed that in some cases where the duration of the absorption burst is small, the depth of absorption can be as high as 70-80 per cent.

3.4b A suggested explanation

The broad-band reductions in the intensity of continuum radiation have been reported at high frequencies (Benz & Kuijpers 1976; Fokker 1982). Benz & Kuijpers (1976) regard that the

continuum radiation in the decimetric wavelengths is due to electrostatic loss-cone instability and the reduction in the continuum is due to the filling of the loss cone by electron streams momentarily, thus stopping the generation of radiation. Fokker (1982) has suggested that the reduction in intensity need not be at the generation stage but can also be at the propagation stage. He proposed that the continuum radiation is ducted through open magnetic flux tubes and the radiation is screened by inhomogeneities created on the path of the radiation by lateral shock waves or solitons impinging on the flux tubes. We are concerned here with the reductions in decametric continuum. The most recent theory on the origin of decametric continuum is due to Levin (1982), who ascribes the continuum to the Rayleigh scattering of plasma turbulence generated by an anisotropic distribution of a diffused electron beam with high transverse temperature. Levin's mechanism does not require a closed magnetic field and hence the loss-cone filling mechanism is not appropriate. So, following Fokker (1982), we assume that the radiation is absorbed on its path, rather than at the generation stage.

It was pointed out by Kaplan & Tsytovich (1973) that ion-sound turbulence can scatter the radio emission of the Sun producing additional maxima or minima in the stationary spectrum. Melrose (1974) explored the possibility of radiation by ion-sound turbulence to expalin Kai's (1973) observations of shadow type III bursts. The generation of ion-sound turbulence can be attributed

to many sources (Melrose 1974, 1982). It has also been theoretically shown that shocks under coronal conditions can generate high level of ion-sound turbulence (Lacombe & Mangeney 1969; Kaplan & Tsytovich 1973; Klinkhamer & Kuijpers 1981). We would like to mention that the shock generated ion-sound turbulence of nonthermal level can cause absorption in the decametric continuum radiation. This is another important consequence of the presence of shock waves, apart from what Fokker (1982) has considered. A shock propagating perpendicular to a magnetic filed can be a source of many types of waves, like the Langmuir, ion-sound, ion-cyclotron, electron-cyclotron etc. As pointed out by Galeev (1976) most of the instabilities other than ion-sound are excited at the intial portion of the shock front. Because of these instabilities, the electrons would be essentially heated and the ion-sound instability with the lowest current threshold would stop the magnetic field profile steepening at a level where all the other instabilities are quenched. Moreover, the saturation level of turbulence for other waves is always much less than the ion-sound turbulence level (Spicer, Benz & Huba 1981; Kaplan & Tsytovich 1973). Therefore, one can regard that the ion-sound turbulence is the most favoured one. We assume that a shock propagates perpendicular to the open magnetic field lines in the region overlying the decametric continuum source, generating ion-sound turbulence. The magnetic field gradient of the shock can induce strong electric fields which can accelerate electrons to velocities U greater than the ion-sound velocity V_s so that

the condition for ion-sound instability is satisfied. The change in magnetic field H, the induced electric field E and the electron drift velocity U are related by:

$$\vec{\nabla} \times \vec{H} = \frac{4\pi}{c} \sigma \vec{E} = \frac{4\pi n_e e}{c} \vec{U} \qquad (3.5)$$

where c is the velocity of light, σ - the plasma conductivity, e the electronic charge and n_e the electron density. The condition for the ion-sound excitation can be obtained by demanding that U must exceed V_s.

$$\frac{\partial H}{\partial L} > \left(\frac{4\pi n_e e}{c} \right) V_s \qquad (3.6)$$

where L is the coordinate along the direction of magnetic field variation. For coronal conditions ($n_e = 10^8$ cm^{-3}, $T_e = 10^6$K), the right-hand side of the above inequality works out to be 1.8 x 10^{-4} G cm^{-1}. Following Klinkhamer and Kuijpers (1981), the left-hand side can be estimated as $\frac{\partial H}{\partial L} \simeq \Delta H(7c/\omega_{p_e})$ where Δ H is the jump in magnetic field across the shock and

is the electron plasma frequency. It is well known (Tidman and Krall 1971) that $\Delta H \lesssim 3H_1$, where H_1 is the upstream (ambient) magnetic field. From frequency splitting and polarisation measurements of type I bursts, the coronal magnetic field at decametric level is obtained approximately as 1 G (ter Haar and Tsytovich 1981). Hence for a magnetic field jump H/H$_1$ 0.18 is sufficient to satisfy the inequality dH/dL > 1.8 x 10^{-4} G cm^{-1}.

The continuum radiation, while propagating towards the observer, encounters the ion-sound turbulence and enters into

a three-wave interaction. In other words, the continuum radiation (t-wave) interacts with the ion-sound (s-wave) producing Langmuir wave (L-wave); thus occurs a reduction in the intensity of the t-waves. The conditions under which such an interaction takes place will be worked out below.

If one accepts Levin's theory, then one should consider the possibility of ion-sound turbulence generation by the return current caused by the one-dimensional beam that separates from the diffused beam. It is easy to show that an unusually high beam density is required to generate the required level of ion-sound turbulence. The fact that the return current is unimportant even in other situations is pointed out by Smith (1974).

Let us now estimate the effective temperature of the ion-sound turbulence needed to absorb the radiation. Let the ion-sound turbulence be described by assigning a central or average frequency $< \omega_s >$ and a width of $\Delta \omega_s \sim \langle \omega_s \rangle$ to be created over a solid angle $\Delta \Omega$ with an effective temperature $< T_s >$. The energy and momentum conservation relations for the three-wave process $t \rightarrow l \pm s$, by which the radiation is absorbed, are given by

$$\vec{k}_t = \vec{k}_l + \vec{k}_s \tag{3.7}$$

and

$$\omega_t = \omega_\ell + \omega \tag{3.8}$$

where ($\vec{k}$, ω) are the wavevector and frequency respectively. These processes cause a net conversion of transverse waves into longitudinal plasma waves, provided they satisfy the condition- under weak turbulence regime-that the effective temperature of the t-waves and (ω_{pe} / ω_s) times the effective temperature of the s-waves exceed that of the generated ℓ waves (Melrose 1970). For such a three-wave process, or its reverse process $\ell \pm s \rightarrow t$ (Shukla et al. 1982), it is shown that the coupling is possible when the wave numbers of the s-wave and ℓ-wave are approximately the same, i.e.,

$$k_L \simeq k_s \quad ; \qquad k_t \ll k_L, \, k_s \quad . \tag{3.9}$$

The dispersion relations for the interacting waves are given by,

$$\omega_\ell = \omega_{pe} \left(1 + \tfrac{3}{2} \, k_\ell^2 \lambda_D^2 \right) \, , \quad k_\ell^2 \lambda_D^2 \ll 1 \tag{3.10}$$

$$\omega_s = k_s v_s \tag{3.11}$$

and

$$\omega_t = \omega_{pe} \left(1 + \tfrac{1}{2} \, k_t^2 c^2 / \omega_{pe}^2 \right) \, , \quad \frac{k_t^2 c^2}{\omega_{pe}^2} \ll 1 \, , \tag{3.12}$$

where λ_D is the Debye radius, V_s is the phase velocity of ion sound waves and ω_{pe} is the plasma frequency. The other symbols

are standard. using the resonance conditions (3.7) and (3.8) and defining $\Delta\omega_t = \omega_t - \omega_{p_e}$ the typical wave number of the generated L-wave is :

$$\overline{k} = \left(\frac{2}{3} \frac{\Delta\omega_t}{\omega_{p_e}}\right)^{1/2} \frac{\omega_{p_e}}{V_e} \quad , \tag{3.13}$$

with

$$\frac{\Delta\omega_t}{\omega_{p_e}} \gg \frac{V_s}{6 V_e} \tag{3.14}$$

and

$$\Delta\omega_t \simeq \frac{3}{2} \frac{\overline{k}^2 V_e^2}{\omega_{p_e}} \tag{3.15}$$

Then, the fractional bandwidth of absorption defined by :

$$B = \frac{\Delta\omega_t}{\omega_{p_e}} \tag{3.16}$$

is obtained as :

$$B = \frac{3}{2} \frac{<\omega_s>^2}{\omega_{p_i}^2} \tag{3.17}$$

because

$$\overline{k} V_s = <\omega_s> \tag{3.18}$$

The observed fractional bandwidth of absorption B is 5×10^{-2}. Hence the central frequency of the ion-sound turbulence should be $<\omega_s> = \sqrt{\frac{2}{3} B \omega_{p_i}^2} \simeq 0.18 \omega_{pi}$. This is a stable frequency range for the ion-sound waves because the waves of low Landau

damping exist with a dispersion relation (3.11) only for $\omega_s \ll \omega_{p_i}$.

The transfer equation for the continuum radiation can be written as

$$\frac{\partial T_t}{\partial s} = -\mu\, T_t \qquad\qquad (3.19)$$

where μ is the absorption coefficient and s is the spatial coordinate along the ray path of the continuum radiation, with an effective temperature T_t. If L is the linear extent of the absorber and μ is independent of spatial coordinates over this region, the optical depth could be written as

$$\tau = \int \mu\, ds = \mu L \qquad\qquad (3.20)$$

A reduction in the intensity (absorption) occurs if the optical depth exceeds unity, as can be seen from the solution to the transfer equation (3.19), i.e., the condition for absorption is :

$$\mu L > 1$$

$$(3.21)$$

Let us now estimate the linear extent of the source. The thickness L of the absorbing layer is defined by the relative bandwidth of absorption and the scale-length of inhomogeneity L_n of the coronal electron distribution. The maximum thickness could be taken to be :

$$L = \beta L_n \,. \qquad\qquad (3.22)$$

where

$$L_n = \left| \frac{1}{\omega_p} \frac{d\omega_p}{ds} \right|^{-1} \tag{3.23}$$

In the undisturbed corona, L_n is calculated from Newkirk's formula for electron distribution as 2×10^{10} cm for the decametric region. Using the observed fractional bandwidth $B \simeq 5 \times 10^{-2}$, the thickness of the absorbing layer can be obtained from Equation (3.22) as 10^9 cm. The absorption coefficient can be estimated as (Melrose 1974):

$$\mu = \frac{r_0 \, c \, \omega_p^2}{24 \sqrt{3\pi} \, V_e^3} \frac{< T_s >}{T_e} \Delta \Omega \tag{3.24}$$

where $r_0 = e^2/mc^2$ is the classical electron radius and T_e is the electron temperature. Under coronal conditions with $V_e \approx 10^8$ cm s^{-1}, one can rewrite the condition (3.21) as

$$f^2 < T_s > \Delta \Omega \; > \; 10^7 \, T_e \tag{3.25}$$

where f is the frequency of the radio-waves in MHz. For $f = 35$, $\Delta \Omega = 3$ steradians and $T_e \sim 10^6$ K, the condition (3.25) becomes

$$< T_s > \; > \; 2.5 \times 10^9 \, K \tag{3.26}$$

This effective temperature is an order of magnitude more than that required for the shadow type-III bursts (Melrose 1974). The reason for this is the fact that our relative bandwidth is

less than that corresponding to the shadow type-III case by an order of magnitude. The l-waves build up due to the decay process, at the cost of the continuum radiation. Once they have sufficient energy density, the condition for net conversion of the t-waves into l-waves, viz.,

$$\text{minimum} \left[\left(\frac{\omega_l}{\omega_t} \right) T_t \, , \, \left(\frac{\omega_l}{\omega_s} \right) T_s \right] > T_l \qquad (3.27)$$

will not be satisfied and hence the saturation of absorption is reached. The reverse process becomes significant and hence the final brightness is determined by the level of the L-wave turbulence produced due to the decay process. Once the level of the ion-sound waves falls below the critical level, the absorption mechanism fails to operate and so the intensity recovers back to the continuum level. Thus the duration of absorption could be attributed to the time during which the ion-sound turbulence exists above critical level, satisfying inequality (3.25).

3.4c Discussion

We have shown that the sudden reductions in the decametric continuum can be ascribed to the absorption by ion-sound turbulence, generated by a shock wave. [In Fig.3.12, a sketch of the suggested model for the decametric absorption bursts is given]. The magnetic field gradient necessary to generate such a turbulence and the level of turbulence necessary to cause absorption are derived.
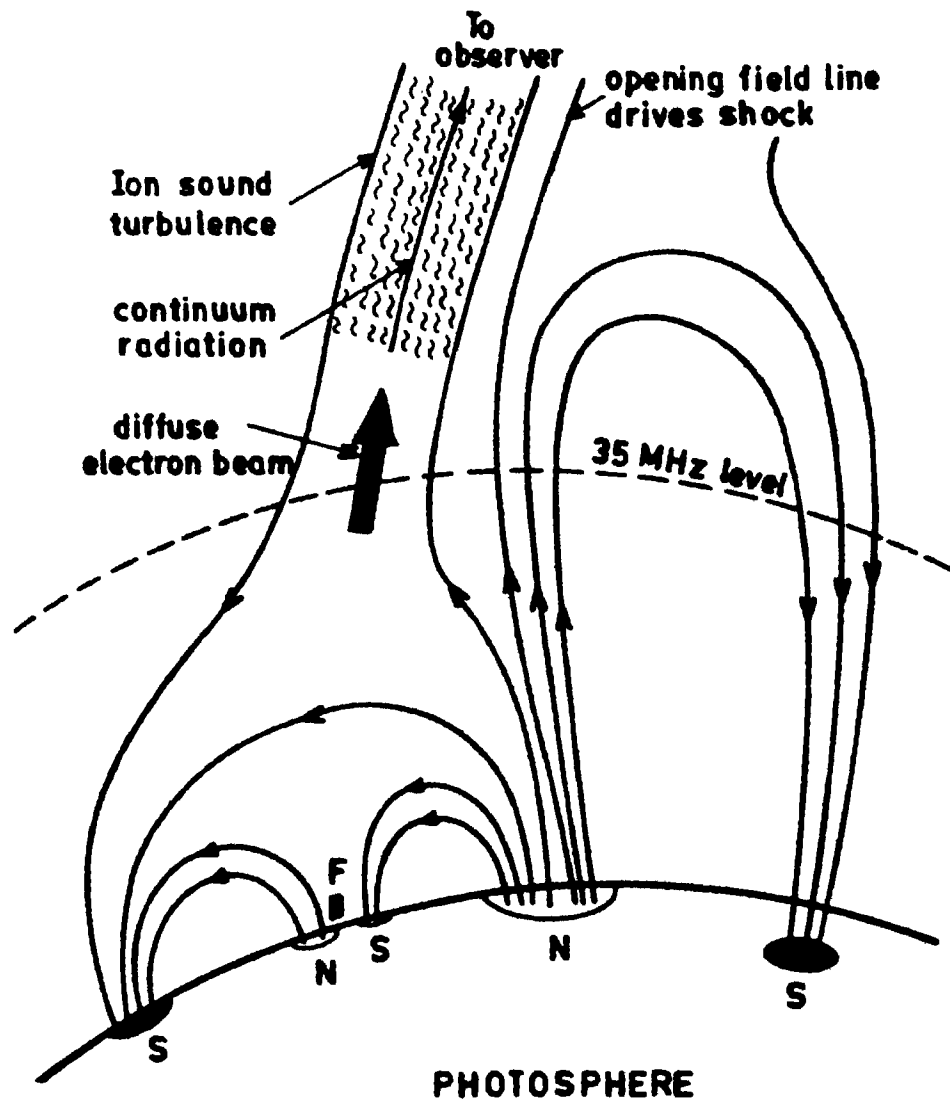
Fig. 3.12. A sketch of the suggested model.

The duration of the absorption could be attributed to the period during which the ion-sound turbulence stays undamped above thermal level. The depth of the absorption is determined by the level of Langmuir turbulence generated as a result of the absorption, after which the reverse interaction between the langmuir waves and ion-sound waves will become important. Since the conditions are most favourable to the generation of ion-sound turbulence and most of the other instabilities are quenched very fast in the front portion of the shock front itself, we did not include any other instability. Nevertheless, one can expect the generation of Langmuir turbulence, though its level is about two orders of magnitude less than the ion-sound level. This small amount of Langmuir waves plays some role in the three-wave interaction process and we have ignored it.

We would like to point out that the ion-sound turbulence could also cause emission by interacting with the Langmuir waves that can originate from two sources: (i) those excited by the shock itself and (ii) those generated during the absorption of continuum radiation. But the conditions under which the emission takes place (the inequalities (3.25) and (3.27))are different from those for absorption considered in this chapter. The presence of the Langmuir turbulence of low level might slightly affect the final brightness tmeperature of the continuum radiation.

Though we have assumed shocks travelling perpendicular to the ambient magnetic field lines, the ion-sound turbulence

could also be generated by oblique shock waves as discussed by Galeev (1976).

Our interpretation is semi-quantitative and we have not calculated, for example, the life-time of the ion-sound turbulence. Actually, the ion-sound turbulence is generated behind the shock where high gradients in magnetic field are formed. These gradients could even be of a stochastic type i.e., distributed randomly behind the shock front (Kaplan, Pikel'ner and Tsytovich 1974). Actual time structure of the absorption could be estimated only when the time dependence of the intensity of ion-sound waves is known. One may estimate the latter by analysing the behaviour of the turbulence in the wake of the shock.

The fractional bandwidth we used in our interpretation is approximate because of the limited bandwidth of our system. The transfer equation for the continuum radiation could be used to estimate the fractional bandwidth of absorption from the absorption coefficient of the ion-sound turbulence calculated by assigning an effective temperature of the ion-sound turbulence $< T_s >$ that satisfied the inequality (3.26). From Equation (3.24) for $< T_s > \sim 2.5 \times 10^9 K$, and $T_e \sim 10^6 K$, μ can be estimated as 2.3×10^{-8} cm. If we take $\mu L \sim 10$, then $L \sim 10/\mu$ so that Equation (3.22) gives $B \sim 0.02$, which is in the range of observed bandwidths.

The above model assumed that the emission and absorption are independent of each other and hence it can not explain the emission preceeding or following the absorption.

It is natural to ask the question as to what happens when the shock passes through the source region itself. If the shock is sufficiently weak so that the diffuse beam is not much affected, then the ion-sound turbulence will interact with the enhanced plasma fluctuations and give rise to radiation that propagates away from the line of sight, thus causing absorption again.

If shocks propagate successively, one after another, then depending upon the time intervals between the shocks and the ion-sound damping time, different time structures will obtain for the absorptions. Hence the multiple time structures could be interpreted as due to multiple shocks.

In the preceeding disucssion we did not address to the question of origin of the shocks. First of all it should be noted that the decametric corona is a region where the magnetic field makes a transition from closed to open structures and hence one expects opening up of field lines. If an emerging magnetic field line opens up adjacent to the site of the decametric source as shown in Fig. 3.12, then it can drive a shock across the magnetic field lines along which the continuum radiation propagates.

In conclusion, the absorption bursts seem to reveal the complex and "transition" nature of the outer corona and the non-drifting character of these bursts indicate no line of sight velocity for the "screen" absorbing. Hence, the shocks must propagate perpendicular to the line of sight.

CHAPTER IV

THE DRIFT PAIR BURSTS

4.1 Introduction

The most prominent and interesting radio emission phenomena, at decametric wavelengths occurring in the solar corona, are the drift pair bursts (DP's). After the first discovery by Roberts (1958) many authors have studied various aspects of DPs (Zheleznyakov (1965), Ellis (1969) de la Noë and Møller Pedersen (1971), Sastry (1972), Abranin et al (1977), Møller Pedersen et al (1978), Zaitsev and Levin (1978), Suzuki and Gary (1979), Melrose (1982). The DPs appear as two parallel drifting ridges in the dynamic spectrum. In most of the cases both the traces start at the same frequency, the second trace being delayed by approximately two seconds. This time delay is almost independent of frequency of occurrence and the drift rate. The DPs can have both positive and negative drifts, although the former is more frequent. The single frequency duration is small ($\sim$ 1 s)and the bandwidth is in the range of a few MHz to few tens of MHz. In a few cases, three traces and in a few other cases, only a single trace were observed. (Abranin et al, 1977).

Though there are a few attempts to interpret the DPs (Roberts (1958), Zehleznyakov (1965), Møller-Pedersen et al (1978), Zaitsev and Levin (1978), Melrose (1982)), the understanding of DPs is not yet complete. We present here a detailed analysis of DPs

observed during Sept. 26-30, 1983, which brings out some additional features like the DP chains, the vertical DPs and the decrease of drift rate with frequency etc. The existing theories are critically examined in the light of the new observational results.

In section 2, we present the observational results and compare them with those available in literature. In section 3, the existing theories are critically examined. In section 4, we give a qualitative interpretation of DP chain and vertical DPs. Finally we present the conclusions in section 5.

4.2 Observations

The observations were made using the swept frequency spectrograph at Nancay (Boischot et al 1980) during Sept. 26-30, 1983. About 1006 events of DPs were observed during the above five days. Using the NS array of the Gauribidanur radio telescope which is described in Chapter III, we have also observed the DPs with a multichannel spectral receiver on 15th, 16th and 19th July 1980. The typical examples of drift pair bursts observed at long wavelengths are shown in Fig.4.1. Previous observations indicate that the DP activity/s prominent only for a few days. For example, Roberts (1958) found that the DP activity was prominent for 38 days out of 250 days of observations and de la Noe and Moller-Pederson (1971) have reported only two days of activity out of 25 days of observations. No unusual feature was found on the sun either in H -pictures or in magneto-
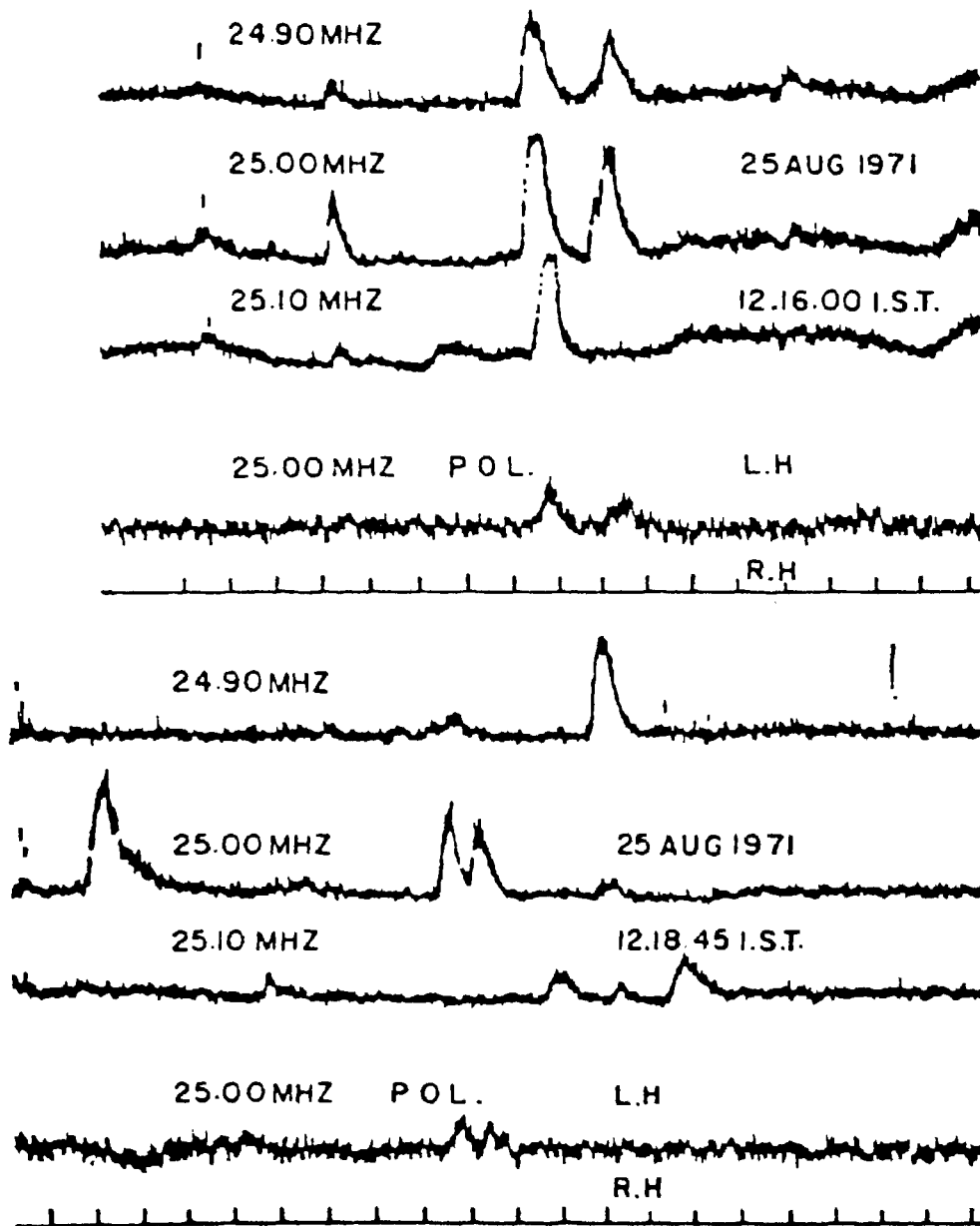
Fig. 4.1. A Typical example of a drift pair bursts (Sastry, 1971)

grams (Dulk et al 1984). The DP events studied in this paper, occurred in the range 25-65 MHz, 85% of which occur in the range 35-60 MHz.

Previous observations are summarised in Table 4.1 depicting the frequency range of occurrence, drift rate, single frequency durations, time delay, etc., in order to compare with our observations.

4.2.1 Time Delay

In the majority of DPs both the traces show identical fine structures precisely at same frequency with a time delay, although in a few cases the starting and ending frequencies are slightly different. The time delay (t_{12}) between the two traces is almost constant and independent of the frequency of occurrence. It does not seem to depend on the frequency drift, intensity or any other parameter. Our analysis shows that for a majority of the DPs, t_{12} lies in the range 1.5 to 1.9s.

4.2.2 Single frequency duration

The single frequency duration of each element lies in the range 0.9s to 2.5s, similar to other observations. The duration at a fixed frequency is not the same for both the traces and it does not depend either on frequency of occurrence or drift rate.

92

TABLE - 4.1

Reference	Roberts (1958)	Ellis (1969)	De la Noe & Moller-Pederson (1971)	*MPSM	Abranin et al (1977)	Suzuki & Gary (1979)	Present study
Frequency Range of Occurrence (MHz)	70-40	25-60	20-40 40-80	25-50	24-26 12-13	24.7.74	25-65
drift rate MHz s^{-1}	2-8	1.2	2-8	2-8	1.47	4	1-3
Duration of a single burst (s)	—	—	—	—	—	—	1.75 2.5
Time delay (s)	1.5-2	1.2	1.5-2	1-2	2	1-2	1.5-1.9

*Moller-Pedersen, Smith & Mangeney (1978).

4.2.3 Frequency drift

The fact that a majority of DPs have reverse drift is brought out in our analysis also where about 70% have reverse drift. About 26% of the observed bursts drift from higher to lower frequencies. The remaining 4% of the bursts appear as vertical traces in dynamic spectrum implying that the drift rate is enormously large or the emission occurs simultaneously at all the frequencies. It is clear from our analysis that in 34% of the cases the two It is clear from our analysis that in 34% of the cases the two traces have similar drift rates while in about 46% of the events show slightly different drift rates for the two elements. The magnitude of the drift rate is almost same for both forward and reverse drift pairs, and lies In the range 1 to 3 MHz/Sec [see fig. 4.2]. It is very intersting to note from the fig.4.3 that the drift rate decreases as the frequency of occurrence increases. Our analysis contradicts the earliest results in that the frequency drift decreases with increasing frequency. Fig.4.4 is an example of vertical DPs.

4.2.4 Polarizon

The DPs occur in both the polarization channels with almost same intensity (see fig.4.1 and fig.4.4) indicating that
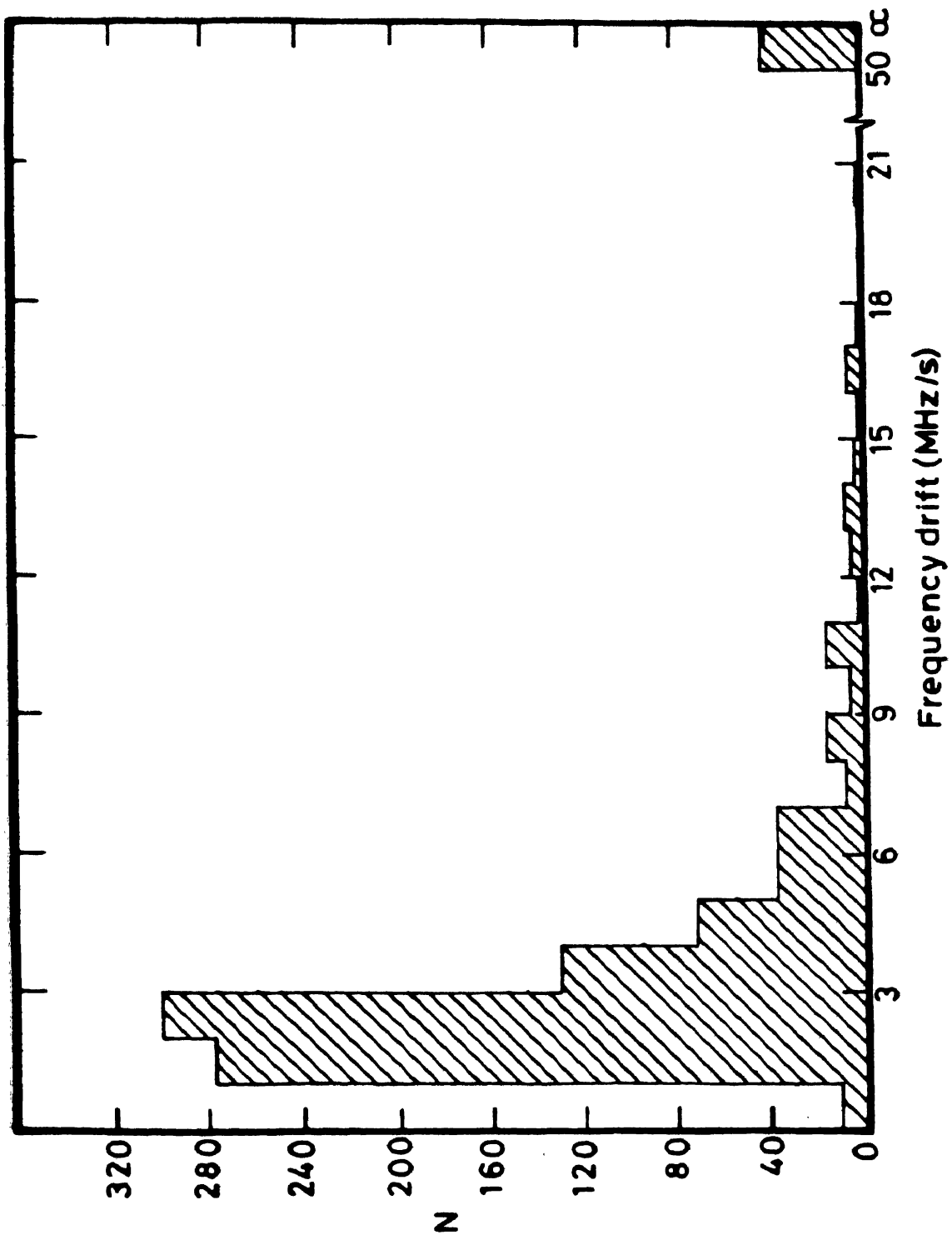
Fig. 4.2. Histogram of frequency drift of the DP bursts.
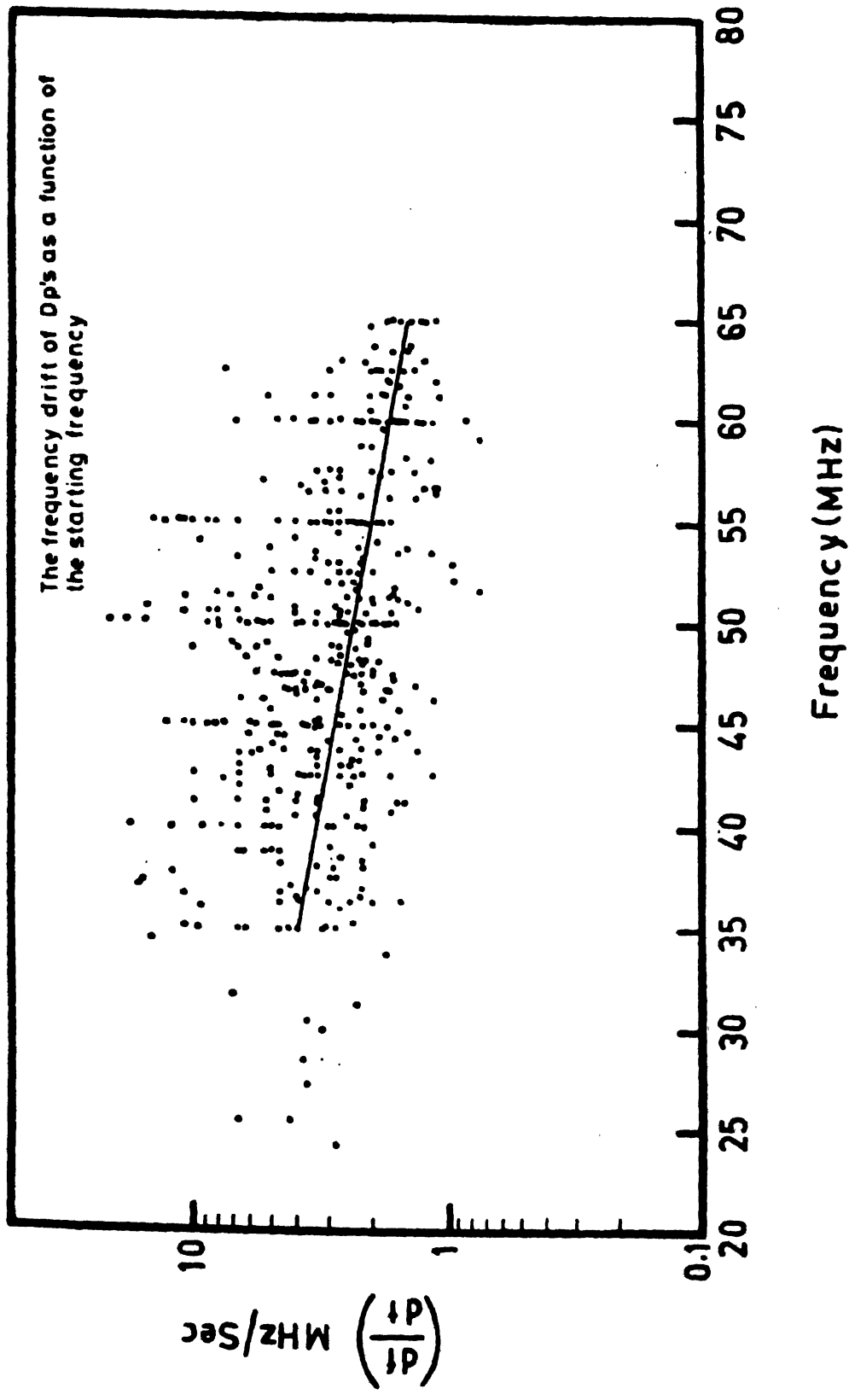
Fig. 4.3. The frequency drift of DP's as a function of the starting frequency.
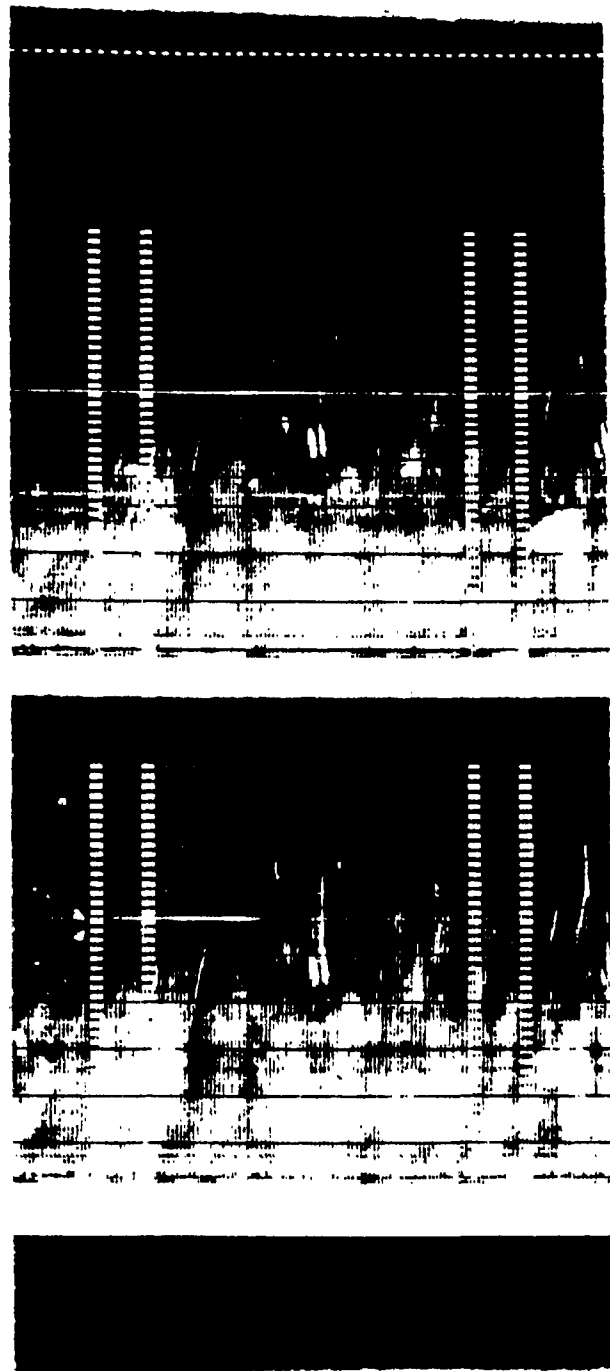
Fig. 4.4. An example of a vertical DP.

the DPs are very weakly polarized. It is also noticed that the background continuum is polarized in the left handed sense, as expected.

4.2.5 Intensity ratios

We have measured the ratio of the intensities of the elements in DPs observed using the Gauribidanur Radio Telescope,and found that the intensity ratio at a fixed frequency is less than or equal to one ($I_R \in [0.6,1]$).

4.3 DP chains

Occasionally the DPs are found to occur in chains (fig.4.5) The number of DP's in a chain ranges from 2 to 4. The chain as a whole also has a slope in the f-t plane indicating that the chains have drift rates similar to that of DPs. The chains occur over a bandwidth of 10 MHz and they drift from lower to higher frequencies in a majority of cases. About 50 DP chains were observed of which 43 have reverse drift 7 have forward drift and one appears like vertical trace. It is also found that the numbers in a chain can have different drift rates as ·in the case of type I chains. The individual members may differ in the duration at a fixed frequency the life time, that total bandwidth etc. Among the fifty chains, 39 contain two DPs, 8 contain 3 members and in three of the chains there are 4 members. The frequency drift of the chains is measured and depicted in the fig. 4.6.
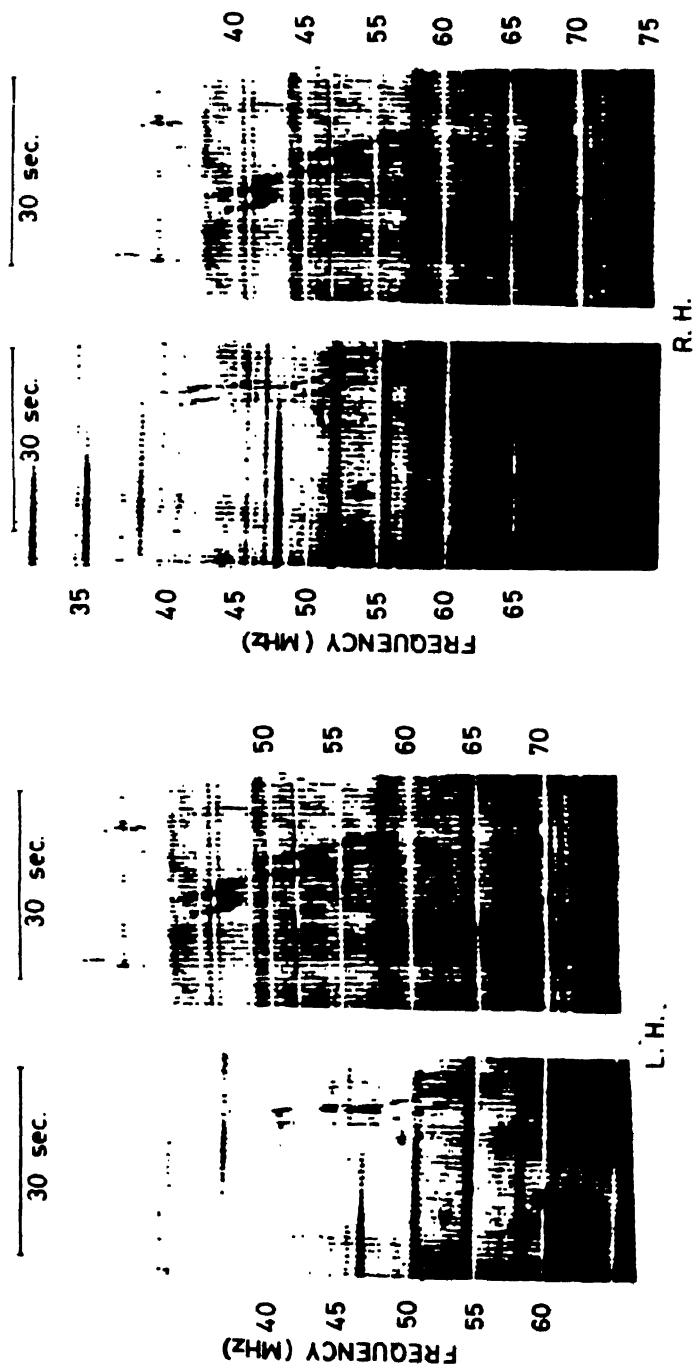
Fig. 4.5. A typical examples of DP chains in both circular polarizations. (Thejappa et al 1986)
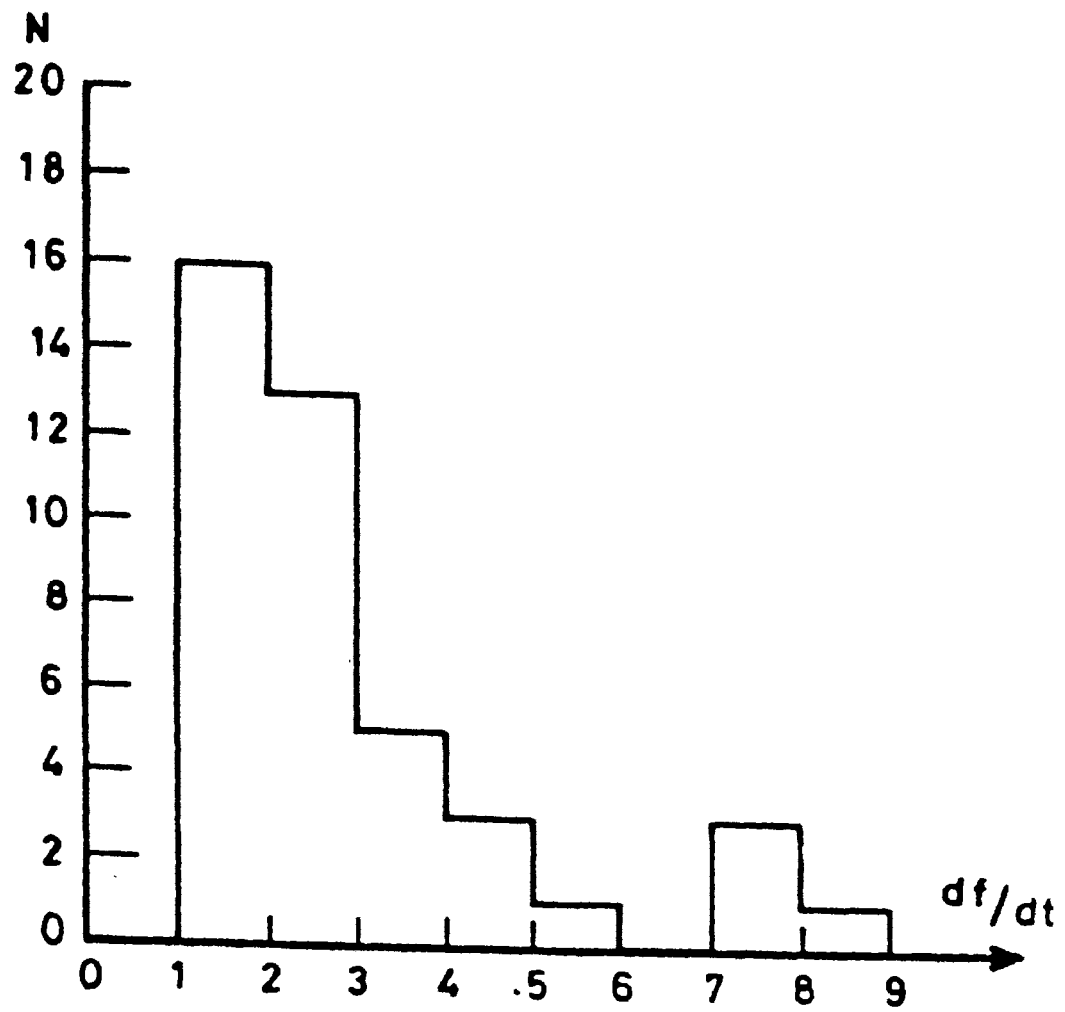
Fig. 4.6. Histogram of the frequency drift of DP chains (in MHz s^{-1}).
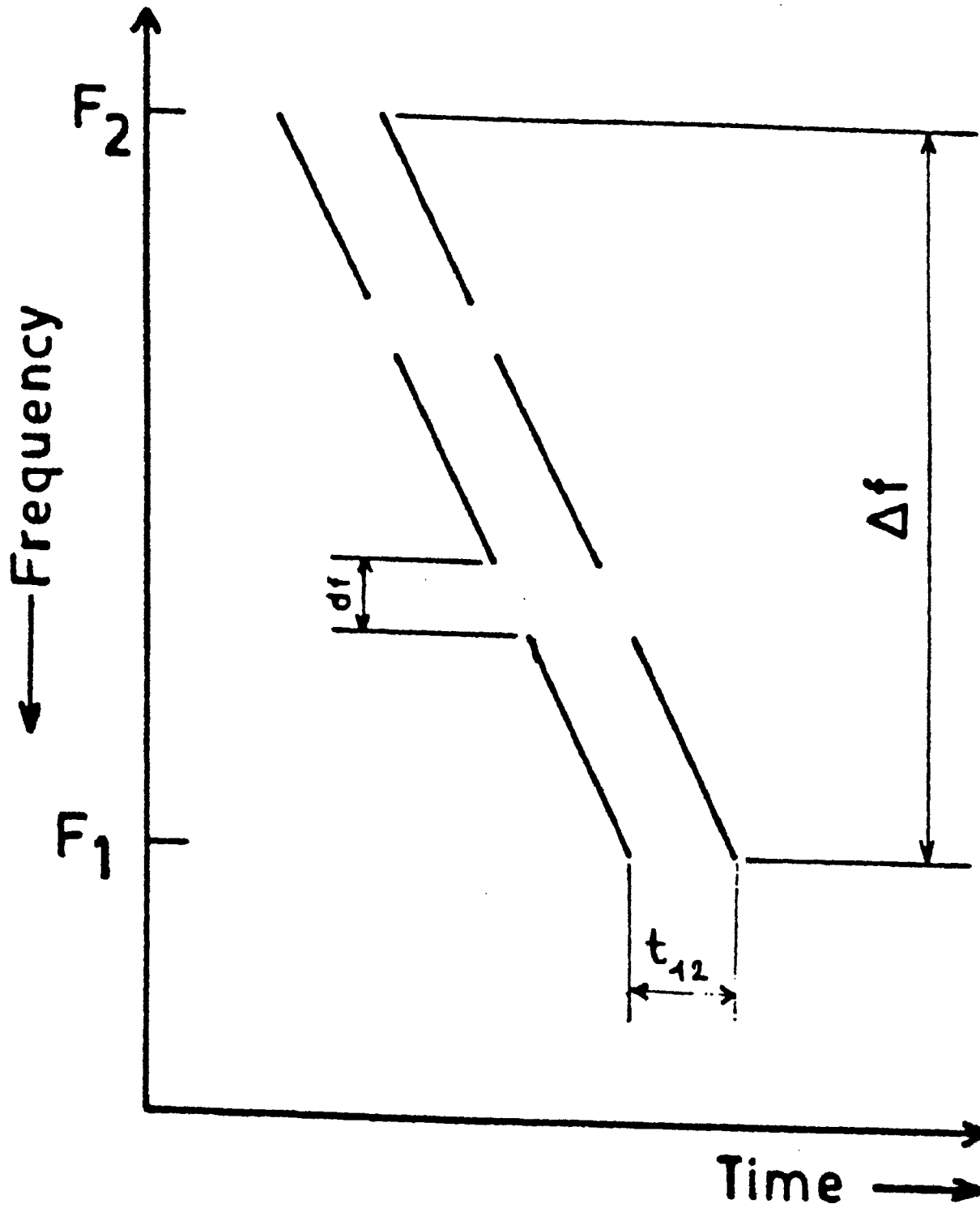
Fig. 4.7. Main characteristics of a typical DP chain, where Δf - Total bandwidth, t_{12} - time difference and df-frequency interval between the two consecutive DPs.

It is clear from the histogram that the frequency drift rate lies between 1 and 3 MHz s^{-1} which is in agreement with the frequency drift measurement of a single DP (Ellis, 1969, de la Noe and Pedersen, 1971; Abranin et al 1977). There are about 11 DP chains whose drift rates are very large and in one among them, the elements look like traces parallel to frequency axis. The least square fit to the data points whose drift rate is less than 6 MHz s^{-1} showed that the drift rate decreases as the frequency increases. The curve fitted for the above data point is

$$f = -0.21f + 1.5 \text{ MHz s}^{-1} \qquad (4.1)$$

where f is the central frequency of the DP chain in MHz. The main characteristics of a typical DP chain is presented in Fig.4.7.

4.4 Vertical drift pairs

Roberts (1952) noted that the frequency drift of some drift pairs, he recorded was very large. In most of these cases the condition existed only at frequencies near 40 MHz and the rate decreased at higher frequencies. In two cases, however all frequencies in the burst occurred simultaneously within the limits of measurement. Abranin et al (1977) also reported detection of bursts with very large drift rates, which appear sometimes like vertical traces in the f-t plane. In the present study we have found that about 4% of the observed 1006 events are similar bursts where the emission occurs simultaneously at all frequencies. The time delay t_{12} between the traces remains as in the case

of the other DPs which is about 2 seconds. The total duration, bandwidth and polarization also are the same as for the other DPs.

Here one should note that in additon to the already reported variants of DPs like hook bursts, triple bursts, etc., there are some peculiar events like four elements with the third trace having a small bandwidth, DP's with curved traces: events where one of the traces appears to have a branch trace etc. The appearance of many DPs in the dynamic spectra is very random, and therefore events like hook bursts or bursts which look as if they diverge from a point or converge to a single point may be just due to coincidence.

4.5 Interpretation

Most of the interpretations in the literature explain only a limited number of characteristics of DPs. The complexity with which the DPs occur in the dynamic spectrum indicates that the processes going on in the decametric corona are complex. Therefore any simple interpretation based on one or two observational facts like drift rate etc will not explain all the features of the DPs self consistently. The corona at decametric wavelengths is a special region because the magnetic field lines are predominently open. This is clear from the transtion of type I to type III bursts. The type I bursts are supposed to occur at the top of closed magnetic fields and when the field lines open up,

electron beams are ejected into the corona which subsequently produce strom type III bursts. Some of these beams might become diffuse due to quasi-one-dimensional relaxation and generate decametric continuum radiation (Levin, 1982). Since DPs also occur in such a region, these electron beams in particular stages of their evolution could supply the necessary energy in DP radiation. It is difficult to think of any other source of free energy available in the decametric corona.

Once the electron beam is fixed as the source of energy, it is tempting to think that the frequency drift of the bursts is caused by the movement of the electron beam in the corona. But the random slopes of DPs in the dynamic spectrum, specially the vertical traces indicate that the drift is not caused by the physical movement of any agency like a shock or an electron beam. Therefore one should look for a radiation mechanism which accounts for the observed drift rates without involving the movement of the exciting agency. Keeping these in mind, let us crtically discuss the existing theories.

Roberts (1958) interpreted that both components of the drift pairs are due to plasma emission at the second harmonic and that the first component escapes directly from the corona, the second component is an echo, i.e. a reflection of the harmonic radiation at the relevant plasma level, lower in the corona. He also puts forward two possible explanations of the reverse drift in RDPs: (1) an exciting disturbance (electron stream),

travels downward in the corona with speed $V \sim (2-5) \times 10^4$ km/s. (2) Type III exciting electron streams encounter 'hills' in the electron density of the corona. If echo hypothesis expalins the DP burst radiation, it should also predict a similar 'echo' for other types of bursts, especially for type III, which is not observed. The other objections for echo hypothesis are : (1) the absence of a single burst at fundamental frequency (2) the scattering of the reflected radiation should make the second element more diffuse, and (3) the appearance of triple bursts etc.

Zheleznyakov (1965) pointed out that, a casual electron stream generates an ordinary type III burst as it moves through the outer layers of the corona. On encountering a coronal irregularity denser than the surrounding corona (hill) and of comparatively small size, the agent will excite plasma waves that get reflected from the hill. The generated and reflected plasma wave interact through combination scattering to produce a short lived burst with reverse drift. He also explains the high brightness temperatures of DPs, since the emission is due to combination scattering of plasma waves. The above interpretation expalins only reverse drift.

Møller-Pedersen et al (1978) assume the existence of magnetosonic solitons propagating at large angles to the ambient magnetic field, of a streamer. Upon entering the streamer, these pulses steepen as they propagate into the higher density,

lower- region towards the axis. At some point the magnetic profile will be so steep that the current density exceeds the critical value at which low-frequency intabilities start. Through these current instabilities, the magnetic energy of the pulse is transferred to plasma layer in a very short time. The layer expands with super Alfenic velocity, generating shock waves on both sides of the inital instability point. These shock waves generate ion sound turbulence which causes the generation of Langmuir turbulence through turbulent bremsstrahlung but only in those regions of the streamer, where plasma β is small. The time delay t_{12} is due to the delay involved in the inward propagating shock crossing the axis of the streamer and entering the low- β region on its far side. The emission is fundamental plasma emission with the band width determined by that of Langmuir waves.

According to Møller-Pederson et al (1978), the two components of the DPs are generated on opposite sides of the streamer. As the magnetic field is oppositely directed in the two source regions, emission in the first component is polarized in one sense and the second component in the opposite sense, contrary to the observations of Sastry (1972) and Suzuki and Gary (1979). The theory predicts more forward DPs than reverse DPs, and when RDPs occur they should be related to the FDPs in the form 'hook' bursts. But observations show relatively less number of FDPs and hook bursts and not all RDPs are related to FDPs. There are problems in the pairing mechanism also. According

to the theory the radiation is confined in a small range of angles about $\psi = \frac{\pi}{2}$ where ψ is the angle between the emerging ray and the streamer axis. Further refractions and/or reflections are required to account for two parallel rays being directed towards the Earth. Moreover, nothing has been mentioned about the origin of the solitons.

Melrose (1982) suggested that the two traces in a DP are due to two rays from a single source (the echo hypothesis), which is within an overdense flux tube inside a conical coronal duct. Fundamental plasma radiation is assumed to be generated over the cross section of the flux tube by an exciter which moves up (forward DP) or down (RDP) the flux tube. Two parallel emerging rays, one reflected from the near side of the duct and the other from the far side of the duct give rise to two parallel traces.

The qualitative explanation given by Melrose (1982) by combining some aspects from Møller-Pedersen et al (1978) and Roberts (1958) is also not satisfactory. This is because the exciting agency is not clearly indicated. Since Melrose (1982) attributes the drift rate to the physical movement of an exciting agency, the DPs which appear as vertical traces are not explained naturally. If the electron beam is assumed as the exciting agency, one should be clear about the origin of the electron beams because in the decametric corona the injection of electron beams, towards the sun is less probable. Since the magnetic field lines are

predominantly open, one expects more of forward DPs than reverse ones due to electron beam movement. This again supports the idea that the drift may not be caused by the movement of the exciting agency. Melrose (1982) predicts a frequency difference between the two traces especially when the viewing angle or the angle made by the flux tube with the axis of the duct are more. Since there are no specific limits set on these anles, one expects more of frequency difference rather than time delay. Melrose (1982) predicts that the two rays producing the DPs should be separated by a distance equal to that of the distance across the duct. This is contradictory to the observations that two rays emanate from the same region (de la Noe and Gegeley, 1977, Suzuki and Gary 1979). According to this conical duct hypothesis one expects a ring rather than two points for a particular frequency because of the three dimensional character of the duct. The conical nature of the duct indicates that the separation between the pair should increase with decrease in frequency whereas observations indicate that the separation is independent of frequency.

Zaitsev and Levin (1978) proposed a new mechanism for the generation of drift pairs. According to them, the same stream of fast electrons which is reponsible for type III radio bursts is responsible for the generation of drift pairs.

The generation of type III burst is due to Cherenkov plasma emission. The interaction of the beam particles and the plasma waves excited, lead to theformation of a beam distribution

function of the 'Quasi-Plateau' type with respect to longitudinal velocities with a certain limiting velocity Vs. Such a distribiution is unstable relative to the excitation of plasma waves through the normal Doppler effect, if the edge of the plateau is deformed in such a way that, in some regions of longitudinal velocities $V_{//} > V_s$ a section develops with a positive derivative of the beam distribtuion function with respect to the transverse velocities. The most efficient excitation of plasma waves in this case occurs in those layers of the corona where the condition of double plasma resonance is satisfied. Since the region of the instability is tied into the limiting velocity V_s of the plateau, while the limiting velocity varies with time, the position of the double plasma resonance i.e., the frequencies of the excited plasma waves also vary with time. The direction of motions of the resonance region and hence the sign of the frequency drift of the narrow-band bursts depend on the local ratio of the magnetic field gradient to the coronal density gradient. Drift pairs with positive and negative frequency drift are both possible.

Abranin et al (1977) Zaitsev and Levin (1978) successfully explain the relatively small number of bursts at a fixed frequency is due the disappearance of the positive derivative of the beam distribution function with respect to the transverse velocities as a result of the intense excitation of plasma waves in several very close regions of double plasma resonance.

Abranin et al (1977) also calculate the time delay as

$$t_{12} = \frac{2 z c}{V_s^2} \frac{\Omega_H}{\Omega_k} \approx \text{const; if } \frac{\Omega_H}{\Omega_k} \approx 1/2, \text{ where } \Omega_H$$

and Ω_k are the electron cyclotron and upper hybrid frequencies, Z is the distance from the injection region, c and V_s are the velocities of light and beam respectively.

The interesting part of this theory is that the drift rate is not attributed to any physical agency but to the shift of the resonance region. The theory of Zaitsev and Levin (1978) does not explain why the majority of DPs not associated with type III bursts and also it does not explain the excess of polarization of DPs in comparison with storm type IIIs (Dulk et al 1984). Also one needs to change the slopes of the curves $\Omega_H(Z)$ and $k_{||} V_{||} + \Omega_H(z)$ very rapidly to explain the appearance of both positive and negative drift bursts within a few seconds.

4.6 Discussion

The drift pair chains and the vertical drift pair bursts reported by us may provide some very important clues to understand the complex plasma processes taking place in the outer corona.

4.6.1 DP chains

The individual members in drift pair chains have the same characteristics as the usual DP bursts. Therefore, the same agency should be responsible for all the members. In this case the conditions for the generation of DPs to be intermittently

satisfied so that one sees a chain. It is interesting to compare these chains with type I chains. In the case of type I chains the condition for generation of individual type I bursts is intermittently satisfied along with path of a weak shock in the corona (Wentzel, 1982). The slow drift rate of the type I chains corresponds to the shock velocity (Wild and Tlamicha, 1964). As pointed out above some of the DP chains have very large frequency drift. Therefore, the physical movement of an agency is probably not the cause of the drift. It has to be caused by some characteristic of the medium such as the double plasma resonance (Zaitsev and Levin, 1978). Abranin et al., (1977) and Zaitsev and Levin (1978) put forward a hypothesis that the DP bursts are generated while the quasiplateau type electron beam with positive derivative of the distribution function with respect to the transverse velocities crosses the regions of the double plasma resonance successively. Depending upon the slopes of $\Omega_h(z)$ and $K_{||} \cdot V_{||}$ $:: + n\Omega_H$ (z) the coordinates of double plasma resonance increase or decrease, causing negative or positive frequency drift. The disappearance of the instability region in the distribution function as a result of the intense excitation of plasma waves in several very close regions of double plasma resonance puts the constraints on the number of bursts at a fixed frequency.

We propose that the condition for double plasma resonance is intermittently satisfied along the extent of the beam. The instability region appears and disappears along the spatial extent of the path of the beam. The structure of the density or the

magnetic field may be oscillatory in space causing the intersection of $\Omega_k(z)$ and $K_{//} \cdot V_{//} + n\Omega_H (z)$ at different points In space at the same time at short intervals. The localized fluctuations in density and magnetic field, as evidenced by observations (Yakobalev, et al, 1980) may be responsible for such an oscillatory nature.

4.6.2 Vertical drift pairs

The drift pairs which occur simultaneously in all the frequencies have the drift rate tending to infinity, which is not feasible physically, because this needs any exciting agency responsible for such bursts to travel with velocities faster than velocity of light.

Abranin et al (1977) and Zaitsev and Levin (1978) proposed that the relative slopes of $\Omega_k(z)$ and $K_{//} \cdot V_{//} + n\Omega_H (z)$ define the drift rate and show that the anomalously high rate of frequency drift arises in those cases where the derivatives with respect to z of the functions $\varphi_n(z) = 1 - n\Omega_H /\Omega_h$ and $V_{//}/c$ are close in value in the region of their intersections (c being the velocity of light).

Assuming similar arguments, Zaitsev and Levin (1978) derived a formula for the drift rate as:

$$\frac{\partial f}{\partial t} = f \frac{V_{//}}{2} \left\{ 1 + \frac{n\Omega_H}{k_{//} V_{//}} \left(\frac{1}{H} + \cdots - \frac{1}{2N} \frac{\partial N}{\partial z} \right) \right\}^{-1} \frac{1}{2N} \frac{\partial N}{\partial z} \qquad (4.2)$$

where f is the frequency, $V_{//}$ is the limiting velocity of the beam. When the frequency drift rate tends to infinity, the denominator of the above expression tends to zero i.e.,

$$1 + \frac{n\Omega_H}{k_{//} V_{//}} \left[\frac{1}{H} \frac{\partial H}{\partial z} - \frac{1}{2N} \frac{\partial N}{\partial z} \right] = 0 \qquad (4.3)$$

since $k_{//} = \frac{\sqrt{3}}{2} \frac{\Omega_p}{c}$ the above equation reduces to

$$\frac{1}{H} \frac{\partial H}{\partial z} - \frac{1}{2N} \frac{\partial N}{\partial z} = - \frac{\sqrt{3}}{2} \frac{\Omega_p}{n\Omega_H} \frac{V_{//}}{c} \qquad (4.4)$$

for n = 1; and $V_{//}$ = 1/3 c; the equation becomes

$$\frac{1}{2N} \frac{\partial N}{\partial z} - \frac{1}{H} \frac{\partial H}{\partial z} = 9.3 \times 10^{-4} \frac{\sqrt{N}}{H} \qquad (4.5)$$

Now if we assume that the density in the corona where the DPs are predominant is the same as in the unperturbed corona and only the magnetic field is perturbed i.e., different from the usual corona, we can write the above equation if we assume that the density and magnetic field obey the following laws:

$$N(z) = 4.2 \times 10^4 \times 10^4 \times 10^{4.32/(a+z)} \qquad (4.6)$$

and

$$H(z = 0) = 0.5 (a-1)^{-1.5} \qquad (4.7)$$

as (Dulk & McLean, 1978)

$$\frac{\partial H}{\partial z} + \frac{4 \cdot 97}{(a+z)^2} H = -0 \cdot 19 \times 10^{(2 \cdot 16/(a+z))} \qquad (4.8)$$

Here we assumed that the upper limit of the DP bursts bandwidth is around 65 MHz which corresponds to a $\approx$ 1.4 solar radii from the center, z corresponds to the radial distance in the corona where the DP activity is confined. The equation (4.7) can be used as a boundary condition to solve equation (4.8), which gives:

$$H = \exp\left(\frac{4 \cdot 97}{a+z}\right)\left\{0 \cdot 5(a-1)^{-1 \cdot 5} \exp\left(-\frac{4 \cdot 97}{a}\right) - 0 \cdot 19 z\right\} \qquad (4.9)$$

Similarly if we assume that the magnetic field is unaffected by the DP activity and only the density is affected, then we get the following differential equation:

$$\frac{1}{2N} \frac{\partial N}{\partial z} - 1 \cdot 86 \times 10^{-3}(a+z-1)^{1 \cdot 5} \sqrt{N'} = -\frac{1 \cdot 5}{a+z-1} \qquad (4.10)$$

here we have used that the magnetic field varies as given by Dulk & McLean (1978) :

$$H = 0.5 (a + z - 1)^{-1.5} \qquad (4.11)$$

If we use
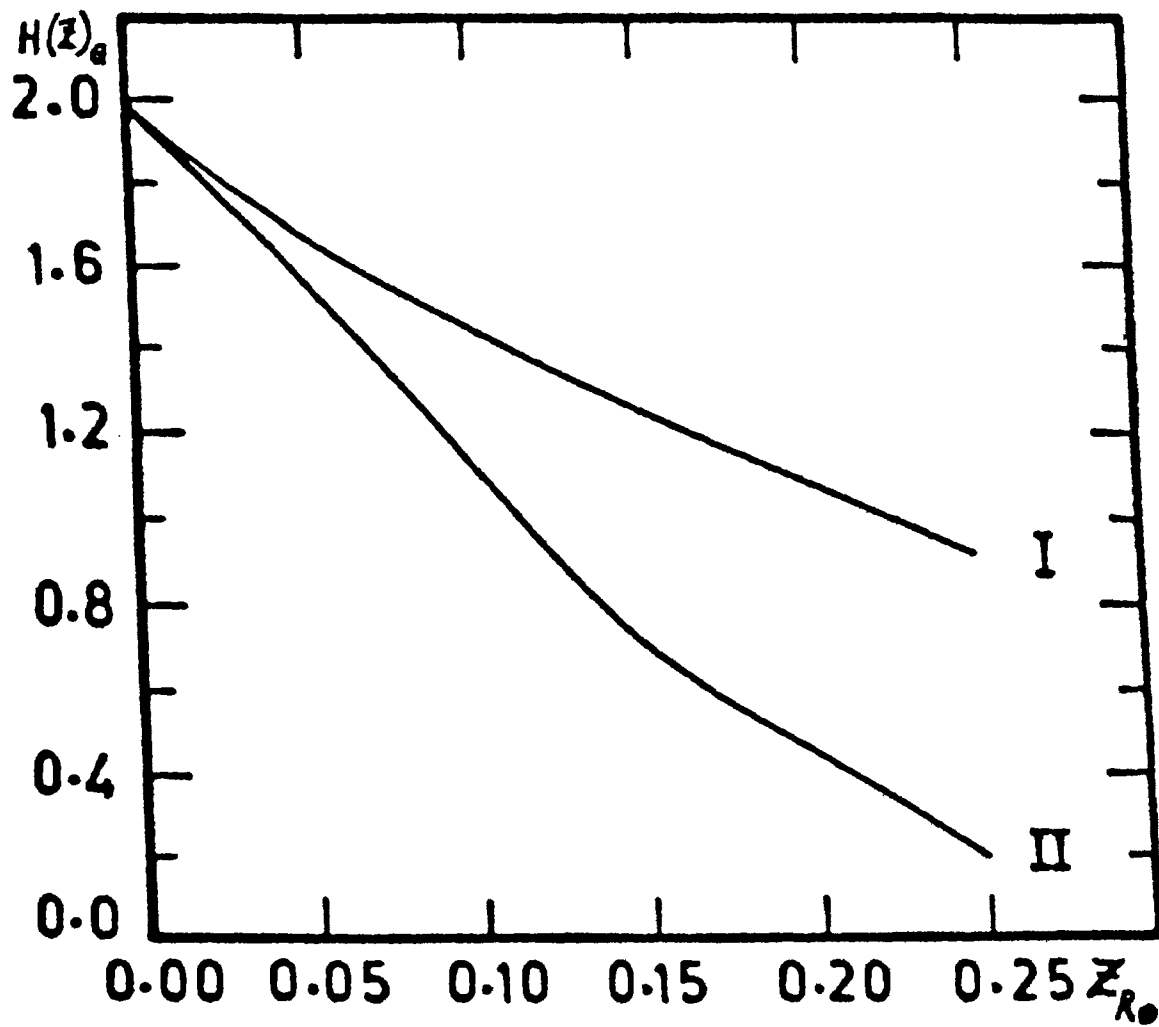
Fig. 4.8.　　Variation of the magnetic field H with radial
distance in the DP active region (I) and in quite
corona (II).
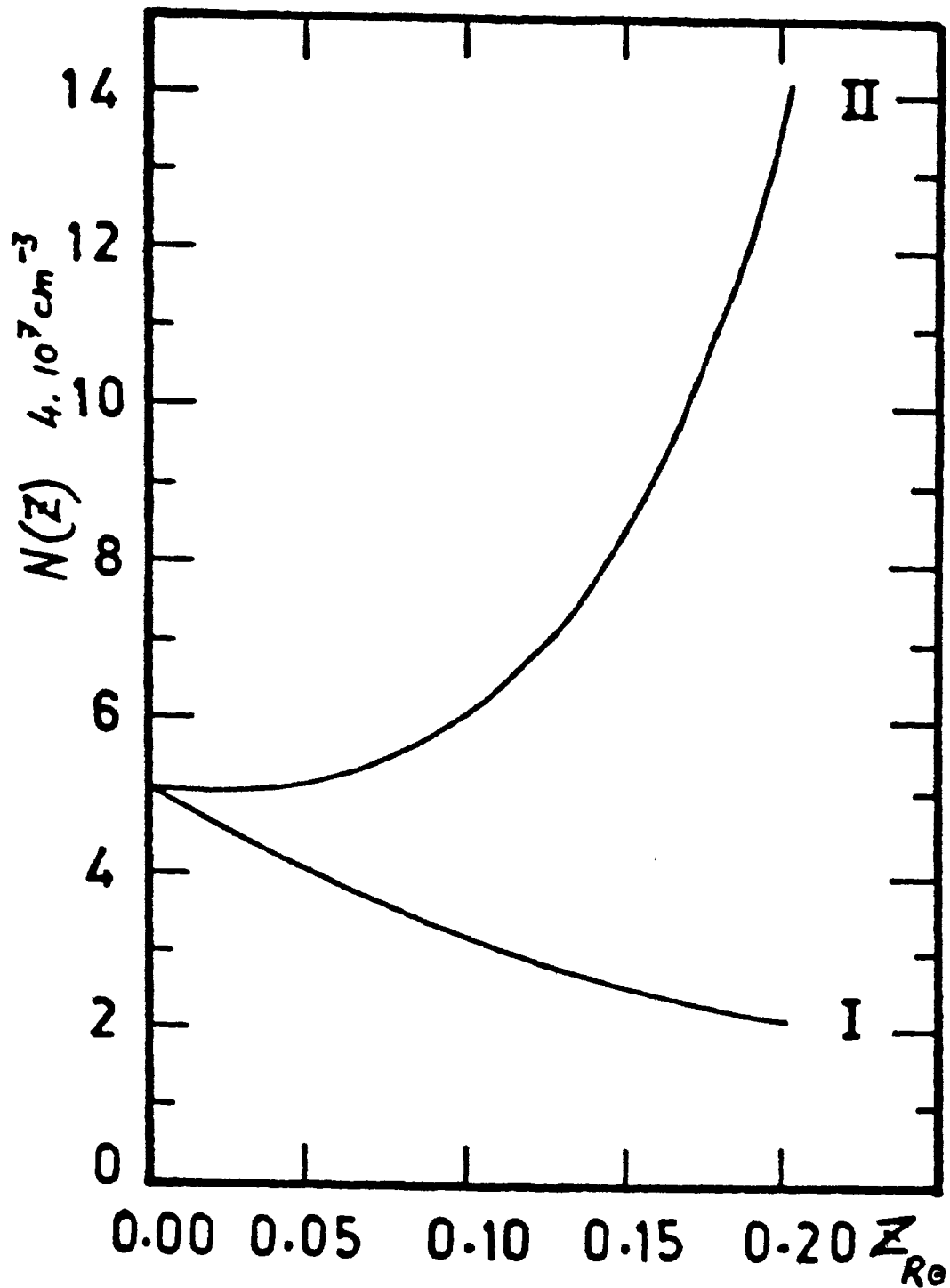
Fig. 4.9. Variation of the density N with radial distance in the DP active region (I) and in quite corona (II).

$$N(z = 0) = N(a) = 4.2 \times 10^{4} \times 10^{4.32/a} \qquad (4.12)$$

as the boundary condition, the equation (4.10) can be solved, the solution of which is :

$$N(z) \sim (a+z-1)^{-3} \left[5(a-1)^{-1.5} \times 10^{-(2.16/a + 2)} - 1.9 \times 10^{-3} z \right] (4.13)$$

In Fig.4.8 and 4.9 we have sketched the variations of H and N in DP active region and also in unaffected variation for comparison. It is clear from the figures that the magnetic field should decrease very steeply when the density is not varied and the density should increase very steeply when the magnetic field is unaffected to produce DPs with very high drift rates.

4.7 Conclusion

We have reported some new observational results regarding the enigmatic DP bursts occurring in the decametric region. The reported drift pair chains and the vertical DPs indicate the complexity of decametric corona with a free energy source which causes these peculiar radio signatures. As the magnetic field in this region is predominantly open, one cannot think of a free energy source propagating sun-ward most of the times to explain the predominant reverse drift pair chains. In addition to this, the appearance of the vertical chains and DPs rules out the possibility of an agency moving in the corona causing the observed

drift. These observations lend support to the idea that the reso-
nance layer in which the radiation is generated is different at
different instant of time so that one gets a slope in the frequency-
time plane. If one assumes considerable fluctuations in some
macroscopic parameters such as density and magnetic field,
supported by observations (Yakobalev, 1980) then it is possible
to have drifts of all directions as the drift rate depends upon
the medium in which the fluctuation occur. Therefore, it has
been shown that the magnetic field decreases steeply if we assume
that the density of the medium is not affected by the DP activity
when the frequency drift is very high and it is shown that the
magnetic field H is given by :

$$H = exp\left(\frac{4.97}{a+z}\right)\left\{0.5(a-1)^{-1.5}\,exp\left(-\frac{4.97}{\alpha}\right) - 0.19\,z\right\}$$

when $N = 42 \times 10^4 \times 10^{4.32/a+z}$ And similarly if we assume
that the magnetic field is unaffected and is given by the formula
$H = 0.5(a + z - 1)^{-1.5}$, then the variation in density in DP activity
region where $\frac{\partial f}{\partial t} \rightarrow \infty$ is given by

$$N(z) \sim (a+z-1)^{-3}\left\{5(a-1)^{-3/2} \times 10^{-\left(2.16/a+z\right)} - 1.9 \times 10^{-3}z\right\}$$

There the fluctuations in the magnetic field and density can
produce very high drift rates.

CHAPTER V

A SELF CONSISTENT APPROACH TO THE THEORY OF TYPE II
SOLAR RADIO BURSTS

5.1 Introduction

Historically, soon after the introduction of the solar radio-spectrograph observations the slowdrift bursts had been recognized as a special phenomenon and were classified as type II bursts by Wild and McCready (1950). A typical example of the dynamic spectrum of a type II burst is shown in the figure 5.1. Usually type II bursts are characterized by:

I. Drifting ridges of emission, with bandwidth as low as a few MHz.

II. Fundamental and harmonic spectra of similar form.

III. Splitting of both components into two bands $\sim$ 10 MHz apart for fundamental, $\sim$ 20 MHz for harmonic (not seen in all type II).

The starting frequency of the fundamental component is usually below 100 MHz, but can also reach higher frequencies, say 250 MHz. Correspondingly the second harmonic features are observed at twice the frequency.

The polarization of type II bursts is typically random; however, complex polarization structures can also be obtained.

Type II bursts, which are characterized by the slow drift

Fig. 5.1. A Typical example of the dynamic spectrum of a type II solar radio burst. (Wild and Smerd 1972)

in their spectral features from high to low frequencies are generally accompanied by a large flare. On the plasma hypothesis the frequency drift is found to correspond to a velocity of the order of 10^3 km/sec and the moving source had been identified with a flare-associated collisionless MHD shock wave (Pikel'ner and Gintzburg (1963), Kundu (1965)). Later, direct evidence for the generation of type II radiation by shock waves was given by the space observations of interplanetary type II bursts and interplanetary shock waves [Malitson et al., 1973, Cane et al., 1982]. The estimates of type II shock speeds are subject to considerable error because of the uncertainty in the coronal density models. Velocities derived from heliograph observations of source positions are even more uncertain because of the imperfectly known effects of coronal scattering and refraction and of ionospheric refraction [See Nelson and Melrose, 1985].

Although it is evident that type II solar radio bursts are produced by collisionless shock waves, there is no general agreement about the microscopic processes that actually give rise to radio emission since the details of the burst generation are not clear yet.

One of the possible means of burst generation by collisionless shock waves moving across the magnetic field was proposed by Pikelner and Gintzburg (1963) and developed by Zaitsev (1977); it is connected with the Buneman instability developing in the shock front. This instability is due to the relative motions of ions and electrons. However, the excited plasma waves have

low frequencies. The rising of the plasma wave frequency ω_{P_e} needs subsequent induced scattering on nonthermal electrons that leads to the broadening of the spectrum upto $2\,\omega_{P_e}$ and to its isotropization. So the transformation of plasma waves into electromagnetic waves gives rise to the radio emission in a wide frequency band $\omega_{P_e} \leq \omega \leq 2\,\omega_{P_e}$. The harmonic structure of the emission spectrum can be obtained only when the plasma wave spectrum is isotropic and has two maxima with respect to k; one in the region of plasma wave pumping and the second in the region of dissipation due to the radiation losses.

Lampe and Papadopoulos (1977) proposed that type II emission can be associated with acceleration of electrons by lower-hybrid waves followed by nonlinear conversion. The lower hybrid waves were assumed to be generated by a current driven instability in the shock front.

Holman and Pesses (1983) proposed that shock dirft acceleration of electrons could be responsible for type II radio bursts. The streaming distribution of reflected electrons produced upstream of the shock front is unstable to the generation of electrostatic plasma waves, which in turn, could interact to produce the observed radio emission.

However, the mechanisms proposed are not general. In particular, they do not describe adequately an analogy between type III and type II bursts, which is often observed (Roberts 1959). Small type III bursts can grow on time scales of seconds from

the type II shock front, caused by electrons emitted from it. Certain type II bursts exhibit the so-called 'herring-bone' pattern in the dynamic spectrum consisting of a succession of fast drifting burst elements (Roberts, 1959).

The type III radio bursts, as it is well known, are produced by fast electron streams propagating along the magnetic field lines. From the analogy between the components of the type II bursts and the type III bursts, one can suppose that type II bursts are also generated by streams of accelerated electrons (McLean and Nelson 1977). It is natural to connect the radio emission of the coronal shock with the fluxes of the electrons as the most general and effective way of direct generation of plasma waves. Therefore in this case the key questions are those of electron acceleration and of the transformation of electron energy into electro-magnetic radiation. It is known that the radio-emission of the type II bursts may be very strong i.e., $T_b \approx 10^{11}$ K (Nelson and Robinson, 1975).

In this chapter we propose, that the majority of the type II shocks are supercritical since the estimated Mach numbers of the most of the type II shocks exceed the recently revised critical Mach number M_c by Edmiston and Kennel (1984), which lies, between 1 and 2 for typical solar wind parameters. This fact is also supported by the studies of the forward interplanetary shocks observed by ISEE-3 [Bavassano-Cattaneo et al 1986] where it has been shown that a majority of the interplanetary shocks

are supercritical. We also propose that many of the shocks responsible for the type II radiation have an overshoot, foot and ramp in the magnetic field structure in consistence with their supercritical character. The reflected ions which behave like a beam in the foot and ramp of the shock front, and like a ring in velocity just behind the overshoot [Leroy et al., 1981, 1982] accelerate electrons to ultra-relativistic energies both in the upstream as well as in the downstream through resonantly excited low frequency waves. [Papadopoulos (1981); Vaisberg et al., (1983); Galeev, (1984); Krasno-selskikh et al., (1985), Thejappa, (1986, 1987)].

Regarding the shock propagation angle relative to the magnetic field Dulk et al (1971) suggested that propagation is likely to be more parallel than perpendicular. These authors, however, could not arrive at any firm conclusions. Later Stewart and Magun [1980] analyzed a case where a transverse shock seemed to be required in order to explain the herringbone structure of a type II burst. Therefore the observational evidence is not consistent with either strictly perpendicular or parallel shock propagation for all type II events. The range of shock angles over which type II bursts can be produced seems to be quite large. The advantage of the proposed acceleration mechanism over the Fast Fermi process or the shock drift acceleration [Wu, 1984; Leroy and Mangeney, 1984; Holmann and Pesses, 1983] is that it is applicable for a wide range of shock angles.

It is well known that in some cases the fundamental and harmonic bands of type II bursts are split in two. The present

model is consistent with the qualitative model suggested by Smerd et al (1975), who attributed the split-band structure of type II bursts to simultaneous plasma-frequency emission from plasma ahead of and behind a type II shock front. Nelson and Robinson (1975) reported that at a given frequency the U and L sources were circular, essentially the same size and in the same position where U and L represent the upper frequency band and lower frequency band respectively. At the fixed observing frequency the L band is observed earlier in time than the U band and so it is inferred that at a given time the L source is further from the Sun than the U source confirming the model of Smerd et al (1975) for band splitting.

5.2 Electron Acceleration

Uchida (1974) proposed that the type II radiation comes both at fundamental and harmonic, from the low-V_A regions, where the shock has a relatively high Mach number. Gary et al., (1983) reported that the Mach number of type II shock lies in the range 1.3 to 3. Kennel et al (1982) first reported that among 10 interplanetary shocks, the fast wave Mach number M_F ranged from 1.3 to 4.7, where the critical Mach number $M_F \approx 2.5$. However Bavassano-Cattaneo et al (1986) reported that among 34 forward interplanetary shock waves observed by ISEE-3 during 1978 and 1979, 19 were supercritical, seven has a Mach number close to the critical Mach number, four were subcritical and the remaining four shock were ambiguous. However, the average critical Mach

number $< M_c >$ was taken as 1.5 due to its strong dependence on shock parameters.

Kennel et al (1982) as well as Bavassano- Cattaneo et al (1986) have detected large amplitude low-frequency electrostatic noise, Whistler turbulence and a high frequency ($\gtrsim f_p$) continuum near each shock and for upto several hours downstream. In the cases observed by Kennel et al (1982) no type II bursts were observed at 1 AU, although intense impulsive Langmuir waves were observed an hour upstream from one shock. Impulsive Langmuir waves were present for a few minutes on either side for other shocks.

It is well known that the structure of a shock wave propagating perpendicular to the ambient magnetic field in a collisionless plasma undegoes a distinct change of shape when the Alfven Mach number is increased above a critical value M_c. In addition to the ramp, the spacedraft observations [Russel and Greenstadt, 1979] show that there is a precursor structure of length equal to a few c/ω_{p_i} which appears closely associated with the presence of ions reflected off the ramp, and is usually called the "foot" where c is the velocity of light and ω_{p_i} is the ion plasma frequency. Also it is seen [Russel and Greenstadt, 1979] that in the immediate post-ramp region the magnetic field exceeds its downstream value (magnetic field overshoot) and develops further downstream a somewhat oscillatory behaviour with a scale length of an ion gyro-radius. Leroy et al (1981, 1982) from numerical computations showed that the reflected ions behave essentially like a beam

in the shock front (in the foot and ramp region), whereas they tend to form a gyrating stream in the downstream region behind the overshoot. Krasnoselskikh et al (1985) approximated the distribution function of the reflected ions in the foot and ramp as:

$$f_b^u = n_b \left(\frac{1}{2\pi \Delta V_b}\right)^{3/2} \exp\left(-\frac{(\vec{V} - \vec{V}_b)^2}{2\,\Delta V_b^2}\right) \tag{5.1}$$

where n_b is the reflected ion beam density, V_b and ΔV_b are the beam velocity and velocity spread respectively. More realistic representation of the reflected ion distribution function in the downstream, which includes thermal effects is the Dory-Guest-Harris distribution (Dory et al 1965):

$$f_b^d = \frac{1}{\pi^{3/2}(N+1)!} \frac{1}{\Delta V_{b_{\parallel}} \Delta V_{b_{\perp}}^2} \left(\frac{V_{\perp}}{\Delta V_{b\perp}}\right)^{2N} \exp-\left(\frac{V_{\parallel}^2}{\Delta V_{b_{\parallel}}^2} + \frac{V_{\perp}^2}{\Delta V_{b_{\perp}}^2}\right) \tag{5.2}$$

where N is the anisotropy index and $\Delta V_{b_{\perp}}$ ($\Delta V_{b_{\parallel}}$) is the thermal speed $\perp(\parallel)$ to the ambient magnetic field. [Thejappa, 1986; Akimoto et al 1985]. The reflected ion beam is the basic energy source of electron acceleration. The acceleration of electrons is due to the ion-beam-induced excitation of very low frequency plasma oscillations propagating almost across the magnetic field. Dealing with the mean parameters of the plasma in solar corona, let us suppose the following inequalities are valid: $\Omega_e \ll \omega_{p_e}$, and $\beta_{e,i} = \frac{8\pi m_o(T_e,T_i)}{B^2} \ll 1$. Here B is the strength of the magnetic field, n_o is the background plasma density, T_e, T_i are the electron and ion temperatures,

$$\omega_{P_j} = \left(\frac{4\pi n_0 \, e_j^2}{m_j} \right)^{1/2} \quad \text{and} \quad \Omega_j = e_j B / m_j c$$

are respectively the plasma frequency and cyclotron frequency of j-sort particles. The low density ion beam ($n_b/n_0 \ll 1$) with small thermal spread ($\Delta V_b \ll V_b$) moves almost perpendicular to the magnetic field and hence can effectively interact with low-frequency plasma oscillations, which have wave vectors almost perpendicular to the magnetic field lines. If we assume that the oscillation frequencies and wave vectors are in the range:

$$\Omega_e \gg \omega \gg \Omega_i \quad , \qquad \text{Im} \, \omega \gg \Omega_i$$

$$k_\perp \rho_{L_i} \gg 1 \gg k_\perp \rho_{L_e} \quad , \quad \frac{\omega}{k_\parallel} \gg V_{T_i} \quad , \quad \frac{\omega}{k_\parallel} \gg V_{T_e} \qquad (5.3)$$

where $V_{T_j} = \sqrt{2 T_j / m_j}$ is the thermal velocity of j-sort particles, $\rho_{L_j} = V_{T_j} / \Omega_j$ is the larmor radius of j-sort particles $k_{\parallel}$ and $k_\perp$ are the components of the wave vector, along and across the ambient magnetic field, it is possible to considedr that electrons are strongly magnetized and ions are not. Then one can easily write the dispersion equation for non-potential waves:

$$\varepsilon \left(\omega, \vec{k} \right) = 1 + \varepsilon_0 + \varepsilon_i + \varepsilon_e \qquad (5.4)$$

where

$$\varepsilon_0 = \frac{\omega_{P_e}^2}{\Omega_e^2} \left(1 + \frac{\omega_{P_e}^2}{k^2 c^2} \right) \frac{k_\perp^2}{k^2} - \frac{\omega_{P_i}^2}{\omega^2} - \frac{\omega_{P_e}^2}{\omega^2} \frac{k_\parallel^2}{k^2} \frac{1}{\left(1 + \frac{\omega_{P_e}^2}{k^2 c^2} \right)} \, , \quad (5.5)$$

is the contribution of the background plasma to the permittivity whereas ε_i and ε_e are the reflected ion beam and accelerated electron beam contributions respectively. The solution of $(1+\varepsilon_0)=0$ is the dispersion relation :

$$\omega^2 = \frac{\Omega_e^2}{\left(1+\omega_{P_e}^2/k^2c^2\right)}\left[\mu + \frac{\cos^2\theta}{\left(1+\omega_{P_e}^2/k^2c^2\right)}\right] \cdot \quad (5.6)$$

Here $\mu = m_e/m_i$ is the electron to ion mass ratio, $\cos^2\theta \equiv k_z^2/k^2 \ll 1$, $\vec{B} = B\,\hat{e}_z$. In the limit of short-wave oscillations $kc \gg \omega_{P_e}$ (5.6) describes the electrostatic oblique Langmuir waves and their frequency is equal (at $k_{//} = 0$) to or higher (at $k_{//} \neq 0$) than, the lower-hybrid resonance frequency ω_{LH}. With wavelength increasing i.e., $kc \ll \omega_{pe}$ the non-potentiality of oscillations becomes essential, and they turn into well-known whistlers. Here we confine ourselves to the case $k_{//}^2 \ll k_{\perp}^2$; this is justified by the fact that, as a rule, the particle energy density in the coronal plasma turns out to be of the same order as the magnetic field energy density; because of this, waves with $k_{11} > k_{\perp}\mu$, have a longitudinal phase velocity of the order of V_{Te} and thus, strongly damp. The quantity ε_i is given by:

$$\varepsilon_i = \frac{\omega_{P_i}^2}{k^2 n_o} \int \frac{\vec{k}\cdot\frac{\partial f_b}{\partial\vec{v}}}{\omega - \vec{k}\cdot\vec{v}+i0}\, d^3\vec{v} \qquad (5.7)$$

and the contribution due to acclerated electrons is :

$$\varepsilon_e = \frac{\omega_{P_e}^2}{k^2 n_o} \int \left(\frac{n\,\Omega_e}{v_\perp}\frac{\partial F_e}{\partial v_\perp} + k_{//}\frac{\partial F_e}{\partial v_{//}}\right)\frac{\zeta_n^2\, d^3\vec{v}}{\left(\omega - n\Omega_e - k_{//}v_{//}\right)}, \quad (5.8)$$

where $f_b(\vec{v})$ is the distribution function of the ion beam; F_e is the distribution function of suprathermal electrons over longitudinal velocities in a drift approximation and

$$\zeta_n = \frac{J_n\left(\frac{k_\perp v_\perp}{\Omega_e}\right)\left(1+ \frac{n\Omega_e}{\omega_k}\frac{\omega_{Pe}^2}{k^2 c^2}\right)}{\left(1+ \omega_{Pe}^2/k^2 c^2\right)} + \frac{\omega_{Pe}^2}{k^2 c^2}\frac{k_\perp v_\perp}{\Omega_e} J_n'\left(\frac{k_\perp v_\perp}{\Omega_e}\right) \quad (5.9)$$

[See Galeev, 1984]

Here $V_{//}$ and $V_\perp$ are the velocities of particles along and perpendicular to the magnetic field, respectively.

5.2a   Acceleration of electrons due to the presence of reflected
ions in the upstream (foot and ramp)

In the shock front (foot and ramp region) it is necessary to consider only waves with $k_\perp d \sim \frac{k V_b}{\Omega_i} > 1$, because the ion beam exists only in a region of finite thickness $d \sim \frac{V_b}{\sqrt{\Omega_i}}$. So the ions are automatically unmagnetized. Since the ion beam distribution in the foot and ramp region can be approximated by a drifted Maxwellian,

$$\frac{\omega_{Pi}^2}{k^2 n_0}\int d\vec{v}\, \frac{\vec{k}\cdot\frac{\partial f_b}{\partial \vec{v}}}{\omega - \vec{k}\cdot\vec{v}+i0} = \frac{2\,\omega_{Pi}^2\, n_b}{k^2 n_0\,(\Delta V_b)^2}\left[1+ \xi_i\, Z(\xi_i)\right] \quad (5.10)$$

where

$$Z(\xi_i) = \pi^{-\frac{1}{2}} \int_{-\infty}^{\infty} dx \; \frac{\exp(-x^2)}{(x - \xi_i)} \qquad (5.11)$$

and

$$\xi_i = \frac{\omega - \vec{k} \cdot \vec{V_b} + i0}{\vec{k} \cdot \Delta \vec{V_b}} \qquad (5.12)$$

The function $Z(\xi_i)$ defined in (5.11) is referred to as the plasma dispersion function. In the present case let us consider that

$$\omega - \vec{k} \cdot \vec{V_b} = \omega - k V_b \cos\varphi \approx k \Delta V_b \quad , \text{ so that}$$

$\xi_i \ll 1$, for which

$$Z(\xi_i) = -2\xi_i + \frac{4}{3}\xi_i^3 - \cdots + i\sqrt{\pi} \; \frac{k}{|k|} \exp(-\xi_i^2) \qquad (5.13)$$

Hence

$$\text{Im} \, \varepsilon_i = \frac{2\sqrt{\pi} \; \mu \; \omega_{Pe}^2 \; n_b}{n_o \; k^2 (\Delta V_b)^2} \; \frac{k}{|k|} \left(\frac{\omega - \vec{k}\cdot\vec{V_b}}{\vec{k}\cdot\Delta\vec{V_b}}\right) \exp-\left(\frac{\omega - \vec{k}\cdot\vec{V_b}}{\vec{k}\cdot\Delta\vec{V_b}}\right)^2 \cdot \quad (5.14)$$

Maximum of Im ε_i occurs when $K V_b \cos\varphi - \omega = \frac{k\Delta V_b}{\sqrt{2}}$. Therefore one can write

$$\text{Im} \, \varepsilon_i = 2\left(\frac{\pi}{2}\right)^{\frac{1}{2}} \frac{\mu \; \omega_{Pe}^2 \; n_b}{n_o \; k^2 \Delta V_b^2} \exp(-\frac{1}{2}) \qquad \cdot \quad (5.15)$$

For a small growth or damping of waves (γ), such that the inequality $\frac{\gamma}{\omega} \ll \omega$, is satisfied, the growth (damping) is given by:

$$\Upsilon = - \text{Im}\, \mathcal{E} \Big/ \Big(\partial \mathcal{E}_{0} \big/ \partial \omega \Big) \qquad (5.16)$$

Using the equation (5.5), one can write:

$$\frac{\partial \mathcal{E}_{0}}{\partial \omega} = \frac{2}{\omega^{3}}\, \omega_{P_{e}}^{2} \left[\mu + \frac{k_{\shortparallel}^{2}}{k^{2}\left(1 + \omega_{P_{i}}^{2}\big/k^{2}c^{2}\right)} \right] \qquad (5.17)$$

Using the dispersion relation (5.6), we get:

$$\omega \frac{\partial \mathcal{E}_{0}}{\partial \omega} = 2\, \frac{\omega_{P_{e}}^{2}}{\Omega_{e}^{2}} \left(1 + \frac{\omega_{P_{e}}^{2}}{k^{2}c^{2}} \right) \qquad (5.18)$$

When the reflected ion beam which is approximated as a drifted Maxwellian is present in the ambient plasma the waves described by the dispersion relation (5.6) are unstable and the growth rate is calculated using (5.15), (5.16) and (5.17) as :

$$\frac{\Upsilon_{b}}{\omega} = \left(\frac{\pi}{2} \right)^{1/2} \frac{\mu\, \Omega_{e}^{2}}{\left(\vec{k} \cdot \Delta \vec{V_{b}} \right)^{2}}\, \frac{n_{b}/n_{o}}{\left(1 + \omega_{P_{e}}^{2}\big/k^{2}c^{2}\right)}\, \exp\left(-\tfrac{1}{2} \right) \qquad (5.19)$$

The growth of oscillations resonant with an ion beam is in principle, limited   (a) by convection of waves through the shock front;   (b) by the energy losses due to the resonance with the electrons, $\omega = k_{\shortparallel} \cdot V_{\shortparallel}$, and their acceleration and (c) by the nonlinear effects.   Here we shall suppose that the quasi-static amplitudes of the excited waves are small and neglect their nonlinear interactions.

In such a case the excitation of waves in the upstream by the reflected ion beam, the relaxation of the beam and the quasilinear acceleration of electrons are described by the following system of equations (Vaisberg et al, 1983 Krasnoselskikh, et al, 1985):

$$\left(\vec{V_g} - \vec{V_o}\right) \cdot \frac{\partial}{\partial x} E_k^2 = 2 E_k^2 \left(\gamma_b + \gamma_e + \gamma_i\right) \tag{5.20}$$

$$\vec{V} \cdot \frac{\partial f_b}{\partial x} + \frac{e}{m_i c} \left[\left(\vec{V} - \vec{V_o}\right) \times \vec{B}\right] \cdot \frac{\partial f_b}{\partial \vec{v}}$$
$$= \Pi \left(\frac{e}{m_i}\right)^2 \int \frac{d^3 k}{(2\pi)^3} \vec{k} \cdot \frac{\partial}{\partial \vec{v}} \frac{E_k^2}{k^2} \delta(\omega - \vec{k} \cdot \vec{v}) \vec{k} \cdot \frac{\partial f_b}{\partial \vec{v}}, \tag{5.21}$$

$$\vec{V} \cdot \frac{\partial F_e}{\partial x} = \Pi \left(\frac{e}{m_e}\right)^2 \int \frac{d^3 k}{(2\pi)^3} \frac{\partial}{\partial V_z} \frac{k_{\parallel}^2 E_k^2}{k^2 \left(1 + \frac{\omega_{pe}^2}{k^2 c^2}\right)^2} \frac{\delta(\omega - k_{\parallel} V_{\parallel})}{\partial V_{\parallel}} \frac{\partial F_e}{\partial V_{\parallel}} \tag{5.22}$$

These equations are valid in the frame of reference moving with the shock wave with velocity Vo. Here the angle is the angle between the ambient magnetic field vector and the normal to the wave front, i.e. the angle between $\vec{H}$ and X axis, $\vec{V_g} = \frac{\partial \omega}{\partial \vec{k}}$ is the group velocity of the waves. The left hand side of (5.20) describes the convection of oscillations from the region of interaction, while the right hand side of (5.20) deals with the growth of the low-frequency waves by an ion beam (γ_b), their damping due to the resonant interaction with the electrons (γ_e) and the ions of the background plasma (γ_i).

Before analysing the system of equations (5.20) - (5.22), let us make some simplifications. First, one can suppose that only a negligible part of the ion beam energy is transmitted to the waves and does not affect the relaxation of the ion beam described by Eq.(5.21). This assumption is confirmed by the observations near the Earth's bow shock and the computer similations mentioned earlier and is in good agreement with the results obtained below.

Second, since the electrons are magnetized, their transverse energy does not change and a one-dimensional distribution function is enough to describe the behaviour of the electrons: $F(v_\perp) = \int \pi \, dv_\perp^2 f_e(v_{||}, v_\perp)$. To calculate the damping one should first estimate $\text{Im} \, \varepsilon_e$, where ε_e is given in (5.8):

$$\text{Im} \, \varepsilon_e = - \pi \frac{\omega_{Pe}^2}{k^2} \int \left(n \Omega_e \frac{\partial F_e}{v_\perp \partial v_\perp} + k_{||} \frac{\partial F_e}{\partial v_{||}} \right) \zeta_n^2 \, \delta(\omega - n\Omega_e - k_{||} v_{||}) \, d v_{||} \quad (5.23)$$

Since $\vec{B}_o$ is very large for the electrons we retain only the $n = 0$ term in the expression (5.23). Moreover, in the small-Larmor-radius approximation, $J_0^2 \left(\frac{k_\perp v_\perp}{\Omega_e} \right) \simeq 1$ and Eq.(5.23) reduces to :

$$\text{Im} \, \varepsilon_e = - \pi \frac{\omega_{Pe}^2}{k^2} \frac{1}{\left(1 + \omega_{Pe}^2/k^2 c^2 \right)^2} \left. \frac{\partial F_e}{\partial v_{||}} \right|_{v_{||} = \omega/k_{||}} \quad (5.24)$$

Using equations (5.16), (5.18) and (5.24), we can write the damping of waves due to the cherenkov resonance with the electrons as:

$$\frac{\gamma_e}{\omega} = \frac{\Pi}{2} \frac{\Omega_e^2}{k^2} \left(1 + \frac{\omega_{Pe}^2}{k^2 c^2}\right)^{-3} \frac{\partial F_e}{\partial v_{||}} \Bigg|_{v_{||} = \omega/k_{||}}$$

(5.25)

The damping of waves due to background ions is:

$$\frac{\gamma_i}{\omega} \approx -\sqrt{\Pi}' \ b^3 e^{-b^2}$$

(5.26)

where $b = \frac{\omega}{k_\perp V_{Tio}}$ is the phase velocity of the waves perpendicular to the magnetic field relative to the background ion thermal speed V_{Tio}. Since $\gamma_i \ll \gamma_e$, γ_i can be neglected. The velocity of the resonant electrons is:

$$V_{||}^2 = \frac{V_A^2 \omega_{Pe}^2/k^2 c^2}{\mu\left(1 + \omega_{Pe}^2/k^2 c^2\right)^2} + \frac{V_A^2 \ \omega_{Pe}^2/k^2 c^2}{\cos^2\theta \left(1 + \omega_{Pe}^2/k^2 c^2\right)}$$

(5.27)

where $V_A^2 = \frac{c^2 \Omega_e^2}{\omega_{Pe}^2} \mu = \frac{B_0^2}{4\Pi n_0 m_i}$ is the Alfven velocity.

The third, and the last simplification. is due to the fact that the term describing the wave convection is small in comparison with γ_b ; $V_b = M V_A > V_g$, V_A, and LHS of (5.20) is

$$\left(V_0 - V_g\right) \frac{\partial E_k^2}{\partial x} \approx \frac{V_0}{d} E_k^2 \approx \alpha \Omega_i E_k^2$$

(5.28)

Here $\alpha \leq 1$ and we use the estimate $\partial/\partial x \sim d^{-1} \sim \frac{\Omega_i}{v_0}$. Comparing (5.28) with $\gamma_b E_k^2$ one can conclude that the convection is important only for long wavelength oscillations for which $\gamma_b < \Omega_i$. For simplicity it is assumed that $\cos^2\theta < \mu$, then :

$$\omega^2 = \frac{\mu \, \Omega_e^2}{\left(1 + \frac{\omega_{Pe}^2}{k^2 c^2} \right)} \tag{5.29}$$

Therefore the inequality $\gamma_b < \Omega_i$ takes the form :

$$\left(\frac{\pi}{2}\right)^{1/2} \frac{\mu \, \Omega_e^2}{\left(k \Delta V_b\right)^2} \sqrt{\mu} \, \frac{\Omega_e}{\left(1 + \frac{\omega_{Pe}^2}{k^2 c^2} \right)^{3/2}} \frac{n_b}{n_0} \exp\left(-\frac{1}{2}\right) < \Omega_i \tag{5.30}$$

which reduces to :

$$\left(\frac{\pi}{2}\right)^{1/2} \frac{V_A^2}{\sqrt{\mu} \, (\Delta V_b)^2} \frac{k c/\omega_{Pe}}{\left(1 + \frac{k^2 c^2}{\omega_{Pe}^2} \right)^{3/2}} \frac{n_b}{n_0} e^{-1/2} < 1 \tag{5.31}$$

which can be rewritten as

$$\frac{k c/\omega_{Pe}}{\left(1 + \frac{k^2 c^2}{\omega_{Pe}^2} \right)^{3/2}} \leq \frac{\sqrt{\mu} \, e^{1/2} \left(\frac{\pi}{2}\right)^{-1/2}}{\frac{n_b}{n_0} \left(\frac{V_A}{\Delta V_b}\right)^2} \tag{5.32}$$

The important parameter $\frac{m_b}{m_o} \left(\frac{V_A}{\Delta V_b}\right)^2 \sim \frac{m_b}{m_o} \frac{1}{\beta}$, connected with the convection, determines, in particular, the threshold of the ion beam instability. Since the LHS of (5.32) is less than 3/8 for all k, for the instability to occur it is necessary to fulfill the condition $\frac{m_b}{m_o} \left(\frac{V_A}{\Delta V_b}\right)^2 > \frac{8}{3} \left(\frac{\pi}{2}\right)^{-1/2} e^{1/2} \mu^{1/2}$. This inequality is satisfied for $\frac{m_b}{m_o} > \beta/_{10}$ and one can take the convection into account only in the small part of phase volume occupied by the oscillations. The energy of these waves is small too. So the energy of the ion beam which is transferred to the waves, is mainly absorbed by the electrons. As a result, strong electron acceleration along the magnetic field lines will occur and $F_e(V_{||})$ will have a non-Maxwellian "tail".

We shall describe this process in more detail. The scheme of the solution for the distribution function of the accelerated electrons is the following. Balancing γ_b with γ_e one can find the fraction of electrons accelerated and determine $F_e(V_{||})$ such that the energy lost by an ion beam is absorbed by the electrons. Note that, when solving Eq. (5.20), we do not take into account the finite size of the system, while the wave convection is considered in a simplified way, see e.g. (5.28). Knowing $F(V_{||})$, one can determine the wave spectrum and estimate the relaxation of the ion beam if it is important.

In that part of phase space $(k_\perp, K_{||})$ where $E_k^2 \neq 0$, it follows from (5.20) that :

$$-\frac{\partial F_e}{\partial V_{\parallel}} \geq \frac{2}{\pi} \frac{\mu}{V_A^2} \left(\frac{\omega_{P_e}^2}{k^2 c^2}\right)^2 \left(1 + \frac{k^2 c^2}{\omega_{P_e}^2}\right)^3 \left[\frac{n_b}{n_o}\left(\frac{V_A}{\Delta V_b}\right)^2 \frac{e^{-\frac{1}{2}}(\Gamma_2)^{\frac{1}{2}}}{\left(1 + \frac{k^2 c^2}{\omega_{P_e}^2}\right)} - \frac{\alpha \Omega_i}{\omega}\right]$$

(5.33)

In the rest of the phase space the LHS of the eq. (5.33) is negative, because the waves should damp. Taking into account the Eqs. (5.19) and (5.25), equation (5.33) can be written as

$$\Upsilon_b + \Upsilon_e - \alpha \Omega_i \approx 0 \qquad (5.34)$$

It should be noted that the resonance condition (5.27) and the dispersion relation (5.6) allow us to find $\cos\theta$ and ω as functions of k and $V_{\parallel}$, so that RHS of (5.33) depends upon both independent variables. The exact equality occurs only for a single $k = k_m$, for which the RHS of (5.34) reaches its maximum. The waves with another k are damped, i.e. the spectrum of the oscillations is streamer-type and the energy is concentrated in a narrow band near the line $k = k_m$ on the phase plane ($k_\perp$ $k_{\parallel}$). (See the fig. 5.2). Now our aim is to find the maximum of RHS of (5.33) for a given electron velocity $V_{\parallel}$. For this purpose we can eliminate $k_{\parallel}$ in the equation (5.6) and write $\omega = \omega$ (k, $k_{\parallel}$, $V_{\parallel}$) using the resonance condition $\omega = k_{\parallel} \cdot V_{\parallel}$ which gives :

$$\omega^2 = \mu \Omega_e^2 \frac{1 + k^2 c^2/\omega_{P_e}^2}{\left(1 + \frac{\omega_{P_e}^2}{k^2 c^2}\right)\left(1 + \frac{k^2 c^2}{\omega_{P_e}^2}\right) - \frac{V_A^2}{\mu V_{\parallel}^2}} \qquad (5.35)$$

Now substitute the above expression in Eq.(5.33). To simplify the formula let us introduce:

$$u = \mu^{1/2} \frac{V_{//}}{V_A} \quad ; \qquad \xi = \frac{k^2 c^2}{\omega_{Pe}^2} \quad ;$$

$$a = \sqrt{\frac{\pi}{2}} \; e^{-1/2} \; \frac{m_b}{m_o} \left(\frac{V_A}{\Delta V_b} \right)^2 \tag{5.36}$$

and write down the eq. (5.33) in the form:

$$-\frac{\partial F}{\partial u} = \frac{2}{\pi} \; \frac{\mu^{1/2}}{V_A} \left(\frac{1+\xi}{\xi} \right)^2 \left\{ a - \alpha \mu^{1/2} \left[\frac{(1+\xi)^3}{\xi} - \frac{1+\xi}{u^2} \right]^{1/2} \right\} \tag{5.37}$$

We are interested in the region of suprathermal velocities $V_{//} > 2 \cdot V_{Te}$, i.e. $u^2 > \left(4 \mu V_{Te}^2 \Big/ V_A^2 \right) = 4 \beta_e$. Hence, if β_e is not too small, one can neglect the term with u^{-2} in (5.37). Then the maximum of the RHS of (5.37) is reached for $\xi = \xi_* = \left(\frac{5}{4} \frac{\sqrt{\mu}}{\alpha} \right)^2 < 1$ and, it does not depend on u. It implies that the distribution function of the accelerated electrons is linear:

$$F_e(V_{//}) = \sqrt{\frac{2}{\pi}} \; e^{-1/2} \; \frac{\mu}{5 \, \xi_*^2} \; \frac{m_b}{m_o} \; \frac{V_A^2}{(\Delta V_b)^2} \; \frac{V_h - V_{//}}{V_A^2} \tag{5.38}$$

Here we do not dwell upon the dependence of ξ_* on other parameters for the convenience and the compactness of formulae.

When $\beta_e < \frac{1}{4} \frac{\sqrt{\mu}}{\alpha}$, $\bar{f}_*$ slightly depends on u for small velocities. Although this dependence $\bar{f}_*(u)$ is easy to find and determines the deviation of Fe $(V_{//})$ from the linear law, this effect proved to be insignificant and it would be ignored.

For small velocities $V_{//} = V_* \approx (2\text{-}3) \, V_{Te}$, the distribution function of the accelerated electrons merges with the thermal electron distribution function, which is supposed to be Maxwellian $(V_h \gg V_*)$:

$$F_e(V_*) = \sqrt{\frac{2}{\pi}} \; \frac{\mu}{5} \; \frac{V_h}{V_A^2} \; \frac{n_b}{n_o} \; \frac{1}{\bar{f}_*^2} = \frac{exp-\left(\frac{V_*^2}{2V_{Te}^2}\right)}{\sqrt{2\pi \, V_{Te}}} \qquad (5.39)$$

5.2b Electron Accelration due to the ring distribution of reflected ions just behind the overshoot

By numerical simulations Leroy et al (1981, 1982) showed that the reflected ions tend to form a gyrating stream in the down stream region behind the overshoot and evolve into a 'ring' with a significantly large velocity spread. A realistic representation of the ring type distribution of reflected ions which includes all thermal effects is given by Dory-Guest-Harris distribution (Dory et al, 1965) as given in (5.2).

The distribution function (5.2) resembles a ring or torus in V-space. When N = 0, it reduces to a Maxwellian distribution,

and when N (the ring anisotropy) is large, the perpendicular energy is concentrated near the maximum:

$$V_{\perp_{max}} = \sqrt{N} \, \Delta V_{b_\perp} \equiv V_b \qquad (5.40)$$

The average gyro energy of expression (5.2) is

$$< \frac{1}{2} m_i \, \Delta V_{b_\perp}^2 > = \frac{1}{2} (N+1) \, m_i \Delta V_{b_\perp}^2 = \frac{1}{2} \left(1 + \frac{1}{N}\right) m_i \, V_\perp^2 \qquad (5.41)$$

The distribution function (5.2) has many of the features expected for monoenergetic injection of ions corresponding to reflected ions. The Quasi-linear wave effects will act to reduce the anisotropy. The model given in equation (5.2) with the free parameter N will suffice to make a determination of the growth rate of waves given in eq. (5.6) which are unstable when such ion beams with $N > 0$ are present in the background plasma.

If we substitute the expression (5.2) into equation (5.15), then we obtain:

$$Im \, \varepsilon_i = \frac{4 \mu \, \omega_{p_i}^2}{(N+1)! \, \omega^2} \, \frac{n_b}{n_0} \, R^3 e^{-R^2} \int_0^\infty dt \, e^{-t^2} \left(R^2 + t^2\right)^N \left(1 - \frac{N}{R^2 + t^2}\right) \qquad (5.42)$$

where $\quad R = \dfrac{\omega}{k_\perp \Delta V_{b_\perp}}$

We can write a necessary condition for growth from inspection of the equation (5.42). It is $R^2 < N$ or, alternatively,

$$\frac{\omega}{k_\perp} < N^{1/2} \Delta v_{b_\perp} = v_b \tag{5.43}$$

If we define

$$I_N = \int_0^\infty dt \; e^{-t^2/a^2} (R^2 + t^2)^N \tag{5.44}$$

we can derive a recursion relation

$$I_{N+1} = \left[R^2 + a^2 \left(N + \tfrac{1}{2} \right) \right] I_N - N R^2 a^2 \, I_{N-1} \tag{5.45}$$

For $a = 1$ equation (5.42) takes the form

$$\text{Im}\,\varepsilon_i = \frac{4\mu}{(N+1)!} \; \frac{n_b}{n_0} \; \omega_{p_e}^2 \, R^3 \, e^{-R^2} \left(I_N - N I_{N-1} \right) \tag{5.46}$$

For integers $N = 0,1$ we have

$$I_0 = \sqrt{\pi/2}$$

$$I_1 = \sqrt{\pi/2} \; \left(R^2 + 0.5 \right) \tag{5.47}$$

from which higher order I_N may be obtained.

The $\text{Im}\,\varepsilon_i$ for the lowest three orders $N = 0,1,2$ are given as:

$$\text{Im}\,\varepsilon_i (N=0) = 2\sqrt{\pi} \; \frac{n_b}{n_0} \, \mu \, \frac{\omega_{p_e}^2}{\omega^2} \, R^3 \, e^{-R^2} \tag{5.48}$$

$$\text{Im } \mathcal{E}_i \left(N=1\right) = 2\sqrt{\pi'} \; \frac{n_b}{n_o} \; \mu \; \frac{\omega_{Pe}^2}{\omega^2} \; R^3 e^{-R^2} \left(R^2 - 0.5\right)$$

(5.49)

and

$$\text{Im } \mathcal{E}_i \left(N=2\right) = \sqrt{\pi'} \; \frac{n_b}{n_o} \; \mu \; \frac{\omega_{Pe}^2}{\omega^2} \; R^3 e^{-R^2} \left(R^4 - R^2 - 0.25\right)$$

(5.50)

$\text{Im } \mathcal{E}_i$ (N = 1) gives instability for $R^2 < 0.5$ and the maximum growth occurs at a value

$$R_o = [0.5 \, (\, 3 - \sqrt{6'} \,)]^{1/2} \approx 0.5$$

(5.51)

(see for example Barbosa et al (1985) for details). Using the equations (5.16), (5.18) and 5.42) one can write the growth rate as:

$$\frac{\gamma_b}{\omega} = - \frac{2}{(N+1)!} \; \frac{n_b}{n_o} \; \frac{\mu \, \Omega_i^2}{\left(1 + \omega_{Pe}^2 / k^2 c^2\right)} \; \frac{R^3 e^{-R^2}}{k^2 v_\perp^2} \times$$
$$\int_0^\infty dt \; e^{-t^2} \left(R^2 + t^2\right)^N \left(1 - \frac{N}{R^2 + t^2}\right)$$

(5.52)

If we assume that $\cos^2\theta < \mu$ and use the relation (5.29) for ω, we can write:

$$\gamma_b = - \frac{2}{(N+1)!} \left(\frac{v_A}{v_\perp}\right)^2 \frac{\omega}{\left(1 + \frac{k^2 c^2}{\omega_{Pe}^2}\right)} \; \frac{n_b}{n_o} \; R^3 e^{-R^2} \int_0^\infty dt \; e^{-t^2} \left(R^2 + t^2\right)^N \left(1 - \frac{N}{R^2 + t^2}\right)$$

(5.53)

Due to the similar arguements as in section 5.2a, by analyzing the inequality (5.33) in this case also we get an equation similar to (5.37) which is:

$$-\frac{\partial F}{\partial u} = \frac{2}{\pi} \frac{\mu^{1/2}}{V_A} \left(\frac{1+\xi}{\xi}\right)^2 \left\{ A - \alpha \mu^{1/2} \left[\frac{(1+\xi)^3}{\xi} - \frac{1+\xi}{u^2} \right]^{1/2} \right\} \quad (5.54)$$

where

$$A = -\frac{2}{(N+1)!} \left(\frac{V_A}{V_1}\right)^2 \frac{m_b}{m_D} R^3 e^{-R^2} \int_0^\infty dt\, e^{-t^2} \left(R^2 + t^2\right)^N \left(1 - \frac{N}{R^2+t^2}\right) \quad (5.55)$$

Agian since RHS of (5.54) reaches its maximum for $\xi = \xi_* = \left(\frac{5}{4} \frac{\sqrt{\mu}}{\alpha}\right)^2 < 1$, it does not depend upon u, which implies that the distribution function of the accelerated electrons is linear which is:

$$F_e\left(V_{\shortparallel}\right) = -\frac{2}{\pi} \frac{A}{5} \frac{\mu}{\xi_*^2} \frac{V_h - V_{\shortparallel}}{V_A^2} \quad (5.56)$$

For small velocities $V_{\shortparallel} = V_* \approx (2\text{-}3)V_{Te}$, the accelerated electron distribution function coincides with the ambinet equilibrium electron distribution function which is supposed to be Maxwellian $(V_h \gg V_*)$:

$$F_e(V_*) = -\frac{2}{\pi} \frac{A}{5} \frac{\mu}{\xi_*^2} \frac{V_h}{V_A^2} = \frac{\exp\left(-\frac{V_*^2}{2 V_{Te}^2}\right)}{\sqrt{2\pi}\, V_{Te}} \quad (5.57)$$

In fig.5.2 a sketch of the distribution function of the accelerated electrons is given.
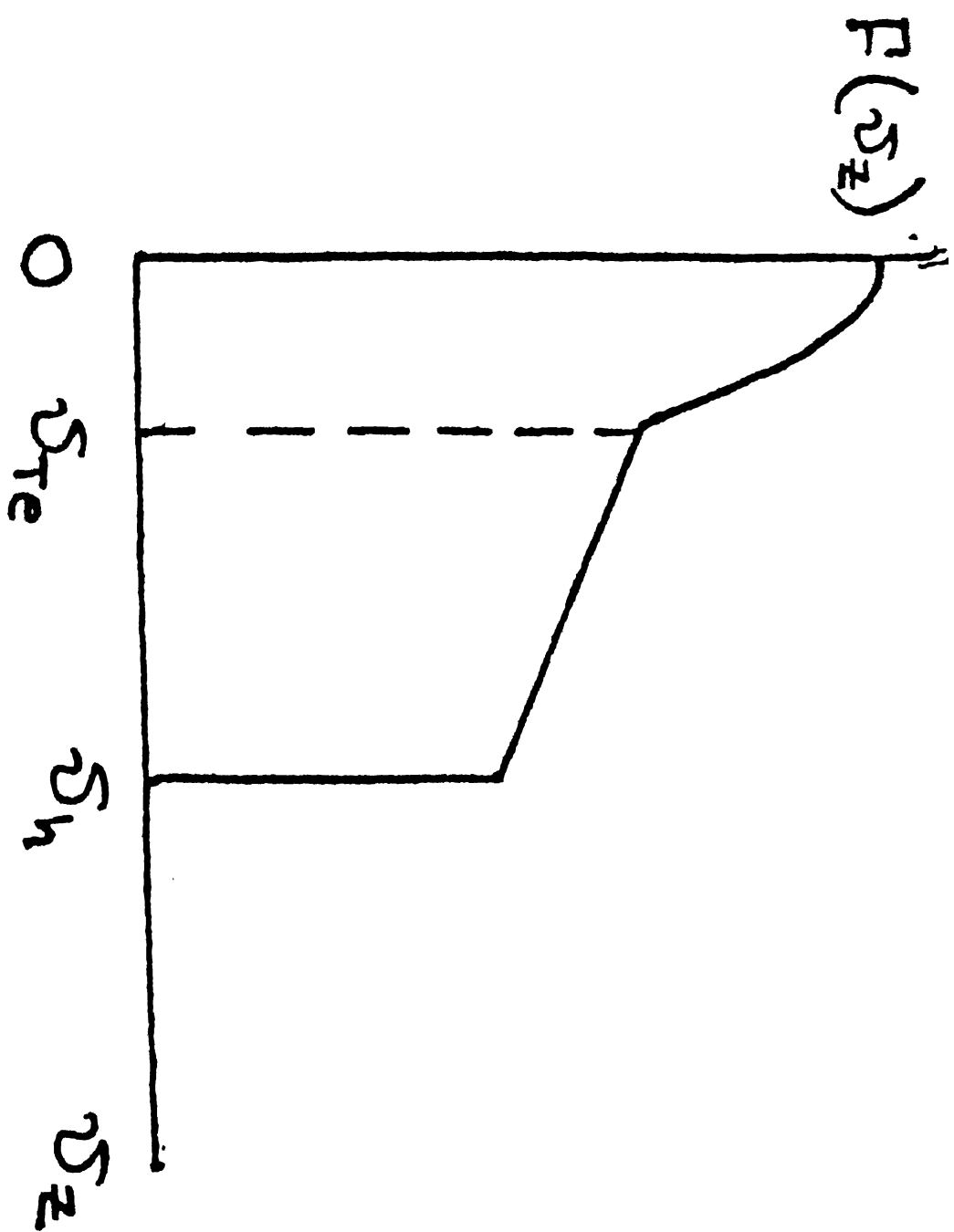
Fig. 5.2. The distribution function of the accelerated electrons.

5.3 Analysis of the streamer-type energy spectrum

As mentioned above, the waves are concentrated near the line $k_\perp = k_\perp (k_{||}) = \frac{\omega_{pe}}{c} \sqrt{\xi_*} = k_* = $ const on a phase plane as shown in fig. 5.3. Therefore the frequency,

$$\omega \approx \left[\frac{\mu \Omega_e^2 \xi_*}{1 - \frac{V_A^2 \xi_*}{\mu V_{||}^2}} \right]^{1/2} \approx k_{||} V_A \approx \Omega_i \left(\frac{\xi_*}{\mu} \right)^{1/2} \tag{5.58}$$

is practically constant for about the whole spectrum, where $V_{||}^2 \gg V_A^2 \xi_*/\mu$. As it follows from the resonant condition $\omega = K \cdot V_b \cos\varphi$, the streamer consists of two straight lines on $(k_x \; k_y)$ making angles $\pm \varphi_*$ with k_x axis. Here

$$\cos \varphi_* = \frac{k_x}{(k_x^2 + k_y^2)^{1/2}} \approx \frac{V_A}{V_b} \tag{5.59}$$

To find the wave spectrum, let us rewrite eq. (5.22) in the following form:

$$-\frac{V_{||} \sin \theta_o}{d} F_e(v_{||}) = \pi \left(\frac{e}{m_e} \right)^{1/2} \frac{\partial}{\partial v_{||}} \left[\frac{V_A^2}{V_{||}^2} \frac{1}{\xi_*} \int \frac{d^2 k_\perp}{(2\pi)^2} E_k^2 \frac{\partial F_e(v_{||})}{\partial v_{||}} \right] \tag{5.60}$$

Here we have used the fact that the spectrum is of the streamer-type. For simplicity we shall consider only the region $V_{||}^2 > \frac{V_A^2 \xi_*^2}{\mu}$ which is the most important for the following. From (5.27) one can obtain that $\cos^2 \theta \approx \frac{V_A^2}{V_{||}^2} \xi_*$. Substituting (5.39) or (5.57) into (5.60) one finds after integration:
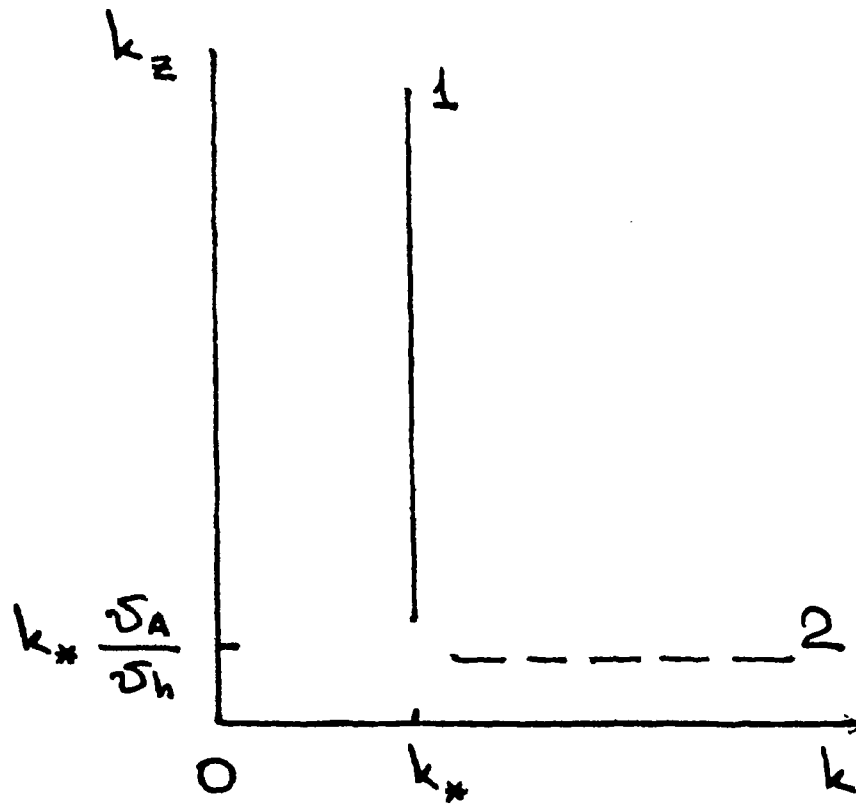
Fig. 5.3. Streamer type spectrum.

$$\int \frac{d^2k_\perp \, E_k^2}{(2\pi)^2} = 4\pi \mu^{3/2} \, \xi_*^{7/2} \sin\theta_0 \left(\frac{V_A}{c}\right)^2 \frac{m_i \, n_0 V_A^2}{2} \left(\frac{\omega_{pe}}{k_\parallel c}\right)^4 \times$$

$$\times \frac{1}{k_\parallel} \left(1 - \frac{2}{3} \frac{V_A}{V_\parallel} \frac{k_\perp}{k_\parallel}\right) \tag{5.61}$$

The wave energy density is:

$$W = \int \frac{dk_\parallel}{2\pi} \left(1 + \frac{c^2}{V_A^2}\right) \int \frac{d^2k_\perp \, E_k^2}{(2\pi)^2 \, 8\pi} =$$

$$= \frac{1}{8} \left(\mu \xi_*\right)^{3/2} \sin\theta_0 \frac{m_i \, n_0 V_A^2}{2} \tag{5.62}$$

5.4 a. Change in the velocity spread, b. Maximum velocity
c. Turbulence level and d. Total density of the accelerated
electrons

Knowing the wave intensity one can easily find the change
of the velocity spread in the beam, $\delta(\Delta V_b)$. In agreement
with (5.21)

$$\delta(\Delta V_b) \approx \sqrt{\frac{D d}{V_b}} \approx \sqrt{D/\Omega_i} \,, \tag{5.63}$$

where the diffusion coefficient D is determined by the waves
as:

$$D = \pi \left(\frac{e}{m_i}\right)^2 \int \frac{d^3k}{(2\pi)^3} \cos^2\varphi \, E_k^2 \, \delta(\omega - \vec{k}\cdot\vec{v})$$

$$= 4\pi^2 \left(\frac{e}{m_i}\right)^2 \frac{(V_A/V_b)^2}{\left[1 - (V_A/V_b)^2\right]^{1/2}} \frac{W_1}{k_\perp V_b} \,. \tag{5.64}$$

The assumption that the change of the growth rate of the ion beam is small and that the energy of the beam is transmitted to the electrons is fulfilled if $\delta(\Delta V_b) < \Delta V_b$ or, as it follows from (5.62) - (5.64), if

$$\frac{\mu V_h^2}{V_A^2} \lesssim \frac{(\Delta V_b)^2 V_b^3}{V_A^5} \frac{\Omega_e^2}{\omega_{P_e}^2} \frac{8}{\xi_*^{1/2} \sin \theta_0} \qquad (5.65)$$

To find V_h it is necessary to balance the energy fluxes, i.e. the energy flux lost by the ion beam must be equal to the energy flux gained by the accelerated electrons:

$$\delta(n_b m_i V_b^3) = n_b m_i V_b^2 \delta(\Delta V_b) = \sin \theta_0 \int n_0 m_e V_h^3 F_e(V_{||}) dV_{||} . \qquad (5.66)$$

From (5.34), (5.63) and (5.64) it follows that:

$$\frac{\mu V_h^2}{V_A^2} = 10 \, \xi_*^{5/4} (\sin \theta_0)^{-1/4} \left(\frac{\omega_{P_e}}{\Omega_e}\right)^{1/2} \left(\frac{V_b}{V_A}\right)^2 \frac{\Delta V_b}{V_A} \qquad (5.67)$$

Note that the maximum velocity of the accelerated electrons does not depend explicitly upon the density of the ion beam. However the ratio n_b/n_0 determines ξ_*. For example, for shock waves with $M \approx M_{cr} = 2$, $\beta_i \sim 10^{-1}$, $\theta_0 \sim 10^{-1}$, $\frac{n_b}{n_0} \sim 10^{-2}$, $\omega_{P_e}^2/\Omega_e^2 = 900$ and $\left(\Delta V_b/V_A\right)^2 \sim \beta_i$, one can find from equation (5.32) that $\xi_*^{1/2} \approx 1/4$ to $1/3$ and after substitution

in (5.67) one obtains:

$$m_e v_h^2 \approx \frac{v_A^2}{\mu} m_e \approx T_e/\beta_e > T_e$$

(5.68)

So the electrons are accelerated up to suprathermal velocities ($\beta_e \sim \beta_i \sim 10^{-1}$). In accordance with (5.62), the level of turbulence appears to be:

$$\frac{W_i}{n_o T_e} \approx \frac{\sin \theta_o}{16} \mu^{1/2} \xi_*^{1/2} \frac{m_e v_h^2}{T_e} \approx 5 \times 10^{-4}$$

(5.69)

and the total density of the accelerated electrons in the upstream:

$$n_{s_u} = \int_{v_*}^{v_h} F_e dv_{||} = \frac{2}{\sqrt{\pi}} \frac{e^{-1/2}}{10 \xi_*^2} \frac{m_b}{n_o} \left(\frac{v_A}{\Delta v_b}\right)^2 \frac{v_h^2}{v_A^2} \mu n_o$$

(5.70)

Here we substitute Eq. (5.38) for Fe. Similarly the total density of the accelerated electrons in the downstream is:

$$n_{s_d} = -\frac{2}{\pi} \frac{A \mu}{10 \xi_*^2} \frac{v_h^2}{v_A^2} \mu n_o$$

(5.71)

for all values of the Anisotropy index N, where Fe is given by (5.56) and A by (5.55).

5.5 A qualitative analysis of nonlinear interactions

The self-consistent theory of electron acceleration near the shock front, developed above, is based on the quasilinear approach. However, in the case of quasilinear theory for waves with $k_{\shortparallel} < \omega/v_h \approx \sqrt{\mu}\, k_{\perp}$, there are no resonant electrons which can limit the growth of these waves. So the growth of the waves in this region of phase space is limited by nonlinear interaction. The full nonlinear analysis is not the main task of this chapter, so we restrict ourselves below only to a qualitative analysis of nonlinear interactions.

For $k_z/k_\perp < \sqrt{\mu}$ the strongest nonlinear effect is the induced scattering of waves by electrons. The physics of this process is the following: the beating of two lower-hybrid waves may have the phase speed close to that of the electron thermal velocity V_{Te}. So the beating will be quickly absorbed by the electrons leading to the nonlinear "coupling" of primary waves and forcing the lower-hybrid waves to move outward the region of k-space where they wer located earlier. Thus, the waves driven by a beam will quickly leave the resonance region in k-space, limiting the density of the waves there.

For potential waves this process and the collapse of the lower-hybrid waves, closely connected with it, studied in the numerous papers (Sturman, 1974; Sotnikov, et al, 1978; Hasegawa and Chen, 1975). With nonpotentiality of waves taken into account the nonlinear increment of induced scattering by

electrons may be found in a similar way:

$$\gamma_{NL}(k) = \sum_{k'} \frac{1}{1 + \frac{\omega_{Pe}^2}{k^2 c^2}} \quad \frac{W(k')}{n_0 T_e} \frac{[\vec{k} \times \vec{k'}]^2}{k^2 \cdot k'^2} (k - k') \cdot$$

$$\left(\frac{k}{\omega} - \frac{k'}{\omega'} \right) v_{Te}^2 \; Im \, \mathcal{E}(k - k') \; \approx$$

$$\approx \frac{\pi}{2} \frac{\omega_{Pe}^2}{1 + \frac{\omega_{Pe}^2}{k^2 c^2}} \frac{\partial}{\partial k_z} \int \frac{d\pi k_\perp^2}{2\pi} \frac{W(k_\perp', k_z)}{n_0 T_e} \frac{\omega - \omega'}{v_{Te}^2} \tag{5.72}$$

Here we use the fact that the spectral "repumping" of the waves occurs in a differential way: for the single act of scattering

$$\Delta k_z \approx (\omega - \omega')/v_{Te} \approx k_\perp v_A/v_{Te} \ll k_z.$$

As the result of the induced scattering the energy of waves is transmitted along the line $k_z = 0$ to the region of greater $k_\perp$, where it is absorbed by the thermal electrons. The part of the energy is lost during the spectral "repumping" because of angular scattering of waves into the region of phase space, where waves are effectively absorbed by the accelerated electrons.

Thus, the streamer-type spectrum $W(k) \sim \delta\left(k_\perp - k_{\perp *} \right)$ for $k_z \sim V_A k_* / V_h$ turns and is continued in a form of a streamer along $k_\perp$ axis. In this branch of a streamer there is a balance between the induced scattering of waves and their generation

by an ion beam: $\gamma_b \approx \gamma_{NL}$. Estimating the thickness of the streamer as $\Delta k_z \sim \omega / V_h$ and substituting in (5.25) $\omega(k) - \omega(k') \approx \sqrt{\mu'}\,\Omega_e$ one obtains

$$\gamma_{NL} \approx \frac{\pi}{2}\,\frac{\omega_{Pe}^2}{1 + \frac{\omega_{Pe}^2}{k^2 c^2}}\,\frac{\sqrt{\mu'}\,\Omega_e}{(\Delta k_z V_{Te})^2} \int \frac{d\pi k_\perp^2\, dk_z}{(2\pi)^3}\,\frac{W(k)}{n_0 T_e} \approx$$

$$\approx \frac{1}{\sqrt{\mu'}} \left(\frac{V_h}{V_{Te}}\right)^2 \left(\frac{\omega_{Pe}}{\Omega_e}\right)^2 \Omega_e\,\frac{W_2}{n_0 T_e} \qquad (5.73)$$

Now, balancing $\gamma_b \approx \gamma_{NL}$, one can find the wave energy density on the streamer, passing along $k_\perp$ axis, supposing the waves are concentrated near the maximum of the increment γ_b and $k_\perp c / \omega_{pe} \approx 1$. The result is

$$\frac{W_2}{n_0 T_e} \approx \mu \left(\frac{V_{Te}}{V_h}\right)^2 \frac{\Omega_e^2}{\omega_{Pe}^2}\,\frac{n_b}{n_0} \left(\frac{V_A}{\Delta V_b}\right)^2 \qquad (5.74)$$

It should be noted that the presence of shortwave oscillations (i.e. the streamer passed along the $k_\perp$ axis) may change the position of the main part of a streamer, $k \approx k_* \ll \frac{\omega_h}{c}$ and thus may change γ_*. To understand this fact one should keep in mind that the nonlinear interaction of waves belonging to the main streamer in k-space is not essential, because the main nonlinear process for $k_z/k_\perp > \sqrt{\mu'}$ is the induced scattering of ions and the corresponding phase velocity of the beatings is $V_{ph} \sim (\omega - \omega')/(k - k') \sim V_A \gg V_{Ti}$, so only exponentially small

fraction of ions takes part in this process. On the contrary, the induced scattering caused by absorbtion of the beatings between the waves from the main part of the streamer, $k \sim k_*$ and the shortwave oscillations from the tail of a streamer, $k_c > c/\omega_{pe}$ is very effective because in this process all the ions may play a role. The increment of the last process is (Sturman, 1974).

$$\gamma_{NL} = \frac{\omega_{pe}^2}{\Omega_e^2} \frac{1}{\sqrt{\mu'}} \frac{W_2}{n_0 T_e} \approx$$

$$\approx \sqrt{\mu'} \, \Omega_e \left(\frac{V_{Te}}{V_h} \right)^2 \frac{n_b}{n_0} \left(\frac{V_A}{\Delta V_b} \right)^2 \qquad (5.75)$$

Thus, for $\left(\frac{n_b}{n_0} \right) \left(\frac{V_A}{\Delta V_b} \right)^2 > \left(\frac{V_h}{V_{Te}} \right)^2 \sqrt{\mu'}$,

$\gamma_{NL} > \Omega_e$; and in this case the just considered "cross-section" induced scattering on ions is more effective in stabilizing the waves with $k < k_*$ than the convection of oscillations considered earlier (see (5.11)). In this case the position of the streamer in k-space does not depend upon n_0:

$$\frac{k_* c}{\omega_{pe}} \sim \left(\frac{V_{Te}}{V_h} \right) \sim \beta_e \qquad (5.76)$$

Since it is difficult to determine $k_* c/\omega_{pe}$ with nonlinear effect taking into account, we estimate it as $\xi_* \sim 0.1 \div 0.3$.

Summarising the results of this section, we come to the following conclusions:

The electrons near the front of the shock may be accelerated up to the energy of the order of $m_i v_A/2$, and the density of the accelerated particles may reach the value of $n_{eh} \sim (10^{-3} \div 10^{-2})$. n_o, depending upon the Mach number M and the angle θ_c. Besides that the acceleration of electrons up to high energies may also take place due to their resonant interactions with waves locating in a narrow cone $k_z \gtrsim 0$ in k-space. However, the number of such electrons is small.

5.6 The radiation caused by electrons moving from the shock front

Let us consider the magnetic field line moving with plasma flow. At some moment of time this field line will touch the front of the shock. From this end the electrons accelerated by the shock, are injected into the background plasma. Since the electrons are magnetized, they move along the field line, and there is an analogy between this process and that considered by Ryutov and Sagdeev (1970), when the flow of the hot plasma enters the half-space occupied by the cold plasma. If $F(v_z)$ is the distribution function of hot electrons, one can suppose that at a given point $z > 0$ a moment $t > 0$ the distribution function of electrons $f_e(v_z, z, t)$ is equal to $F(v_z)$ for $v_z > z/t$ and is small for all the other velocities (we consider $t = 0$ as the moment of injection). However, this distribution function is unstable and can drive Langmuir waves, which, in turn, cause fast diffusion

in v-space and form a plateau:

$$f(z,t,v_{\shortparallel}) = \begin{cases} p(z,t) & , \quad v_{\shortparallel} < u(z,t) \\ f_0(v_{\shortparallel}) & , \quad v_{\shortparallel} > u(z,t) \end{cases}$$

$$(5.77)$$

The quasihydrodynamic equations for p and u were obtained and solved by Ryutov and Sagdeev (1970). Knowing $p(z,t)$ and $u(z,t)$, one can find the energy density of plasma waves. This approach was successfully used in a number of papers for explaining some features of type III Solar radio bursts (Zaitsev et al, 1972; Zaitsev et al, 1974). In these papers it was shown that at a given point on the field line the wave density grows when the first group of hot electron comes, reaches its maximum value and then decreases during the passing of slow electrons. Since we do not know the details of the injection process, following Ryutov and Sagdeev (1970) and Zaitsev et al. (1972, 1974) we estimate that the energy density of Langmuir waves is approximately equal to one tenth of the energy density of hot electrons:

$$W_L \approx \frac{1}{10} \; n_{eh} \cdot \frac{m_e v_h^2}{2}.$$

$$(5.78)$$

Substituting the density and the energy of the hot electrons, obtained in Section 5.4 in (5.78), one can find $W_L > (10^{-5} \div 10^{-4}) \cdot n_0 T_e$.

Now let's consider the processes responsible for the radio emission of the shocks moving in the Solar corona.

The high level of turbulence ensures the high efficiency of nonlinear transformation of Langmuir waves into electromagnetic ones at the frequencies close to ω_{pe} or $2\omega_{pe}$. A number of processes causing the generation of electromagnetic waves by plasma turbulence were studied in connection with Solar type III radio bursts and kilometric radio emission of Earth and Jupiter. Among them are induced scattering of Langmuir waves by ions (Melrose, 1970, 1974; Tsytovich, 1966; Kaplan and Tsytovich, 1972), merging of two Langmuir waves (Tsytovich, 1966; Smith, 1977; Papadopoulos et al., 1974; Smith et al., 1979), coalescense of upper-hybrid waves with the low-frequency electrostatic waves (Galeev and Krasnoselskikh, 1978), the radiation due to the collapse of Langmuir waves (Galeev and Krasnoselskikh, 1976; Kruchina et al 1980; Goldman et al, 1980).

Returning to the process considered in our paper, one can argue that the collapse of Langmuir waves does not play any role, since the spectrum of plasma waves driven by hot electrons is broad enough, $(k\lambda_D)^2 \sim V_{Te}^2/V_{hot}^2 \sim \beta_e > W_L/n_o T_e$, and the condition of modulational instability (OTSI) is not valid. The ion-sound waves are absent because the plasma of the Solar corona is considered to be isothermal $(T_e = T_i)$. In such a case the generation rate for electromagnetic waves with $\omega \approx \omega_{pe}$ is determined by the induced scattering on ions. If W_T is the

energy density of electromagnetic waves and v_{ph} is the phase velocity of Langmuir waves this generation rate is (Tsytovich, 1966; Melrose, 1974):

$$\frac{d}{dt} W_T \approx \omega_{P_e} \frac{W_L}{n_o T_e} \cdot \frac{V_{T_e}^3}{c^2 V_{ph}} \cdot W_T \tag{5.79}$$

To estimate the brightness temperature of the emission one should know the optical depth of the radiative region, which, in turn, is determined by the length at which Langmuir waves exist in the background plasma. This length may be estimated as $l \sim (1/2 - 1/3) \, v_h \cdot t_{in}$, where t_{in} is the time of electron injection into the given field line, sliding along the surface of the shock wave.

It is easy to understand that the acceleration of electrons along the given line continues only till the moment when the angle between the shock surface and this line exceeds some critical value $\Theta > \Theta_{cr} \approx 30°$. Thus, if R is the curvature radius of the shock, the time of the injection may be estimated as $t_{in} \sim R/2v_o \sin \Theta_{cr} < R/4v_o$, which gives $l \sim \frac{R}{10} \frac{v_{hi} t}{v_o}$. So, one can conclude that electrons, accelerated in the shock, excite the intense Langmuir oscillations ($W_L/n_o T_e \sim 10^{-4} \div 10^{-5}$) in the wide foreshock region. The size of this region is comparable with the radius of curvature of the shock wave or is determined by the long-scale irregularities of the magnetic field in the solar corona (if their typical size is $l_i \ll R$). Using Eq.(5.79)

and estimating l as $1/10 \div 1/30$ of the shock wave front curvature, $l \sim 10^{11}$ cm, one can find that plasma layer emitting the radiation is optically thick for $W_L/n_o T_e > 10 \, (c/\omega_{pe} \, R) \, (c^2 v_h/v_{T_e}^3) \sim 10^{-5}$. In this case there is an equilibrium between the electromagnetic and Langmuir waves, and the brightness temperature of the radioemission is equal to the effective temperature of Langmuir waves:

$$T_b \sim T_{eff} \sim T_e \left(n_o \lambda_D^3 \right) \frac{W_L}{n_o T_e} \tag{5.80}$$

For $n_o = 10^8$, $T_e = 10^6$ one obtains $T_b \sim 10^{11}$ K

We are not going to treat the machanisms of radioemission at harmonics in details. It should be only pointed out that the optical depth in this case is large too, so the brightness temperature of the harmonic emission is appeared to be approximately equal to that of fundamental emission. This conclusion is confirmed, at least for a part of type II bursts, by observations.

The value of brightness temperature obtained for $W_L / n_o T_e = 10^{-3} - 10^{-5}$, $T_b \sim 10^9 - 10^{11}$ K is also in good agreement with the observational data. For $W_L/n_o T_e < 10^{-5}$ the plasma becomes optically thin, the brightness temperature may stay at the same level $\sim 10^9$ k, but the difference between the rates of generation of fundamental and harmonic emission becomes significant, and their brightness temperatures will differ, the fundamental emission should be brighter.

5.7 Bandwidth, polarization and the frequency splitting in type II radio bursts

The self-consistent theory of radio emission by shocks moving in the Solar corona developed above allows us to explain in a natural way at least three more features of the type II radio bursts. One is the finite band width $\Delta\omega / \omega_{pe} \sim 10^{-1}$, the second - the relatively high degree of burst polarization at ω_{pe} (Suzuki et al., 1980). The former may be explained by the finite width of Langmuir wave spectrum: $\Delta\omega \sim 3/2 \ \omega_{pe} \cdot (k\lambda_D)^2 \sim \omega_{pe} \cdot v_{Te}^2/v_h^2 \sim 0.1 \ \omega_{pe}$. Besides that, the density irregularities in the emitting volume may also play a significant role. To explain the polarization one should keep in mind that ordinary and extraordinary waves are generated in different ways.

The induced scattering of ions considered above, $L + i \longrightarrow t$, is a very effective way to generate the ordinary waves, since the frequency of this electromagnetic mode slightly differs from the frequency of Langmuir (upper-hybrid) waves, while the frequency of the extraordinary waves is shifted from that of upper-hybrid waves at the value of the order of Ω_e. So the process of induced scattering gives raise mainly to the ordinary waves.

The extraordinary waves may be, in principle, generated due to the merging of Langmuir waves with the lower branch of electrostatic oscillations. However, as it was pointed out

by Galeev and Krasnoselskikh (1978) this process occurs only in the quadrupole approximation and so it is very slow.

Early interpretations of the splitting of fundamental and harmonic bands involved magnetic splitting or Doppler splitting. As pointed out by Wild and Smerd (1972), the magnetic splitting in some cases requires unacceptably strong magnetic fields, and Doppler splitting requires a current which would cause electrons to flow at unacceptably high speed relative to ions in a laminar shock model.

McLean (1967) proposed an interpretation in terms of a local inhomogeneous structure in the corona. The parts of the shock front which are parallel to the surfaces of constant electron density should emit intensely at a single frequency whereas the emission from other parts of the shock front will be spread thinly across a range of frequencies. McLean (1967) analyzed an idealized quantitative model for a shock encountering a streamer and found that the simulated dynamic spectrum resembled a split-band Type II burst. A variant of McLean's mechanism could explain split bands in terms of emission from two related low V_A regions in Uchida's (1974) blast wave.

Smerd et al (1975) suggested that two bands correspond to emission in front of and behind the shock front. The electron density jumps at a shock front by a factor related to the shock Mach number M_A; Smerd et al (1975) estimated that values in the range $M_A \approx 1.2$ to 1.7 (which are plausible) are sufficient

to account for the observed splitting.

Observations of slightly different positions for the two components of split bands have been interpreted as evidence in favour of McLean's (1967) model (Wild and Smerd, 1972). However, Smerd et al (1975) pointed out that at a fixed frequency the components from the two sides of a shock front would be emitted at different times. Nelson and Robinson's (1975) inference that the L source is further from the Sun than the U source at the same time is qualitatively consistent with the mechanism proposed by Smerd et al (1975).

Our model self consistently explains the frequency splitting, which is one of the main characteristics of the type II bursts. It is due to the character of the reflected ions, which excite low frequency waves both in the upstream as well as in the downstream. Due to anisotropy in the phase velocities the electrons are accelerated by these waves to very high energies along the field lines. The detailed observations of the electron and ion distribution functions in the downstream of the Earth's bow shock as well as interplanetary shocks will support the present model. The energy density of the Langmuir waves excited by these electron beams can be approximately written as

$W_{L_{u(d)}} \approx 0.1 \; n_{s_{u(d)}} \frac{m_e v_h^2}{2} \approx 10^{-4} \; n_0 T_e$. If one assumes that all the energy is converted into transverse waves and the source size is $\approx 1 \; R_\theta$, the brightness temperature can be estimated which lies in the range 10^9 K to 10^{11} K. Nelson and Robinson

(1975) reported that $T_B^{(L)}/T_B^{(u)} \approx 2.3$. The difference in the number density of the electron beams in the upstream and downstream will account of this difference in the brightness temperature in the two bands. If the anisotropy index N is large, the number density in the electron beam accelerated in the upstream will be decreased which may not be sufficient to excite observable radiation leading to disappearance of the bandsplitting [Thejappa, 1987].

5.8 Conclusions

1. The majority of the shocks responsible for type II radiation are supercritical, and they are characterized by the ion reflection.

2. The reflected ions behave like a beam in the foot and the ramp whereas they behave like a ring in the downstream. The resonantly excite low frequency waves whose frequency is near the lower-hybrid frequency both in the upstream as well as in the downstream.

3. The electrons are accelerated by these low frequency waves to ultra-relativistic energies due to the anisotropy in the phase velocities.

4. The hot electrons enter the background plasma of both in the upstream and downstream along the magnetic field lines and drive the Langmuir oscillations which may reach a rather high energy levels ($\frac{W_L}{n_0 T_e} \approx 10^{-4} - 10^{-5}$).

5. The Langmuir waves are scattered by ions and transformed into ordinary electromagnetic waves of the same frequency $\omega \approx \omega_{pe}$. Since the optical depth of the emitting plasma layer is large, the brightness temperature of the radiation does not depend upon the fine structure of the spectra and appears to be of the order of 10^{11} K. The radiation at second harmonic is due to the merging of two Langmuir waves. For typical parameters of the coronal plasma, the brightness temperature of harmonics may reach that observed at ω_{pe}.

6. The present model fully agrees with the suggestion of Smerd et al (1975) regarding the generation of the L and U bands in the upstream and downstream respectively.

7. The brightness temperature in the L and U bands depends on the number density in the accelerated beams. Since the number density of the electron beam in the downstream is less than that of upstream, the U band is fainter than L band as experimentally observed (Nelson and Robinson, 1975].

CLOSING REMARKS AND FUTURE OBSERVATIONS

In the introduction of our study we had broadly indicated the difference between inner and outer corona, and classified the types of disturbances that perturb the corona into two classes: (1) particle beams and (2) shock waves. We had also argued that both of them are interpreted since the electron beams are mainly accelerated by shocks.

The radio bursts at long wavelengths give very important clues for understanding the various physical processes taking place in the corona in the presence of the above disturbances.

In chapter II we studied theoretically the problem of type I noise storms which is believed to be caused by weak shocks driven by the newly emerging magnetic flux from the sunspots. We derived an expression for the growth rate of the ion-sound waves generated by the shock gradients and the energy density of the ion-sound (IS) turbulence saturated by quasilinear effect. We compared the energy density of the lower hybrid (LH) turbulence with that of IS turbulence generated under similar conditions and show that IS turbulence grow to higher levels. It was also shown that there is a better overlap in the wave number space in the case of IS waves. Therefore we showed that IS turbulence could be a better candidate for the low frequency turbulence needed to generate type I solar radio bursts.

In the same chapter we derived an empirical formula

for coronal magnetic fields based on the type I chain observations assuming that the chain is caused by a weak shock and the emission is at local plasma frequency. The velocity of the shock calculated from the drift rate of the chains and the density jump across the shock obtained from the observed bandwidth are used as the input in the Rankine Hagoniot relations and the magnetic field is calculated. We recommend that observational programs should be designed to test whether parallel current or perpendicular current in type I shocks is responsible for the low frequency turbulence. The excitation of upper hybrid waves by trapped particles is to be investigated.

In chapter III we described the Gauribidanur Radio Telescope operating at decameter wavelengths. The unusual time profiles of type III radio bursts and absorption bursts in decametric continuum observed using this telescope were studied. It was shown that the unusual time profiles of type III bursts are not due to random superposition of bursts with varying amplitudes and also they are not probable manifestations of fundamental and harmonic pairs. Some of the observed time profiles could be due to the superposition of bursts caused by ordered electron beams ejected with a constant time delay at the base of the corona. This has to be further investigated both theoretically and observationally. We had also shown that the sudden reductions in the decametric continuum can be explained as due to the absorption by ion-sound turbulence generated by a shock wave propagating laterally with respect to magnetic field. The duration

of the absorption was interpreted as the period during which the IS turbulence stays undamped above thermal level. The depth of the absorption is due to the level of Langmuir turbulence generated as a result of the interaction between ionsound waves and transverse waves.

Actually there is a build up of Langmuir waves upto a level after which the reverse interaction, $L + s \rightarrow t$ becomes important, i.e., the saturation stage of the absorption.

In chapter IV we studied in detail the drift pair bursts. The data on drift pair bursts, obtained using the swept frequency spectrograph at Nancay,France, had been analysed. We detected for the first time features like drift pair chains and vertical drift pair bursts. We showed that the drift pair bursts and their related phenomena like chains and vertical DPs can be understood selfconsistently if one assumes that the double plasma resonance layer, where the radiation is generated, is different at different instants of time so that one gets a slope in the frequency-time plane. It was also shown that the bursts can have all types of drift rates if there are considerable fluctuations in some macroscopic parameters such as density and magnetic field. A steep variation in the magnetic field was derived in the case of vertical DPs when the density was assumed not to be affected by DP activity. A more detailed high resolution observations of DPs are necessary to build any new theory.

In chapter V we proposed that the majority of shock waves

responsible for the generation of type II radio bursts are super-
critical. It was also proposed that the reflected ions behave
like a beam in the foot and the ramp and like a ring in the
downstream, i.e., just behind the overshoot. These were described
by drifted Maxwellian and Dory-Gust-Harris distributions respective-
ly. The ion beams were unstable and could drive the low frequency
waves, whose frequency lies between the electron and ion cyclo-
tron frequencies. These waves were absorbed by the ambient
electrons, leading to the formation of electron "tails", in upstream
as well as downstream. On entering the cold background these
hot electrons, in turn, drive the high frequency Langmuir oscilla-
tions to high level energy densities $\frac{W_L}{n_0 T_e} \sim 10^{-5} - 10^{-4}$, in the upstream
as well as in the downstream. The conversion of plasma waves
into electromagnetic waves was caused by the induced scattering
of plasma waves off ions or by merging of two Langmuir waves.
The brightness temperatures in the lower and upper bands depend
on the number densities in the accelerated beams. Since the
number density of the electron beams in the downstream is
less than of upstream, the U band is fainter than L band as
experimetally observed. Thus it naturally explained the band
splitting in type II bursts. The role of nonlinear processes was
also studied in this chapter. Theoretically the herringbone
structure in type II bursts remains to be explained. Observa-
tionally also it is to be confirmed whether herringbones and
type II bursts are completely related.

In conclusion we believe that a combination of high resolution radio observations from the ground and space will enable us to confirm the predictions like shock acceleration, shock excited low frequency turbulence etc.

REFERENCES

Abranin,E.P., Bazelyan,L.L., Goncharov,V.Yu., Zaitsev,V.V., Zinichev,V.V., Levin,B,N., Rapoport,V.O. and Tsybko,Ya.G. 1977, Sov. Astron. 21, 82.

Akimoto,A., Papadopoulos,K. and Winske,D. : 1985, J.Plasma Phys. 34, 445.

Aubier,M.G. and Boischot,A. : 1972, Astr. Astrophys., 19, 343.

Aubier,M.G., Leblanc,Y. and Moller-Pedersen,B. 1978, Astr. Astrophys., 70, 685.

Aurass,H., Bohme,A., Kruger,A., Fomichev,V.V., Gnezdilov,A.A. Mercier,C., Tlamicha,A. and urpo,S. : 1981, in Elgaroy,O., Mervier,C., Tlamicha,A., Zlobec,P. (eds) Supplement to 'Solar Radio Storms' - Proceedings of the 4th CESRA workshop on Solar Noise Storms, Duino Castle (Trieste, Italy), p.17.

Barbosa,D.D., Coroniti,F.V., Kurth,W.S. and Scarf,F.L. : 1985, Astrophys. J. 289, 392.

Bavassano-Cattaneo,M.B., Tsurutani,B.T. Smith,E.J. and Lin,R.P.: 1986, J. Geophys. Res. 91, 11929.

Benz,A.O. Kuijper,J. : 1976, Solar Phys., 46, 275.

Benz,A.O. and Wentzel,D.G. : 1981, Astr. Astrophys. 94, 100.

Boischot,A., Rosolen,C., Aubier,M.G., Daigne,G., Genova,F., Leblanc,Y., Lecacheux,A., De La Noe,J. and Moller-Pedersen,B. : 1980, Icarus, 43, 399.

Cane,H.V., Stone,R.G.,Fainberg,G., Steinberg,J.L. and Hoang,S.: 1982, Solar Phys., 78, 187.

Caroubalos,C., Poquerusse,M. and Steinberg,J.L. : 1974, Astr. Astrophys., 32, 255.

Daigne,G. and Moller-Pedersen,B. : 1974, Astr. Astrophys. 37, 355.

De Groot,T. : 1966, Bull. Astr. Inst. Nath. 15, 229.

De Groot,T., Loonen,J. and Slottje,C. : 1976, Solar Phys. 48, 321.

de La Noe,J. and Moller-Pedersen,B. : 1971, Astr. Astrophys. 12, 371.

de La Noe, J. and Gergely,T.E. : 1977, Solar Phys., 55, 195.

Dory,R.A., Guest,G.I. and Harris,E.G. : 1965, Phys. Rev. Letters, 14, 131.

Dulk,G.A., Altschuler,M.D. and Smerd,S.F. : 1971, Astrophys. Lett. 8, 235.

Dulk,G.A., and McLean,D.J. 1978, Solar Phys. 57, 279.

Dulk,G.A., Suzuki,S. and Sheridan,K.V. : 1984, Astr. Astrophys. 130, 39.

Duncan,R.A. : 1981 Proc. Astr. Soc. Aust., 4.

Edmiston,J.P. and Kennel,C.F. : 1984, J.Plasma Phys., 32, 429.

Elgaroy,O. and Ugland,O. : 1970, Astr. Astrophys. 5, 372.

Elgaroy,O. : 1977, Solar Noise Storms (Oxford; Pergmon).

Ellis,G.R.A. : 1969, Aust. J. Phys. 22, 117.

Fokker,A.D. : 1982, Solar Phys., 77, 255.

Galeev,A.A. : 1976, in Physics of Solar Planetary Environments (Ed.) D.J.Williams, American Geophysical Union, Vol.1, p.464.

Galeev,A.A. and Krasnoselskikh,V.V. : 1976, JETP Letters 24, 558.

Galeev,A.A. and krasnoselskikh,V.V. : 1978, Fizika Plasmy, 4, 111.

Galeev,A.A. : 1984, Exper. Teor. Fiz., 86, 1655.

Gary,D.E., Dulk,G.A., House,L., Illing,R., Sawyer,C., Wagner,W.J., McLean,D.J. and Hildner,E. : 1984, Astron. Astrophys. 134, 222.

Gergeley,T.E. and Kundu,M.R. : 1975, Solar Phys. 41, 163.

Gergeley,T.E. : 1982, in Solar Radio Storms (Ed.) A.O.Benz and P.Zlobec, proc. of 4th CESRA Workshop on Solar Noise Storms, Trieste.

Goldman,M.V., Reiter,B.F. and Nicholson,D.R. : 1980, Phys. Fluids, 23, 388.

Gopalswamy,N., Thejappa,G. and Sastry, Ch.V. ; 1983, J.Astrophys. Astr. 4, 215.

Gopalswamy,N., Thejappa,G. and Sastry,Ch.V. : 1984 Kodaikanal Obs. Bull. 4, 47.

Gopalswamy,N., Thejappa,G. : 1985, Pramana, 25, 575.

Gopalswamy,N., Thejappa,G., Sastry,Ch.V. and Tlamicha,A.: 1986, Bull. Astron. Inst. Czechos, 37, 115.

Grognard,R.J. : 1980, in IAU Symp. 86 : Radio Physics of Sun, (Eds.) M.R.Kundu and T.E.Gergeley,D. Reidel, Drodrecht, p.303.

Hansaz,J. : 1966, Aust. J. Phys. 19, 635.

Hasegawa,A. and Chen,L. : 1975, Phys. Fluids, 18, 1321.

Hey,J.S. : 1946, Nature, 157, 47.

Holman,G. and Pesses,M.E. : 1983, Astrophys.J. 267, 837.

Kai,K. : 1973, Proc. Astr. Soc. Aust., 2, 219.

Kakinuma,T. and Swarup,G., : 1962, Astrophys. J. 136, 975.

Kaplan,S.A. and Tsytovich,V.N. : 1973, Plasma Astrophys., Pergamon Press, Oxford.

Kaplan,S.A., Pikel'ner,S.B. and Tsytovich,V.N. : 1974, Phys. Rep., 15c, 1.

Karlicky,M. and Jiricka,K. : 1981, in Elgaroy,O., Mercier,C., Tlamicha,A., Zlobec,P. (eds.), Supplement to "Solar Radio Storms" - Proceedings of the 4th CESRA workshop on Solar Noise Storms, Duino Castle (Trieste, Italy).

Kaufmann,P., Iacoma,P., Koppe,E.H., Marvues des Santos,P. and Schaal,R.E. : 1975, Solar Phys. 45, 189.

Kennel,C.F. and Petschek,H.E. : 1966, J.Geophys. Res. 71, 1.

Klinkhamer,F.R. and Kuijpers,J., : 1981, Astr. Astrophys. 100, 291.

Krall,N.A. : 1968, Advances in Plasma Physics (eds.) A.Simon and W.B.Thompson (New York : Interscience) Vol.1, p.162.

Krall,N.A. and Book,D.L. : 1969, Phys. Fluids, 12, 347.

Krall,N.A. and Travelpiece,A.N. : 1973, Principles of Plasma Physics (Tokyo : McGraw-Hill).

Krasnoselskikh,V.V., Kruchina,E.N., Thejappa,G. and Volokitin, A.S. : 1985, Astr. Astrophys. 149, 323.

Krishan,V., Subramanian,K.R. and Sastry,Ch.V. : 1980, Solar Phys., 66, 347.

Kruchina,E.N., Sagdeev,R.Z. and Shapiro,V.D. : 1980, JETP
Letters, 32, 443.

Kruger,A. : 1979, Introduction to Solar Radio Astronomy and
Radio Physics (Dordrecht : D.Reidel).

Kundu,M.R. : 1965, Solar Radio Astronomy (New York : Wiley
Interscience).

Lacombe,C. and Mangeney,A. : 1969, Astr. Astrophys.,1, 325.

Lacombe,C. and Moller-Pedersen,B. :1971, Astr. Astrophys.
15, 406.

Lampe,M. and papadopoulos,K. :1977, Astrophys. J. 212, 886.

Le Squeren,A.M. : 1963, Ann. Astrophys., 26, 97.

Leroy,M.M., Goodrich,C.C., Winske,D., Wu,C.S. and Papadopoulos,K.:
1981, Geophys. Res. Letters, 8, 1268.

Leroy,M.M., Goodrich,C.C., Winske,D., Wu,C.S. and papadopoulos,K.:
1982, J.Astrophys. Res. 87, 5081.

Leroy,M.M. and Mangeney,A. : 1984, Ann. Geophys., 2, 449.

Levin,B.N. : 1982, Astr. Astrophys., 111, 71.

Magelsson,G.R. and Smith,D.F. : 1977, Solar Phys., 55, 211.

Malara,F., Veltri,P. and Zimbardo,G. : 1984, Astr. Astrophys.
139, 71.

Malitson,H.H., Fainberg,J. and Stone,R.G. : 1973, Astrophys.
Lett. 14, 111.

McLean,D.J. : 1967, Proc. Astron. Soc. Aust., 14, 47.

McLean,D.J. and Nelson,D.J.: 1977, Izv. Vyssh. Uchebn. Zaved.
Radiofizika, 20, 1359.

Melrose,D.B. : 1970, Australian,J. Phys. 23, 871.

Melrose,D.B. : 1974a, Solar Phys. 35, 441.

Melrose,D.B. : 1974b, Austr. J. Phys. 27, 271.

Melrose,D.B. : 1980, Solar Phys. 67, 357.

Melrose,D.B. : 1982a, Solar Phys., 79, 173.

Melrose,D.B. : 1982b, in Benz,A.O. and Zlobec,P. (eds.), Proc. of the 4th CESRA Workshop on "Solar Noise Storms" Trieste Observatory, Trieste, p.182.

Moller-Pedersen,B., Smith,R.A. and Mangeney,A. : 1978, Astr. Astrophys. 70, 801.

Nelson,C.J. and Melrose,D.B. : 1985 in Solar Radio Physics (eds.) McLean,D.J. and Labrum,N.R., Cambridge University press, Cambridge, p.333.

Nelson,G. : 1967, Ann. Rev. Astron. Astrophys. 5, 213.

Newkirk,G.Jr. : 1971, in Macris (ed.) Physics of the Solar Corona, (D.Reidel, Dordrecht, Holland) p.66.

Papadopoulos,K., Goldstein,M.L. and Smith,R.A. : 1974, Astrophys.J. 190, 175.

Papadopoulos,K., : 1981, in Plasma Astrophysics, (eds.) T.D.Guyenne, G.Levy, ESA Sp-161 p.313.

Pikelner,S.B. and Gintzburg,M.A. : 1963, Astron. Zh. 40, 842.

Roberts,J.A. : 1958, Aust. J. Phys. 11, 215.

Roberts,J.A. : 1959, Aust. J. Phys. 12, 327.

Robinson,R.D. : 1985, Solar Phys. 95, 343.

Rosenberg,H.L. : 1975, Solar Phys. 42, 247.

Russel,C.T. and Greenstadt : 1979, Space Sci. Rev., 23, 3.

Ryutov,D.D. and Sagdeev,R.Z. : 1970, JETP 58, 739.

Sastry,Ch.V. : 1969, Solar Phys., 10, 429.

Sastry,Ch.V. : 1971, Astrophys. Lett. 8, 115.

Sastry,Ch.V. : 1972, Astrophys. Lett. 11, 47.

Sastry,Ch.V. : 1973, Solar Phys. 28, 187.

Sastry,Ch.V., Subramanian,K.R. and Krishan,V. : 1983, Astrophys. Lett., 23, 95.

Sawant,H.S. : 1982, in Solar Radio Storms, [Ed.] A.O.Benz and P.Zlobec, Proc. of 4th CESRA workshop on Solar Noise Storms, Trieste.

Shodura,R. : 1975, Nuclear Fusion 15, 55.

Shukla,P.K., Yu,M.Y., Mohan,M., Varma,R.K. and Spatschek,K.H. 1982, Plasma Physik Bochum/Julich, SFB No.162, Ruhr-Universitat, Bochum.

Slottje,C. : 1972, Solar phys., 25, 210.

Slottje,C.: 1978, Nature, 256, 520.

Smerd,S.F., Sheridan,K.V. and Stewart,R.T., : 1975, Astrophys. Lett. 16, 23.

Smith,D.F.: 1977, Astrophys. J. 216, L53.

Smith,R.A., Goldstein,M.L. and Papadopoulos,K. : 1979, Astrophys. J. 234, 348.

Sotnikov,V.I., Shapiro,V.D. and Shevchenko,V.I. : 1978, Fizika Plasmy, 4, 450.

Spicer,D.S., Benz,A.O. and Huba,H.O., 1981, Astr. Astrophys., 105, 221.

Sturman,B.I. : 1974, Izv. Vyassh. Uchebn. Zaved., Radio Fizika, 17, 12.

Stewart,R.T. and Magun,A. : 1980, Proc. Astron. Soc. Aust., 4, 53.

Subramanian,K.R., Krishan,V. and Sastry,Ch.V. : 1980, Solar Phys. 66, 347.

Suzuki,S. and Gary,D.E. : 1979, Proc. Astron. Soc. Australia, 3, 379.

Suzuki,S., Stewart,R.T. and Magun,A. : 1980 in Radio Physics of the Sun, (eds.) M.R.Kundu,T.E. Gergely, D.Reidel Dordrecht, p.241.

Takakura,T. : 1966, Space Sci. Rev. 5, 80.

Takakura,T. and Shibahashi,H. : 1976, Solar phys., 46, 323.

Tanstrom,G.L. and Benz,A.O. : 1978, Astr. Astrophys. 63, 147.

ter Haar,D. and Tsytovich,V.N. : 1981, Phys. Rep. 73, 175.

Thejappa,G. and Sastry,Ch.V. : 1982, J.Astrophys. Astr. 3, 151.

Thejappa,G., Sastry,Ch.V. and Gopalswamy,N. : 1984, In Nonlinear and Turbulent Processes in Physcis (eds.) R.Z.Sagdeev, Harwood Academic publ. N.Y.

Thejappa,G. : 1986, Kodaikanal Obs. Bulletin, 6, 97.

Thejappa,G. : 1987, Submitted for publication.

Tidman,D.A. and Krall,N.A. : 1971, Shock waves in Collisionless Plasmas, Interscience, New York.

Tlamicha,A. : 1982, in Proc. of the 4th CESRA Workshop on "Solar Noise Storms" (eds.) A.O.Benz and P.Zlobec, Trieste Observatory, Trieste, p.52.

Tsytovich,V.N. : 1966, Uspekhi Fiz. Nauk, 89, 89.

Uchida,Y. : 1974, Solar Phys., 39, 431.

Vaisberg,O.L., Galeev,A.A., Zastenker,G.N., Klimov,S.I.,
Norzdrachev,M.N., Sagdeev,R.Z., Sokolov,A. and Shapiro,A.:
1983, Zhur, Exper. Teor, Fiz., $\underline{85}$, 1232.

Vlahos,L., Gergely,T.E. and papadopoulos,K. : 1982, Astrophys.
J. $\underline{258}$, 812.

Wentzel,D. 1984, Astr. Astrophys. $\underline{100}$, 20.

Wentzel,D. : 1982, in Proc. of the 4th CESRA Workshop on
"Solar Noise Storms" (eds.) Benz,A.O. and Zlobec,P.
Trieste Observatory, Trieste, p.145.

Wild,J.P. and McCredy,L.L. : 1950, Austral. J. Sci. Res. $\underline{A3}$,
387.

Wild,J.P. and Tlamicha,A. : 1964, Nature, $\underline{203}$, 1128.

Wild,J.P. and Smerd,S.F. : 1972, Ann. Rev. Astron. Astrophys.
$\underline{10}$, 159.

Wu,C.S. : 1984, J. Geophys. Res., $\underline{89}$, 8847.

Yakobalev,O.I. Efimov,A.I., Razmanov,V.M. and Shtrykov,V.K.:
1980, Sov. Astron. $\underline{24}$, 454.

Young,C.W., Spencer,C.L. Moreton,G.E. and Roberts,J.A. :
1961, Astrophys. J. $\underline{133}$, 243.

Zaitsev,V.V., Mityakov,N.A. and Rappoport,V.O. : 1972, Solar
Phys. $\underline{24}$, 441.

Zaitsev,V.V. and Fomichev,V.V. 1973, Sov. Astron. $\underline{16}$, 666.

Zaitsev,V.V., Kunilov,M.V., Mityakov,N.A. and Rappoport,V.O.,
1974, Astron. Zh. $\underline{50}$, 252.

Zaitsev,V.V. ; 1977, Izv. Vyssh. Uchebn. Zaved. Radiofizika,
$\underline{20}$, 1379.

Zaitsev,V.V. and Levin,B.N. : 1978, Sov. Astron. 22, 223.

Zheleznyakov,V.V. : 1965, Sov. Astron. 9, 191.

Zheleznyakov,V.V. and Zlotnik,E.Ya : 1977, Izv. Vyssh. Uchebn.

    Zaved. Radiofizika, 20, 1444.

BIO-DATA

Name   G.Thejappa

Date of Birth   1st July 1951

Address   Research Associate
                            Indian Institute of Astrophysics
                            Bangalore 560034

Academic Qualification   1. B.Sc.(Hons) in physics 1971-74.

                               Bangalore University, Bangalore
                               English Medium

                            2. M.Sc. in physics & mathematics
                               1974-80

                               Patrice Lumamba University, Moscow.

                            3. Diploma in Russian Language as
                               an Interpretor from Russian

                               Language into English, PFU Moscow.

                            4. Certificate for the completion
                               of preparatory Dept. of PFU in
                               Russian Language, PFU Moscow.

                            5. Certificate as a teacher in Physics,
                               PFU Moscow.

Membership of Societies   Member, Astronomical Society of India

Specialization in M.Sc.   Plasma Physics

Current Research Interests Solar Radio Astronomy

Research Experience

Visiting Research Scientists: Space Research Institute, Moscow, USSR and SibISMIR, IRKUTSK, USSR Aug - Nov 1983.

Space Research Institute, Moscow, USSR, Solar Station, Kislovodsk, USSR and ISMIRAN, Troisk, USSR, May–June, 1986.

Institute for Astronomy, ETH–Zurich, Switzerland, June 1986.

Astronomical Observatory, Trieste Italy, July, 1986.

Meetings Attended

I.   International Conference on Nonlinear and Turbulent Processes, Kiev, 1983.

II. Astronomical Society of India, Hyderabad, 1983, Bombay, 1984.

III. Winter School on Extragalactic Energetic Sources Organized

IV. Indo-USSR workshop on plasma Astrophysics, Chandigarh, India, 1985.

V.   IAU General Assembly, New Delhi, India, 1985.

VI. All India meeting on Solar Physics, Kodaikanal, India, 1985.

VII. Plasma Astrophysics – An International Course and Workshop, Sukhumi, Georgian SSR, 1986.

VIII. II CESRA Workshop on 'Particle Acceleration and Trapping in Solar Flares' Aubigny-Sur-France, 1986.

IX. XXVI COSPAR, Toulouse, France, 1986.

List of Publications

1.   Investigation of the structure of ECR absorption curves in decaying afterglow Ar–plasma. G.Thejappa, M.Sc. Thesis, Patrice Lumumba University, Moscow, 1980 (in Russian).

2.   Time structure of solar decameter type III radio bursts - G.Thejappa and Ch.V.Sastry, J.Astrophys. Astr. 3, 151-159, 1982.

3. Observation and interpretation of decametric absorption bursts. N.Gopalswamy, G.Thejappa and Ch.V.Sastry, J.Astrophys. Astr. 4, 215, 1983.

4. Fine structure in solar decametric radiation - G.Thejappa, Ch.V.Sastry and N.Gopalswamy, in Nonlinear and Turbulent processes, hardwood publication, (eds.R.Z.Sagdeev) Vol.1 P547-561, 1984.

5. Observations of the fine structure in solar decametric radio emission. N.Gopalswamy, G.Thejappa and Ch.V.Sastry, Kodaikanal Observatory Bulletin, 4, 47-54, 1984.

6. An interpretation of decametric absorption bursts, N.Gopalswamy, G.Thejappa and Ch.V.Sastry, Proc. of II Indo-US workshop on solar-terrestrial physics, (eds. M.R.Kundu, Biswas, B.M.Reddy and S.Ramadurai) p.197-207, 1984.

7. Fast electron generation in quasi-perpendicular shocks and type II solar radio bursts - V.V.Krasnoselskikh, E.N.Krachina, G.Thejappa and V.S.Volokitin - Astron & Astrophys. 149, 323-329, 1985.

8. Estimation of coronal magnetic fields using type I emission. N.Gopalswamy, G.Thejappa, Ch.V.Sastry and A.Tlamicha - Bull. Astron. Inst. Czech. 37 (1986), 115-120.

9. Ion-sound turbulence due to shock gradients in collision-less plasmas. N.Gopalswamy and G.Thejappa, Pramana, Vol.25, p.575, 1985.

10. A model of the generation mechanism of type II solar radio bursts - G.Thejappa, Kodaikanal Obs. Bulletin, 1986, Vol.6, p.97.

11. Some interesting features in the drift pair phenomena of solar decametric radiation, G.Thejappa, N.Gopalswamy, Ch.V.Sastry and M.G.Aubier, in plasma astrophysics, proceedings of the Internal Course and Workshop, (ED. 7.D.Guyenne), ESA publications, P.121.

12. Type II solar radio emission - G.Thejappa - A self consistent approach, presented at CESRA Workshop, Aubigny, to appear in Solar Physics.

13. On type II solar radio bursts, G.Thejappa, presented at XXVI COSPAR Meeting, Toulouse, 1986, To appear in Advances in Space Research.

14. Preferential acceleration of He^3 by lower hybrid waves, S.Ramadurai and G.Thejappa, presented at XXVI COSPAR meeting, Toulouse, 1986, To appear in Advances in Space Research.